

ISSN 0973-3302

# THE JOURNAL OF ACOUSTICAL SOCIETY OF INDIA

Volume 51

Number 4

October 2024



A Quarterly Publication of the ASI  
<https://acoustics.org.in>



**ASI**

# The Journal of Acoustical Society of India

The Refereed Journal of the Acoustical Society of India (JASI)

**CHIEF EDITOR:**

**B. Chakraborty**

CSIR-National Institute of Oceanography

Dona Paula,

Goa-403 004

Tel: +91.832.2450.318

Fax: +91.832.2450.602

E-mail: bishwajit@nio.org

**ASSOCIATE SCIENTIFIC EDITOR:**

**A R Mohanty**

Mechanical Engg. Department

Indian Institute of Technology

Kharagpur-721302, India

Tel. : +91-3222-282944

E-mail : amohantyemech.iitkgp.ernet.in

**Editorial Office:**

**MANAGING EDITOR**

**Mahavir Singh**

**ASSISTANT EDITORS:**

**Yudhisther Kumar**

**Devraj Singh**

**Kirti Soni**

ASI Secretariat,

C/o Acoustics and Vibration Metrology

CSIR-National Physical Laboratory

Dr. KS Krishnan Road

New Delhi 110 012

Tel: +91.11. 4560.8317

Fax: +91.11.4560.9310

E-mail: asisecretariat.india@gmail.com

The Journal of Acoustical Society of India is a refereed journal of the Acoustical Society of India (ASI). The ASI is a non-profit national society founded in 31st July, 1971. The primary objective of the society is to advance the science of acoustics by creating an organization that is responsive to the needs of scientists and engineers concerned with acoustics problems all around the world.

Manuscripts of articles, technical notes and letter to the editor should be submitted to the Chief Editor. Copies of articles on specific topics listed above should also be submitted to the respective Associate Scientific Editor. Manuscripts are refereed by at least two referees and are reviewed by Publication Committee (all editors) before acceptance. On acceptance, revised articles with the text and figures scanned as separate files on a diskette should be submitted to the Editor by express mail. Manuscripts of articles must be prepared in strict accordance with the author instructions.

All information concerning subscription, new books, journals, conferences, etc. should be submitted to Chief Editor:

*B. Chakraborty, CSIR - National Institute of Oceanography, Dona Paula, Goa-403 004,  
Tel: +91.832.2450.318, Fax: +91.832.2450.602, e-mail: bishwajit@nio.org*

Annual subscription price including mail postage is Rs. 2500/= for institutions, companies and libraries and Rs. 2500/= for individuals who are not ASI members. The Journal of Acoustical Society of India will be sent to ASI members free of any extra charge. Requests for specimen copies and claims for missing issues as well as address changes should be sent to the Editorial Office:

*ASI Secretariat, C/o Acoustics and Vibration Metrology, CSIR-National Physical Laboratory, Dr. KS Krishnan Road, New Delhi 110 012, Tel: +91.11.4560.8317, Fax: +91.11.4560.9310, e-mail: asisecretariat.india@gmail.com*

The journal and all articles and illustrations published herein are protected by copyright. No part of this journal may be translated, reproduced, stored in a retrieval system, or transmitted, in any form or by any means, electronic, mechanical, photocopying, microfilming, recording or otherwise, without written permission of the publisher.

Copyright © 2024, Acoustical Society of India

ISSN 0973-3302

Printed at Alpha Printers, WZ-35/C, Naraina, Near Ring Road, New Delhi-110028 Tel.: 9810804196. JASI is sent to ASI members free of charge.

**B. CHAKRABORTY**  
Chief Editor  
**MAHAVIR SINGH**  
Managing Editor  
**A R MOHANTY**  
Associate Scientific Editor  
**Yudhishter Kumar Yadav**  
**Devraj Singh**  
**Kirti Soni**  
Assistant Editors

## EDITORIAL BOARD

**M L Munjal**  
IISc Bangalore, India  
**Michael Vorländer**  
ITA Aachen, Germany  
**S Narayanan**  
IIT Chennai, India  
**V R SINGH**  
PDM EI New Delhi-NCR, India  
**R J M Craik**  
HWU Edinburg, UK  
**Trevor R T Nightingale**  
NRC Ottawa, Canada  
**N Tandon**  
IIT Delhi, India  
**J H Rindel**  
Odeon A/S, Denmark  
**G V Anand**  
IISc Bangalore, India  
**Gopu R. Potty**  
University of Rhode Island, USA  
**S S Agrawal**  
KIIT Gurgaon, India  
**Yukio Kagawa**  
NU Chiba, Japan  
**D D Ebenezer**  
NPOL Kochi, India  
**Sonoko Kuwano**  
OU Osaka, Japan  
**Mahavir Singh**  
CSIR-NPL, New Delhi, India  
**A R Mohanty**  
IIT Kharagpur, India  
**Manell E Zakharia**  
ENSAM Paris, France  
**Arun Kumar**  
IIT Delhi, India  
**Ajish K Abraham**  
IISH Mysore, India  
**S V Ranganayakulu**  
GNI Hyderabad, India



# The Journal of Acoustical Society of India

A quarterly publication of the Acoustical Society of India

Volume 51, Number 4, October 2024

## ARTICLES

**Measured reverberation time as a basis for predictive acoustic modelling of Kashivishweshwar Temple's Domed Hall**

*Anirvan Gupta and Arun Sulkunte Iyengar ..... 213*

**Advanced acoustic emission methods for non-destructive weld inspection in nuclear materials**

*S.V. Ranganayakulu and B. Ramesh Kumar ..... 223*

**Ultrasonic investigation on the physicochemical behaviour of acidum lacticum homoeopathic dilutions at different temperatures by using acoustic, volumetric and viscometric methods**

*Anil Kumar Nain, Neha Chaudhary, Preeti Droliya, Raj Kumar Manchanda, Anil Khurana and Debadatta Nayak ..... 238*

**Structure-borne sound source localization using sound level meter measurements in urban residential buildings**

*Arun Sulkunte Iyengar ..... 261*

**Fundamental frequency perturbation is a consequence of the biomechanics of voicing and not due to phonological status**

*Indranil Dutta and Molly Varghese ..... 268*

## INFORMATION

Information for Authors

Inside back cover

# Measured reverberation time as a basis for predictive acoustic modelling of Kashivishweshwar Temple's Domed Hall

Anirvan Gupta<sup>1</sup> and Arun Sulkunte Iyengar<sup>2</sup>

<sup>1</sup>*Department of Physics, School of Basic and Applied Sciences, JSPM University, Pune, India*

<sup>2</sup>*Principal Acoustic Consultant, dB Acoustique, Bangalore, India*

*e-mail: g.anirvan@gmail.com, arun@dbacoustique.in*

[Received: 21-08-2024; Accepted: 08-12-2024]

## ABSTRACT

This study presents the results of RT60 measurements conducted in the domed hall located in front of the Garbha-Griha (Sanctum-Sanctorum) of the Kashivishweshwar Temple in Wai, Maharashtra. Using dimensional measurements, a 3D model of the domed hall was created with approximated geometry, excluding sculptural and fine details. This model was then imported into ODEON room acoustics software to simulate the acoustics of the enclosure. The material properties were adjusted to match the measured RT60. Based on this calibrated model, key acoustic parameters, including Speech Transmission Index (STI), Clarity (C50), and Early Decay Time (EDT), were evaluated. This study aims to connect these findings to the field of archaeoacoustics, offering insights into the acoustic properties of ancient structures and their implications on speech intelligibility and ritual practices.

## 1. INTRODUCTION

The Kashivishweshwar Temple, located in Wai, Maharashtra, is an architectural marvel with significant historical and cultural importance. Dating back to the 17<sup>th</sup> century, this temple is not only a place of worship but also a testament to the intricate architectural skills of the period. The temple's domed hall, situated in front of the Garbha-Griha (Sanctum-Sanctorum), is a prominent feature where rituals and gatherings take place. The dome's unique geometry and materials are designed to enhance the acoustic experience during these events, playing a crucial role in the spiritual and communal activities within the temple.

Understanding the acoustic properties of this space is essential for both: preserving its historical integrity and enhancing the experience of visitors and worshippers. Acoustic analysis can provide insights into how the temple's design influences sound propagation, which can help in maintaining and restoring the temple to its original acoustic conditions. This is particularly important as changes over time, due to environmental factors and human intervention, might have altered the temple's original acoustic characteristics.

Archaeoacoustics, the study of sound within archaeological contexts, provides valuable insights into how ancient structures were designed to enhance or manipulate acoustics for various purposes<sup>[1,2]</sup>. This

interdisciplinary field combines principles of archaeology, acoustics, and architecture to understand the auditory dimensions of historical spaces. Research in archaeoacoustics has revealed that many ancient structures, from Greek amphitheaters to Mayan temples, were acoustically engineered to amplify sound and enhance auditory experiences during rituals and ceremonies<sup>[3,4]</sup>.

This paper focuses on the acoustic analysis of the domed hall in the Kashivishweshwar Temple, providing data that can contribute to the broader field of archaeoacoustics. By conducting detailed RT60 measurements and utilizing advanced acoustic modeling software, this study aims to offer a comprehensive understanding of the acoustic environment within the temple. The findings not only shed light on the acoustic properties of this historical site but also underscore the importance of acoustics in the cultural and religious practices of ancient Indian temples.

## 2. METHODOLOGY

### 2.1 RT60 Measurements

Reverberation time (RT60) is a crucial parameter for understanding the acoustic characteristics of a space, defined as the time required for sound to decay by 60 dB after the source has ceased. RT60 measurements for this study were conducted on the 1<sup>st</sup> of June 2024, in the domed hall of the Kashivishweshwar Temple, utilizing a calibrated NTi XL2 Sound Analyzer equipped with a Class 1 frequency response M2211 microphone. The combined measurement system holds a Class 2 certification.

The measurements were taken over three sessions, each lasting approximately 15-30 seconds, and were conducted in Indian Standard Time (IST) as follows:

**Session 1:** Start: 16:24:14, End: 16:24:29

**Session 2:** Start: 16:27:16, End: 16:27:45

**Session 3:** Start: 16:41:02, End: 16:41:22

During each session, multiple measurements were recorded across different frequency bands, ensuring a comprehensive analysis of the acoustic environment. The measurement uncertainty was documented wherever applicable to account for any variations and to ensure the reliability of the data.

The methodology employed ensures a systematic and detailed approach to capturing the acoustic properties of the temple's domed hall, providing a robust dataset for subsequent analysis and interpretation within the field of archaeoacoustics.

### 2.2 3D Model Creation

Dimensional measurements of the domed hall were meticulously taken (using both mechanical measuring instruments and laser distance meter HTC LD-50) to construct a 3D model. The model was created using approximated geometry, intentionally excluding intricate sculptural and fine details to focus on the primary architectural elements. This simplified model served as the foundational basis for the subsequent acoustic simulation. The dimensions captured were essential for ensuring that the model accurately represented the spatial characteristics of the hall, thereby providing a reliable framework for analyzing its acoustic properties.

### 2.3 Acoustic Simulation using ODEON Room Acoustics Software

The constructed 3D model of the domed hall was imported into ODEON room acoustics software, a sophisticated tool for simulating and analyzing the acoustic properties of architectural spaces. Within the software, the material properties of the model were adjusted iteratively to match the measured RT60 values. This iterative process ensured that the model accurately represented the actual acoustic environment of the domed hall, thereby providing a reliable basis for further acoustic analysis.

### 2.4 Determining Acoustic Parameters

Based on the calibrated model, the following acoustic parameters were determined:

Measured reverberation time as a basis for predictive acoustic modelling of Kashivishweshwar Temple's Domed Hall

**Speech Transmission Index (STI):** A measure of speech intelligibility, indicating how clearly speech can be understood within the space.

**Clarity (C50):** The ratio of early sound energy (within 50 ms) to late sound energy, which indicates how clear sounds are perceived in the space.

**Early Decay Time (EDT):** The time it takes for the sound level to decay by 10 dB, representing the initial rate of reverberation in the space.

These parameters were essential for comprehensively understanding the acoustic environment of the domed hall and its impact on speech intelligibility and overall acoustic experience.

## **2.5 Position of Receiver**

In this study, the receiver was placed approximately below the apex of the domed hall. This strategic positioning was chosen for several reasons: it optimizes the capture of the hall's reverberant characteristics, as the apex serves as a focal point for sound reflections due to the curved surface of the dome, leading to a more accurate representation of the overall reverberation time (RT60) and other acoustic parameters within the space<sup>[5,6]</sup>. The central location under the dome's apex provides a symmetrical sound field, ensuring that the measurements reflect the averaged acoustic response of the entire space rather than localized anomalies<sup>[7]</sup>. The dome's geometry tends to distribute sound energy evenly across the space, resulting in a more uniform measurement of acoustic parameters such as EDT, C50, and C80<sup>[8]</sup>. In the context of Vedic chanting and rituals, activities are often performed centrally within the hall, making this position relevant to the practical usage of the space and ensuring that the data correlates with the actual experience of participants during rituals<sup>[9]</sup>. In small enclosures with high reverberation, the diffuse nature of the sound field makes the specific position of the receiver less critical for capturing overall acoustic characteristics<sup>[10]</sup>. The high level of reverberation ensures that sound persists uniformly throughout the enclosure, resulting in consistent RT60 and other acoustic parameters across different positions within the hall<sup>[11]</sup>. Small, reverberant spaces exhibit spatial homogeneity in their acoustic response, making measurements at different positions yield similar results due to the consistent reverberant environment<sup>[12]</sup>. Therefore, placing the receiver below the apex of the domed hall was a deliberate choice aimed at capturing a comprehensive and representative acoustic profile of the space, ensuring that the measured acoustic parameters reflect the overall acoustic environment effectively, regardless of slight variations in receiver placement.

## **3. RESULTS AND DISCUSSIONS**

### **3.1 RT60 Analysis**

The RT60 measurements across the three sessions revealed varying reverberation times at different frequencies. These results are critical for understanding the acoustic characteristics of the domed hall in the Kashivishweshwar Temple.

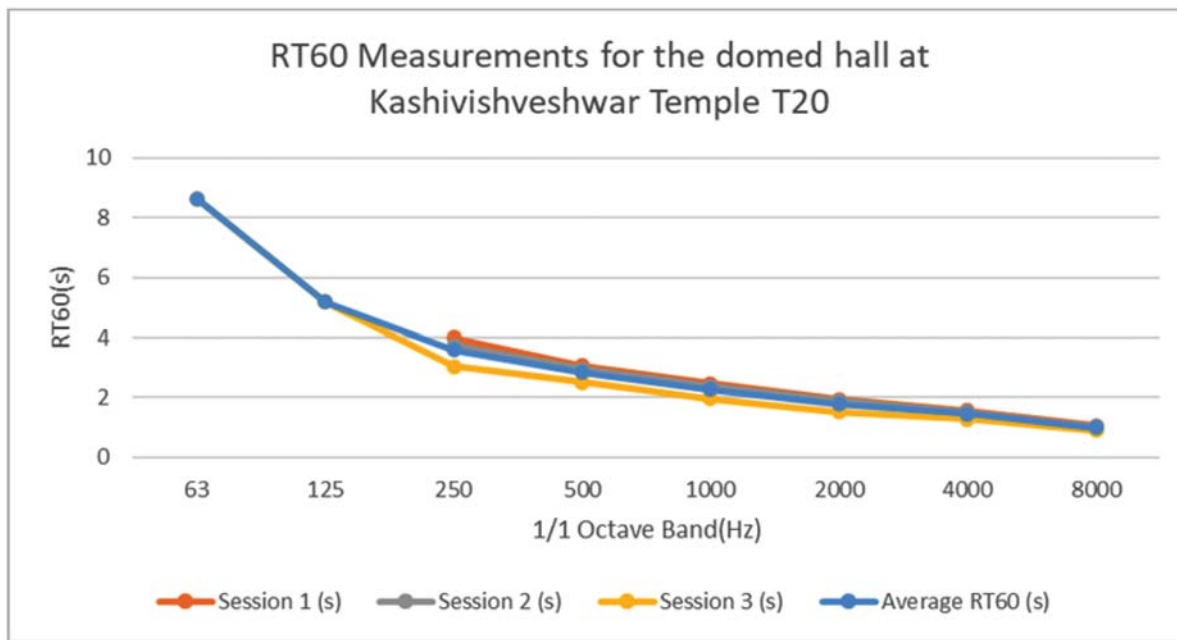
### **3.2 Combined Results and Measurement Uncertainty**

The following table provides a clear and concise representation of the RT60 measurements for each session, highlighting the variability across different frequency bands. The average RT60 values are calculated by taking the mean of the measurements from the three sessions (where available). The quantity in the brackets depict the uncertainty of the measurements (this could be found only in the session 2).

The measured and simulated RT60 values were compared to validate the accuracy of the acoustic model. Discrepancies between the measured and simulated values were identified and addressed by iteratively adjusting the material properties within the ODEON software. This calibration process ensured that the model accurately reflected the acoustic characteristics of the domed hall.

**Table 1.** RT60 Measurements and Average Values Across Different Frequency Bands.

Frequency (Hz)	Session 1 (s)	Session 2 (s ± %)	Session 3 (s)	Average RT60 (s)
63	-	-	8.63	8.63
125	-	-	5.19	5.19
250	4.00	3.74 (± 2.62%)	3.04	3.59
500	3.07	2.96 (±2.08%)	2.51	2.85
1000	2.47	2.39 (±1.64%)	1.97	2.28
2000	1.94	1.90 (±1.30%)	1.52	1.79
4000	1.56	1.53 (±1.02%)	1.28	1.46
8000	1.07	1.03 (±0.88%)	0.90	1.00

**Fig. 1.** Graph of the RT60 measurements in each session and the Average RT60 Measurements

### 3.3 Speech Intelligibility (STI)

The Speech Transmission Index (STI) values were computed to assess the hall's suitability for speech-related activities. Higher STI values reflect better speech intelligibility, which is essential for effective communication<sup>[13]</sup> and ritual activities within the temple. This measure helps determine how well speech is transmitted and understood in the acoustical environment of the hall. The measured STI value of 0.43 was recorded when the receiver was positioned at coordinates (-0.05, 2.62, 1.20) within the domed hall.

An STI value of 0.43 falls within the range that is generally considered as "fair" intelligibility<sup>[14,15]</sup>. This suggests that while speech can be understood, there may be some difficulty in clarity, particularly in a reverberant environment like that of the domed hall. This level of speech intelligibility is likely influenced by the high reverberation times previously measured, which tend to prolong sound reflections and can mask the direct sound, making speech less clear.

In the context of the Kashivishveshwar Temple, where Vedic chanting and other ritualistic activities are performed, an STI of 0.43 indicates that the space is acoustically supportive of prolonged vocalizations

Measured reverberation time as a basis for predictive acoustic modelling of Kashivishweshwar Temple's Domed Hall

but may pose challenges for more precise verbal communication. This acoustic profile aligns well with the intended use of the space for chants and rituals rather than for everyday speech. Overall, the measured STI highlights the unique acoustic environment of the temple, balancing between creating a resonant space for spiritual practices and maintaining a level of speech intelligibility that, while not optimal for everyday conversation, supports the temple's ritualistic needs.

### 3.4 Clarity ( $C50$ and $C80$ ) and Early Decay Time (EDT)

Clarity ( $C50$  and  $C80$ ) and EDT were analysed to assess the quality of sound and its decay characteristics within the domed hall. These parameters provide insights into how well speech and music can be perceived.

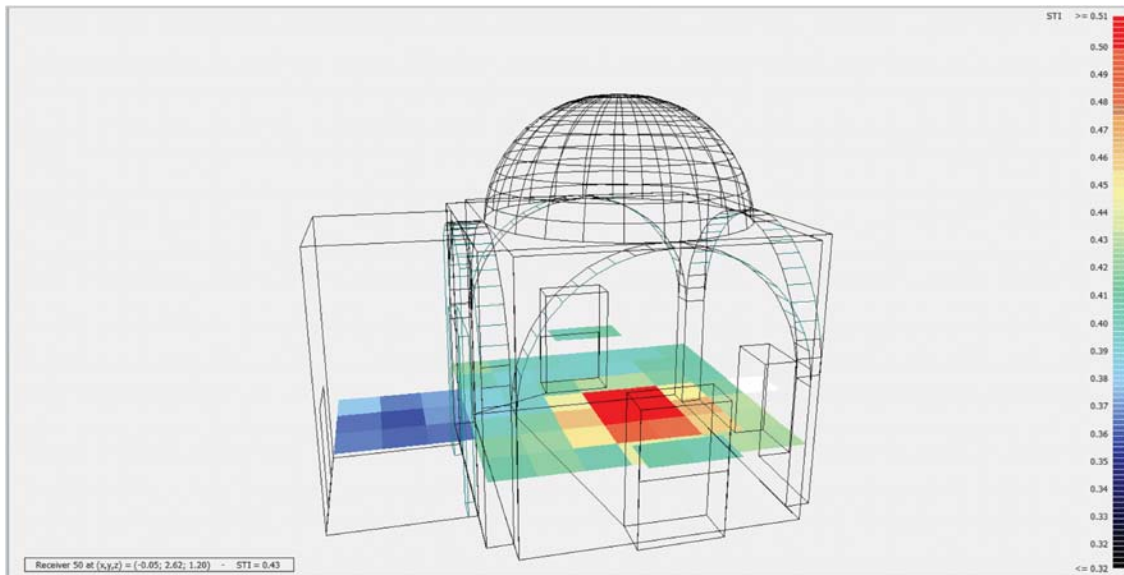


Fig. 2. Grid-wise Speech Transmission Index (STI) based on Ray Tracing Modelling using ODEON Software

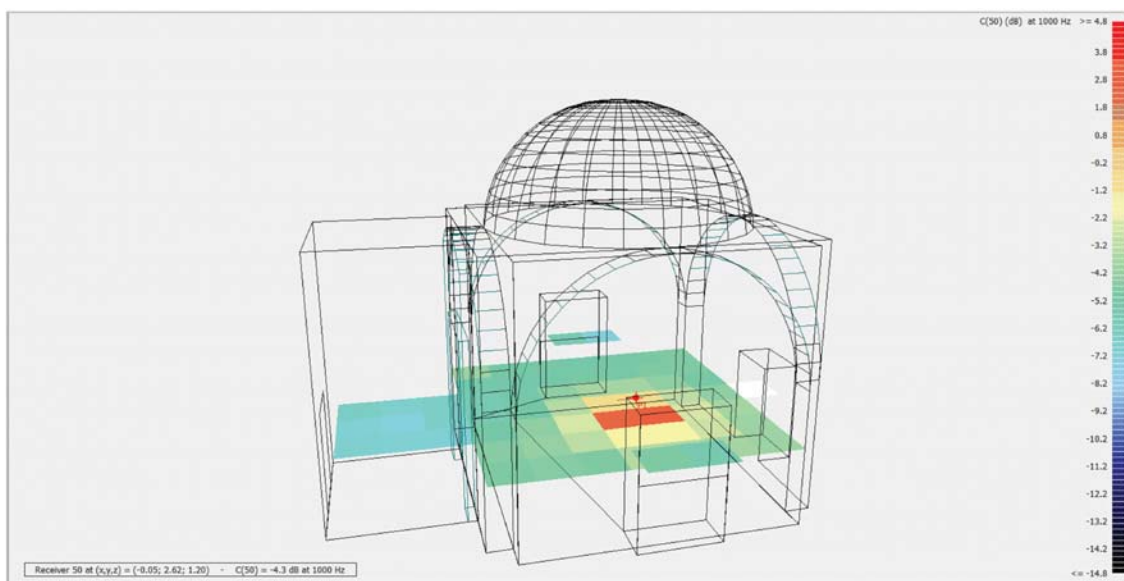


Fig. 3. Grid-wise Clarity ( $C50$ ) based on Ray Tracing Modelling using ODEON Software

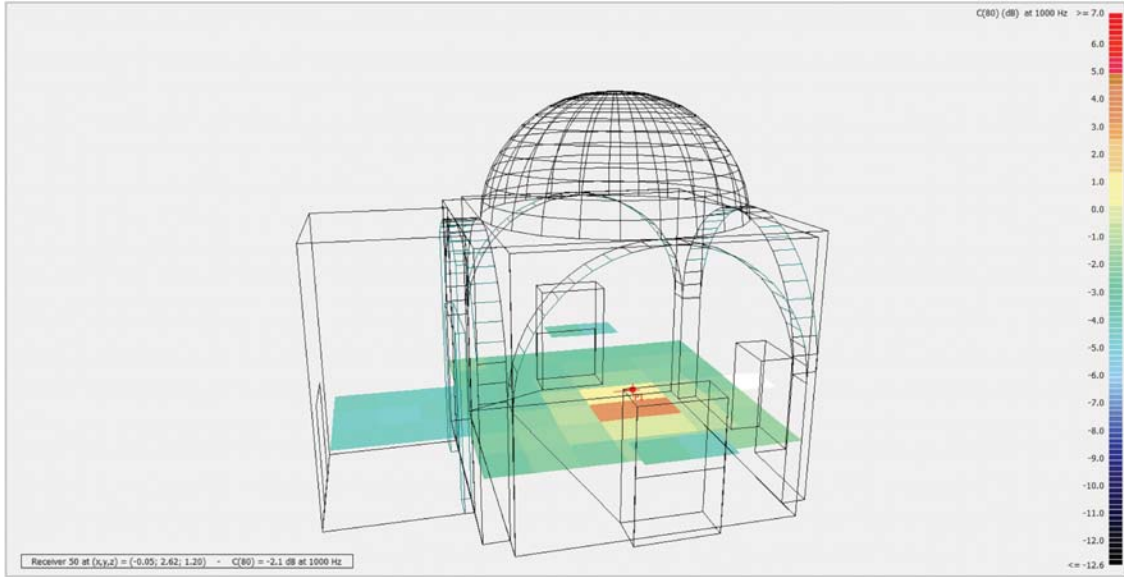


Fig. 4. Grid-wise Clarity(C80) based on Ray Tracing Modelling using ODEON Software

Table 2. EDT, C50 and C80 Measurements Across Different Frequency Bands.

Octave Band (Hz)	EDT (S)	C50 (dB)	C80 (dB)
63	5.01	-4.0	-2.9
125	4.94	-3.8	-2.7
250	3.56	-2.2	-1.0
500	2.80	-1.0	0.3
1000	2.49	-0.2	1.2
2000	1.80	1.6	3.2
4000	1.45	2.9	4.6
8000	0.95	5.5	7.6

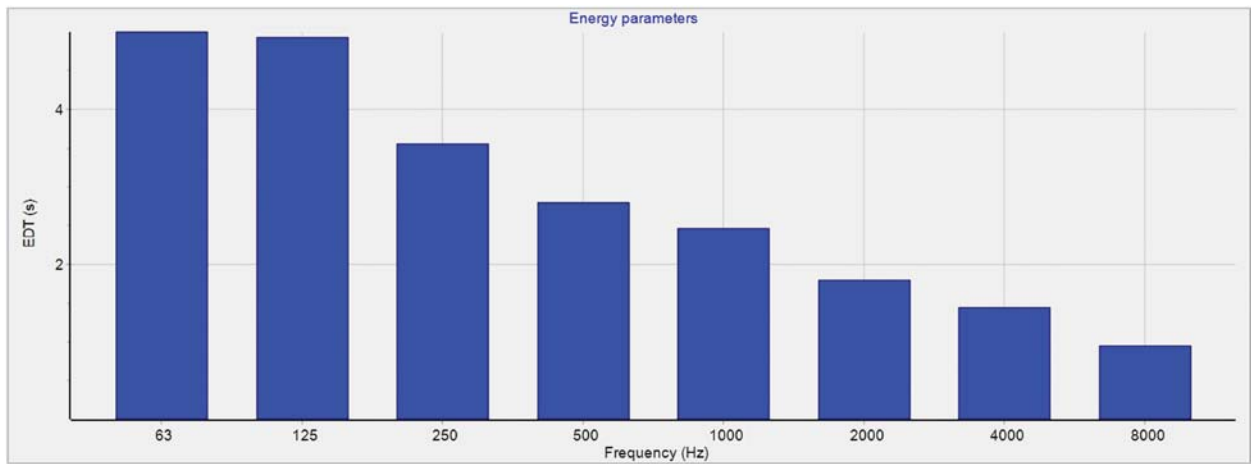


Fig. 5. Grid-wise Early Decay Time (EDT) based on Ray Tracing Modelling using ODEON Software

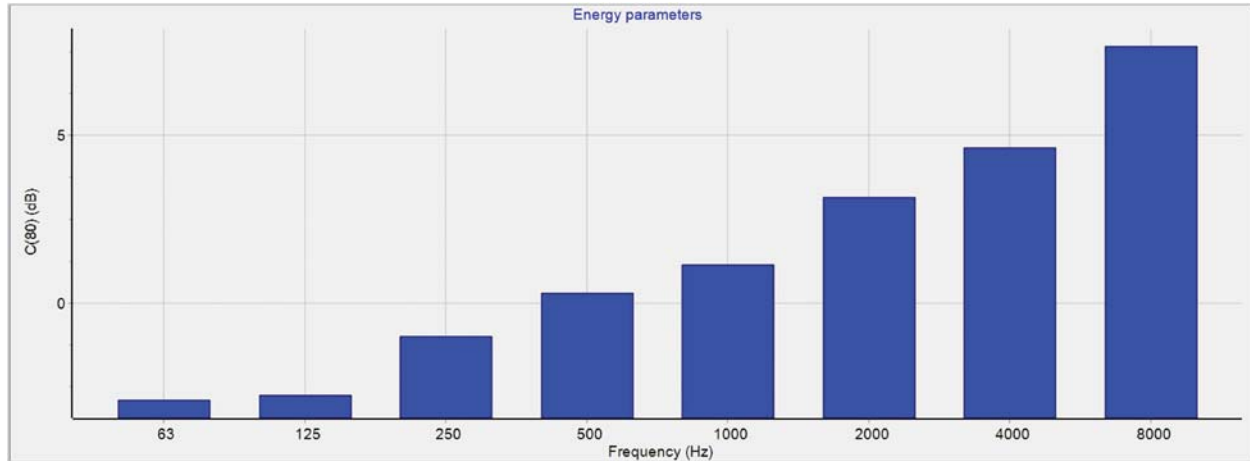


Fig. 6. EDT as a function of frequency

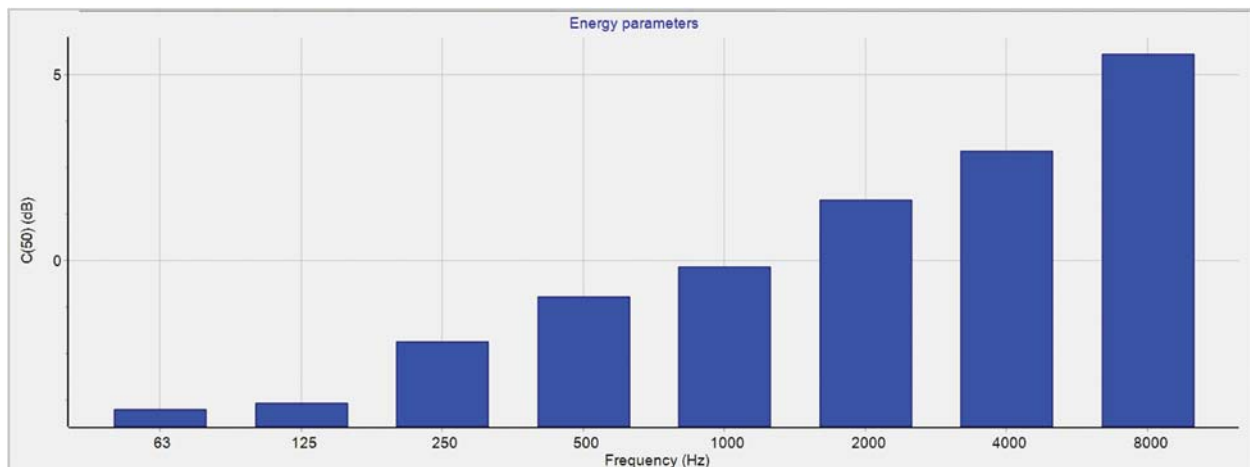


Fig. 7. C80 as a function of frequency

**Early Decay Time (EDT) : 63 Hz - 125 Hz:** The EDT values at the lower frequencies are relatively high (5.01 s and 4.94 s), indicating a long reverberation time. This suggests that low-frequency sounds linger in the space, contributing to a rich and enveloping auditory experience which is beneficial for the bass components of Vedic chanting.

**250 Hz - 1000 Hz:** The EDT values decrease progressively from 3.56 s to 2.49 s, indicating that mid-frequency sounds decay faster than low-frequency sounds. This trend improves speech intelligibility slightly, as evident from the STI measurement, as these frequencies are crucial for the clarity of spoken words.

**2000 Hz - 8000 Hz:** The EDT values continue to decrease significantly (1.80 s to 0.95 s), indicating that high-frequency sounds decay more quickly. This is advantageous for reducing excessive brightness and echoes, helping to maintain a balanced sound field.

**Clarity (C50 and C80): 63 Hz - 125 Hz:** The C50 and C80 values are negative, indicating poor clarity at these low frequencies. This is typical in large, reverberant spaces where low frequencies are less directional and more prone to scattering and diffusion. While this can create a warm and immersive environment, it is less ideal for precise speech intelligibility.

**250 Hz - 1000 Hz:** As the frequency increases, C50 values become less negative and approach positive values at 1000 Hz. Similarly, C80 values improve from -1.0 dB to 1.2 dB. This indicates that mid-frequency sounds are becoming clearer, which is beneficial for understanding speech and the nuances of chanting.

**2000 Hz - 8000 Hz:** At higher frequencies, both C50 and C80 values are positive and increase significantly (C50: 1.6 to 5.5 dB; C80: 3.2 to 7.6 dB). This indicates excellent clarity at these frequencies, which helps in distinguishing consonants and finer details of sound, making spoken words and chants more intelligible and enhancing the overall acoustic experience<sup>[17]</sup>.

**Comments on Temple Acoustics:** The acoustic profile of the Kashivishweshwar Temple, as indicated by the measured parameters, reveals a space that is well-suited for its intended use in Vedic chanting and ritualistic practices:

**Low Frequencies (63 Hz - 125 Hz):** The long EDT and poor clarity at low frequencies contribute to a resonant and immersive environment. This supports the temple's need for a rich, encompassing sound field during chants and rituals, which often include sustained vocalizations that benefit from extended reverberation.

**Mid Frequencies (250 Hz - 1000 Hz):** Improved clarity and reduced EDT at mid frequencies help in achieving a balance between reverberance and intelligibility. This is important for rituals that involve speech and chant, ensuring that the words remain comprehensible.

**High Frequencies (2000 Hz - 8000 Hz):** The significant increase in clarity and rapid decay at high frequencies ensure that the space does not become overly bright or echoic. This helps maintain a clear and pleasant auditory environment, enhancing the intelligibility of speech and the detailed components of chants.

In conclusion, the acoustic characteristics of the domed hall in the Kashivishweshwar Temple are well-aligned with the requirements of Vedic chanting and ritualistic activities. The space provides a balanced reverberant environment that supports both the spiritual ambiance and the practical needs of speech intelligibility during rituals. The combination of high reverberation times at low frequencies and improved clarity at higher frequencies creates a unique acoustic setting that enhances the overall sensory experience of the temple's users.

### **3.5 Acoustic Environment and Vedic Chanting**

The high reverberation time observed in the domed hall is particularly conducive for Vedic chanting, which often involves prolonged vocalizations and long pauses. The sustained reverberation allows for the chants to resonate throughout the hall, creating a profound and immersive auditory experience. This acoustic characteristic not only enhances the spiritual ambiance but also aligns with traditional practices where acoustics play a vital role in ritualistic chanting.

The high reverberation time observed in the domed hall of the Kashivishweshwar Temple is particularly conducive to Vedic chanting, which frequently involves prolonged vocalizations and extended pauses. The sustained reverberation allows the chants to resonate throughout the hall, creating a profound and immersive auditory experience. This acoustic characteristic not only enriches the spiritual ambiance but also aligns with traditional practices in which acoustics play a crucial role in ritualistic chanting. Such acoustic environments enhance the auditory perception of vocal rituals, making them more impactful and immersive for practitioners<sup>[18]</sup>.

### **3.6 Material Characteristics**

The domed hall's construction is characterized by the exclusive use of granite stone. This choice of material, typical of the Hemadpanti architectural style, involves massive granite slabs assembled without mortar, resulting in a robust structural framework. Granite's inherent density and rigidity contribute to

the hall's unique acoustic properties, facilitating long reverberation times that are ideal for Vedic chanting and other ritualistic practices. The acoustic implications of using such materials have been noted in various studies on historic architecture<sup>[19,20,21]</sup>. Granite's properties amplify sound and sustain reverberation, thus enhancing the effectiveness of ritualistic vocalizations.

#### 4. IMPLICATIONS FOR ARCHAEOACOUSTICS

The findings from this study provide a valuable contribution to the field of archaeoacoustics by offering a detailed acoustic profile of a historically significant structure. Analyzing the acoustic properties of the Kashivishweshwar Temple's domed hall offers insights into the architectural strategies employed by ancient builders to enhance acoustic experiences. This understanding helps elucidate how acoustics were integrated into the design of ritual spaces.

##### 4.1 *Ritual and Acoustic Design*

In archaeoacoustics, the role of acoustics in ritual practices is a significant area of study. The design of the domed hall may have been intentionally crafted to amplify and enhance certain sounds, thus contributing to the overall spiritual experience. The relationship between architectural design and ritualistic acoustics reflects an intentional integration of acoustic principles into the spatial and cultural context of the temple<sup>[22]</sup>.

##### 4.2 *Comparative Studies*

Comparing the acoustic properties of the Kashivishweshwar Temple with those of other ancient structures can reveal common design principles and regional variations in acoustic practices. Such comparative studies can deepen our understanding of how different cultures approached acoustic design, offering insights into historical practices and architectural ingenuity. Examining similarities and differences in acoustic features across various sites provides a broader perspective on ancient acoustic engineering<sup>[23]</sup>.

#### 5. CONCLUSION

This study presents a comprehensive analysis of the acoustic properties of the domed hall at the Kashivishweshwar Temple. By connecting these findings to the broader field of archaeoacoustics, we gain valuable insights into the intersection of architecture, sound, and ritual practices in ancient structures. Future research is expected to explore additional aspects of the temple's acoustics and compare them with other historical sites to further our understanding of ancient acoustic environments. The observed high reverberation time supports the notion that the space was designed to enhance prolonged vocalizations and chanting, a characteristic feature of Vedic rituals. This understanding of the acoustic environment provides a richer interpretation of ancient practices and their intended sensory experiences.

#### 6. REFERENCES

- [1] C. Scarre and G. Lawson, 2006. Archaeoacoustics. *McDonald Institute for Archaeological Research*.
- [2] R. Till 2011. Songs of the Stones: An investigation into the acoustic culture of Stonehenge. *Journal of the Acoustical Society of America*, **130**(5), 2748-2756.
- [3] P. Devereux and R.G. Jahn, 1996. Preliminary investigations and cognitive considerations of the acoustical resonances of selected archaeological sites. *Antiquity*, **70**(269), 665-671.
- [4] D. Lubman and B. Kiser, 2001. The Acoustics of Ancient Theatres Conference. *Institute of Noise Control Engineering*.

- [5] L. Sabatini, 2014. Acoustics of domed spaces: An experimental and numerical investigation. *Journal of Sound and Vibration*, **333**(16), 3721-3734.
- [6] L. Shtrepi, A. Astolfi and G.E. Puglisi, 2018. The role of early reflections in the perception of reverberation in large historical churches. *Applied Acoustics*, **130**, 161-172.
- [7] U. Berardi and G. Iannace, 2017. Acoustic performance of an Italian historical theatre. *Journal of Cultural Heritage*, **26**, 72-83.
- [8] L. Álvarez-Morales, R. Martínez-Sala and J.M Navarro, 2016. Acoustic simulation and auralization in a virtual model of the Catholic Cathedral of Murcia. *Building Acoustics*, **23**(4), 233-252.
- [9] M. Bisesi and G. Brambilla 2017. Soundscapes of urban parks and open spaces: A comparative study in Italy. *Applied Acoustics*, **127**, 160-168.
- [10] H. Kuttruff, 2016. *Room Acoustics* (6<sup>th</sup> ed.). CRC Press.
- [11] M. Long, 2014. *Architectural Acoustics* (2<sup>nd</sup> ed.). Academic Press.
- [12] D. Cabrera and J. Tichy, 2019. Diffusion and reverberation in small rooms. *Journal of the Acoustical Society of America*, **145**(2), 904-914.
- [13] ISO 9921:2003 Ergonomics - Assessment of Speech Communication. International Organization for Standardization, Geneva, Switzerland (2003).
- [14] Jens Holger Rindel, 2014. ODEON Application Note - Calculation of Speech Transmission Index in Rooms, pp. 9-16.
- [15] Herman J.M. Steeneken, 2002. The Measurement of Speech Intelligibility. TNO Human Factors, Soesterberg, *The Netherlands*, pp. 4-8
- [16] A.B. Gupta, L.M. Chaudhari and V.H. Raybagkar, 2019. Analysis of Acoustic Parameters to Determine the Appropriateness of Temple Enclosures for Speech and Music - Reference to Temples in Pune, *Annals of the Faculty of Engineering Hunedoara*.
- [17] A.B. Gupta, L.M. Chaudhari and V.H. Raybagkar, 2018. Analysis of Acoustical Characteristics for Understanding of Sound Quality and Acoustic Environment inside Temples, *Intl. J. Engg. Tech. Sci. and Res.*, **5**(3), 1908-1920.
- [18] L.E. Kinsler, A.R. Frey, A.B. Coppens and J.V. Sanders, 2000. *Fundamentals of Acoustics*. Wiley.
- [19] Trekbook, 2020. The Hemadpanthi Architectural Style. Retrieved from [Trekbook website].
- [20] NewsBharati, 2021. Granite in Ancient Architecture. Retrieved from [NewsBharati website].
- [21] EcoHeritage, 2022. The Acoustic Properties of Historical Buildings. Retrieved from [EcoHeritage website].
- [22] C. Baker and A. Bradley, 2008. *Acoustics and Architecture: Theories and Applications*. Cambridge University Press.
- [23] C. Tilley, S. Hamilton and B. Bender, 2000. *Handbook of Material Culture*. Sage Publications.

# Advanced acoustic emission methods for non-destructive weld inspection in nuclear materials

S.V. Ranganayakulu<sup>1\*</sup> and B. Ramesh Kumar<sup>2</sup>

<sup>1</sup>Center for Non Destructive Evaluation, Gurunanak Institutions Technical Campus,  
Hyderabad-501 506, Telangna State, India

<sup>2</sup>Institute for Plasma Research(under Dept of Atomic Energy), Bhat,  
Gandhinagar-382 428; Gujarat, India  
e-mail: svrnayakuluj@gmail.com

[Received: 10-07-2024; Accepted: 08-12-2024]

## ABSTRACT

This paper describes the acoustic emission investigation on Tungsten Inert Gas welding welded Stainless Steel (SS 316L) material with dimensions of 140\*16\*10 mm has been taken for these studies and fabricated with Tungsten Inert Gas welding (TIG) with implanted defects like porosity and pinhole in the welded area to get Acoustic Emission signatures by Acoustic Emission Linear Location Technique(AELLT) using AEWIN software procured from Physical Acoustic Corporation U.S.A. Constant load was applied on the material by using mechanical JIG to get the deformation in the welded region where the sensors are acquiring the test data for post analysis. The tests were conducted on two samples of the same defect weld material. The test is carried out and the acoustic emission signatures are recorded. X-ray Radiography testing is conducted on material to identify the defects to correlate with the acoustic emission signatures.

## 1. INTRODUCTION

Acoustic Emission (AE) is the study and practical use of elastic waves generated by a material subjected to external stress<sup>[1]</sup>. The phenomenon was recognized by early miners who exited a mine when the rocks or supporting timbers started groaning. Tin cry, the sound produced when a tin bar is bent, was known soon after the production of metallic tin. More recently, C.S. Barrett mapped a low-temperature phase transition in Lithium-Magnesium alloys by sticking a phonograph needle into the crystal and recording the output as the temperature was changed. J. Kaiser investigated the signals produced by samples undergoing tensile testing and discovered the Kaiser effect, i.e., that no signals were generated by a sample upon the second loading until the previous maximum load was exceeded. After Kaiser's thesis was published in 1950, several groups investigated the phenomena for possible use in testing structures. In the early 1960s, Allen Green and a group at Aero Jet Corporation started using AE in the testing of Saturn Rocket propellant tanks. They used a form of triangulation based on the arrival times of the acoustic pulse at several acoustic emission sensors. Acoustic Emission, according to ASTM, refers to the generation of transient elastic waves during the rapid release of energy from localized sources within a material<sup>[2]</sup>. Other sources of Acoustic Emission are melting, phase transformation, thermal stresses, cool-down cracking, and stress build-up.

## 2. EARLIER WORK ON ACOUSTIC EMISSION

The main function of an acoustic emission test is to identify flaw growth in a structure as it undergoes increasing or continuing stress. Ideally, the test should both locate the flaws and describe their growth rate as the stress level increases or the stress state continues over time. On simple structures, a single AE sensor can report how the structure itself is behaving. However, complex structures will have many possible flaw sites. Such a structure, when large or constructed of multiple materials, will best be monitored with multiple sensors. Thus, most of the growth in the field of AE in the last 40 years has been in the design of multi-sensor systems and their analysis techniques. The focus of these techniques has been the location of acoustic emission sources on large structures. Starting with the early work of Green et al. at Aero Jet Corporation, a primary structure of interest has been pressure vessels. Now, almost any structure that experiences changes of stress in normal operation is a candidate for acoustic testing, and most of these tests involve source location.

The basic idea in source location is to cover a surface with a network of sensors. If one can determine the arrival times of an emission signal at several sensors, then, knowing the acoustic velocity<sup>[3]</sup>, it is possible to triangulate back to the location of the source of that emission.

As discussed above, most acoustic emission mechanisms involve a permanent change in the microstructure of the material<sup>[4]</sup>. Once a microfracture occurs, it will not happen again unless there is some sort of healing mechanism. The ratio of the load value, when emission starts on subsequent loadings, to the maximum load value reached on the previous loading, known as the Felicity ratio, indicates possible damage induced by the previous loading. Many NDT tests of FRP structures apply the test load in a series of steps, returning to zero between each step. The appearance of Felicity ratios much less than 1.0 is a good indication that significant damage occurred in previous loadings.

## 3. EXPERIMENTAL SETUP OF MECHANICAL JIG

All the samples were subjected to visual, ultrasonic, and radiographic examinations before conducting the AE. The defect location and magnitude were well established by these conventional methods. As mentioned earlier, it is necessary to subject these samples to external loading to activate the defects and generate AE. The generated AE is monitored with the help of two transducers in "Linear localization" mode for locating the defects<sup>[5]</sup>. The following is a brief principle of the linear mode of detection in AE.

### **Flaw Location :**

The samples were tested using the above-mentioned linear localization method. To activate the defects, an external force needed to be applied to the specimens. The following setup was used for testing these samples in a unique jig made specifically for this purpose. This special jig was designed for ease of loading and to minimize unwanted external noise. The jig has provisions for placing the samples on an anvil at the lower side and in the center. This anvil has two vertical supports with rounded tops on which the sample can be placed and pressed to obtain deformations. A mandrel attached to a screw loading system can be lowered onto the anvil

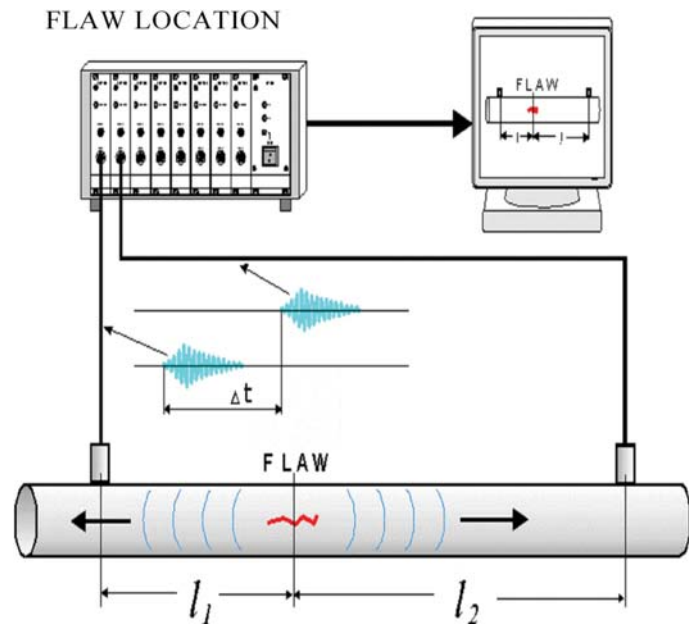


**Fig. 1.** Setup For Linear Localization of AE from a Flaw.

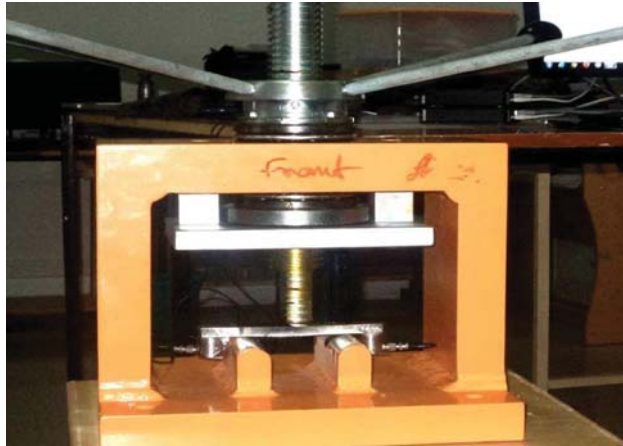


**Fig. 2.** Sensors attached with sample.

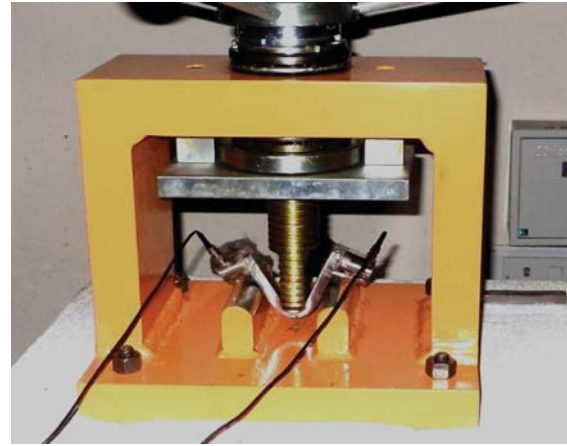


**Fig. 3.** After bending the sample.

for pressing the samples. The samples are placed on the anvil in a flat position, and the mandrel is lowered slowly by rotating the lever attached to the screw, thus loading the samples

Two broadband acoustic sensors were placed on either side of the sample, and acoustic data was collected while slowly loading the samples. A linear location program was used during data collection. Suitable filters were applied to avoid unwanted noise from various sources. AE signatures were recorded in terms of energy, count, and amplitude. At least two samples were tested from each of the weld categories mentioned above. The specimens were bent to an angle of less than 45 degrees between their two legs.

Acoustic emission data was collected while slowly loading the specimens. Copious emission activity was detected from both good and defective specimens. However, it was noticed that the emission activity started much earlier in the defective specimens than in the good specimens. Additionally, the activity from the defective samples was higher, and some of the signals were distinctly sharper. Some signals showed higher frequencies, possibly due to crack formation during loading and deformation<sup>[6]</sup>. Overall, it was observed that the embedded defects resulted in extra acoustic emission activity compared to specimens from good welds.

The AE data was recorded for various good and defective samples of SS304L and SS316R. NDT evaluation was also carried out on the specimens earlier, and the results are being correlated with the AE response of the specimens. Currently, experiments are being conducted on more specimens to obtain a reasonable statistical distribution and correlation of the AE data concerning the sound and defective specimens, as well as for different defect types.

#### 4. EXPERIMENTAL SETUP OF AE HARDWARE AND SOFTWARE

The USB-AE Node System is a high-performance, computerized Acoustic Emission (AE) system packaged in a small anodized aluminum case. Once linked with a PC running AEwin for USB software, the USB-AE Node system has all the performance features of a larger, more expensive AE system, including AE bandwidth, speed, AE features, sampling rates, and waveform processing capabilities, all in a compact package. The USB-AE Node System is capable of performing any AE application that one of our larger AE systems can and is an excellent field survey tool, especially in situations where plug-in power is not readily available. It can be used with a notebook or netbook PC in the laboratory and is capable of carrying out lab tests, utilizing its channel AE capabilities and four-channel parametric inputs for correlating load or stress with AE activity.

The generation of transient elastic waves occurs when there is a sudden redistribution of stress in a material. When a structure experiences an external stimulus like changes in pressure, load, or temperature,

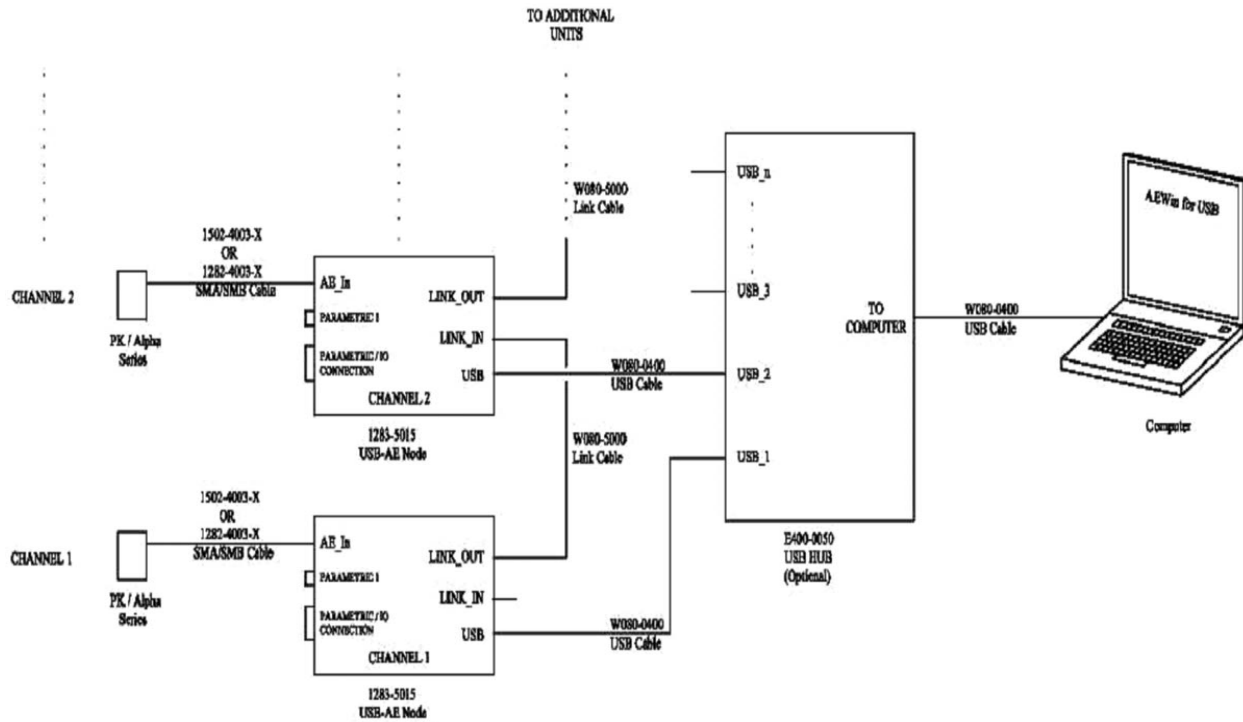


Fig. 4. USB-AE Node and Accessories (Sensor and Sensor Cable), 2) Typical Daisy-Chain Configuration.

localized sources trigger the release of energy in the form of stress waves. These waves propagate to the surface and are detected by sensors<sup>[7]</sup>. With suitable equipment and setup, movements as small as picometers ( $10^{-12}$  m) can be identified. Sources of acoustic emissions (AE) vary from natural events such as earthquakes and rock bursts to internal processes like crack initiation, growth, slip, dislocation movements, melting, twinning, and phase transformations in metals.

The elastic component of strain occurs immediately upon the application of a load, redistributing the internal force field to achieve balance within the material. This redistribution happens at the speed of sound.

The plastic component of strain often takes longer to manifest. Some deformation occurs immediately, while some is delayed<sup>[8]</sup>. This behavior is akin to how materials like silly putty behave: over time, they exhibit plastic creep and stretching, causing phenomena like sagging in wooden beams. Steel shows minimal plastic behavior, but acoustic emission serves as a sensitive indicator that

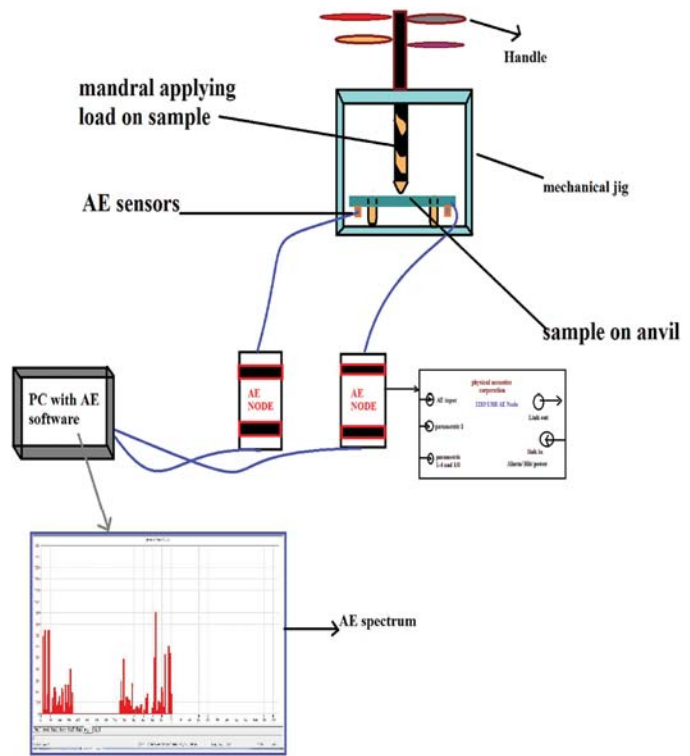


Fig. 5. Schematic diagram for AE testing process.



Fig. 6. Emission continuing during load hold indicates instability.

can reveal time-dependent behavior otherwise unnoticed. This characteristic behavior pattern is evident in newly fabricated components. In Figure 6, both load and AE are plotted against time<sup>[9]</sup>. During the first load hold, no emissions occur, but during the subsequent higher stress level, emissions continue for a period before stabilizing. Emissions during load holds often indicate significant structural defects, making them crucial in many testing procedures. Emissions during load rises in previously unloaded structures are less straightforward to interpret and may originate from defects or natural material response.

Experiments involving cyclic loading with fixed loads have shown that primary emissions from active crack growth occur only at peak load levels. Secondary emissions and noise at lower load levels are typically disregarded. Initially, when cracks are small, not every cycle produces emissions. However, as cracks approach critical lengths for unstable propagation, emissions become consistent across cycles. This aligns with statically loaded specimens, where insignificant flaws exhibit the Kaiser Effect, while structurally significant flaws show the Felicity Effect.

Damage assessment becomes feasible because AE activities correlate with parameters such as stress levels in the crack zone. AE activity can directly inform fracture mechanics parameters, which in turn relate to crack growth rates and fatigue failure.

The primary goal of AE inspections is often to pinpoint the source of significant acoustic emissions. While AE analysis may not determine the extent of damage, subsequent testing at identified sources can provide these answers.

### **Linear Location Technique**

Several source location techniques have been developed based on acoustic emission (AE) methods, categorized into two types: zonal location and point location. In planar materials, when using AE to pinpoint a source, three or more sensors are typically employed, with the optimal source position being between these sensors.

One commonly used technique for computed-source location is the linear location principle, illustrated in the figure to the right. This method is often applied in evaluating struts on truss bridges. When the source is positioned at the midpoint between two sensors, the difference in arrival times for the wave at these sensors is zero<sup>[10]</sup>. If the source deviates closer to one sensor, a measurable difference in arrival times occurs. To determine the distance of the source from the midpoint, the arrival time difference is multiplied

by the wave velocity. The direction (right or left of the midpoint) is determined by which sensor records the wave first<sup>[11]</sup>. This linear relationship applies to any event source located between the sensors.

It's important to note that this method assumes implicitly that the source lies along a line passing through the two sensors, making it applicable only to linear problems.

## 5. SAMPLE PREPARATION DETAILS

For acoustic testing, SS316L material was selected due to its high strength, commonly used in nuclear reactors<sup>[12]</sup>. Various welded specimens were prepared to study signals around the welded regions. To monitor weld defects accurately, intentional defects were introduced during the welding of several weld plates. Plates of suitable dimensions were chosen for these experiments.

**Details of the welding process are as follows:**

- Plate material: SS316L
- Plate thickness: 10 mm
- Plate length: 300 mm
- Plate width (before welding): 70 mm

**Main welding method used:**

- TIG (Welding current: 110 to 130 Amperes)

**Other welding methods used (for creating porosity and slag defects):**

- Manual Metal Arc (MMA) (Welding current used: 200 Amperes)

After welding, the plates measured 140 mm in width and 300 mm in length. Different categories of welds were created, including:

1. Pinholes
2. Porosity



(a) Pinhole

(b) Porosity

**Fig. 7.** SS 316L Samples containing (a) pinhole (b) porosity for AE Study under Stress or load.

## 6. EXPERIMENTAL PROCEDURE

- A. Radiography Testing :** Radiography testing involves exposing a test object to penetrating radiation, allowing the radiation to pass through the object being inspected, with a recording medium placed opposite to it<sup>[13,14]</sup>.
- B. Positioning :** The test part is positioned between the radiation source and a piece of film. Areas of varying thickness and density within the object will attenuate the radiation differently. The



**Fig. 8.** Radiographic film shows (a) pinhole and (b) porosity defects.

darkness (density) of the film will correspond to the amount of radiation reaching it through the test object.

**C. Radiographic Source :** The radiography testing techniques demonstrate that the required sensitivity has been achieved. Iridium-190 is used as the radiation source in this test, meeting the minimum thickness requirements for steel of 0.75 mm. The minimum recommended thickness may be adjusted when the radiography techniques verify the necessary sensitivity has been attained.

**D. Radiographic Film :** Commercially available industrial radiography films are used according to the SE 1815 (ASTM) standard test method for film systems in industrial radiography. The radiography film used is fine grain, high definition, and high contrast (e.g., Kodak type AA 400, FUJI 100, or AGFA D7)<sup>[15]</sup>. D4 film is specifically employed for SS316L to inspect defects as follows.

Radiography tests are conducted on samples to correlate with acoustic emission (AE) testing, determining whether emissions observed in AE testing relate to defects in weld specimens. Two samples, each containing pinhole and porosity defects separately, are subjected to the test cycle using Gamma ray as the source. Wire-type and hole-type penetrameters are used to ensure test accuracy<sup>[17]</sup>. The achieved sensitivity is good, allowing defects in the films to be easily observed. Subsequent AE testing is conducted for further analysis.

## 7. ACOUSTIC EMISSION TESTING

The primary purpose of acoustic emission testing on a structure is to detect and monitor flaws that affect its integrity. It's important to note that acoustic emission testing is not considered a nondestructive test as the emissions detected result from irreversible changes in the material under test.

Acoustic emission tests can be categorized based on the type of loading applied. The first category involves a single loading up to either the maximum applied load or failure, which may be applied continuously or in steps. In tests involving fiber-reinforced plastics (FRP), steps may include returns to zero load between each step, allowing for determination of the Felicity ratio at the start of each step. Continuous loading with steps allows observation of how emission rates decrease as loading halts. As a specimen approaches failure, emissions often continue during load holds, indicating a critical period to end the test and reduce the load, unless the objective is to deliberately fail the specimen<sup>[18]</sup>.

Analysis of acoustic emission tests primarily involves detecting emissions and measuring emission rates relative to changes in stress levels during the test. In tests using multi-channel setups<sup>[19]</sup>, the goal is to locate emissions and measure emission rates for each identified area. Analysis can be performed in real-time (if the goal is to prevent structural failure) or in post-test analysis<sup>[20]</sup>. Real-time analysis heavily relies on the operator's experience and knowledge, particularly in high-energy loading scenarios, which are typically learned through practical experience.

Graphical analysis of tests in real-time is guided by the AE system operator, who relies on predefined graphs. In the early stages of AE testing, key instruments included the oscilloscope and audio channels, displaying output from individual AE channels.

One could glean valuable insights from the oscilloscope, noting the rapidity of emission occurrence, its amplitude, and the overall shape of emission bursts. Non-emission noise signals were immediately discernible. Impending specimen failure was clearly indicated as the entire scope illuminated. The audio channel utilized beat frequencies to bring main AE frequencies into the audible range, allowing experienced operators to gather additional information from changes in audio amplitude and frequency. Alongside these instruments, an x-y recorder plotting summed counts against load or time provided experienced operators with a comprehensive view of test progress.

A graph depicting hits, events, counts, or absolute energy versus load or time is crucial. The author favors cumulative graphs over rate graphs, as they visually distinguish cumulative trends more effectively than integrating rate data. The classic parameter-versus-time graph has been a staple since the early days of AE testing. The choice of AE parameter depends on the test's objectives. Hits or counts display all detected AE, with counts being more sensitive to emission intensity. Located events counts are sensitive to emissions from actual flaws but may miss regions where only one or two sensors activate<sup>[21]</sup>. Counts or absolute energy per event provide detailed information on flaw growth state but can be complex with multiple flaws. A rate of absolute energy per load interval graph is likely the most useful but is best used in post-test analysis, requiring a comprehensive understanding of all cluster behaviors.

Changes in the slope of cumulative graphs indicate shifts in acoustic emission rates<sup>[22]</sup>. A steady rate amidst external noise suggests controlled flaw growth, while an increasing rate indicates uncontrolled flaw propagation. A curve slope approaching exponential or showing a distinct knee typically signals impending structural failure.

## 8. RESULTS AND DISCUSSIONS

Testing involved two samples from each defect category, along with good samples previously mentioned. Linear localization techniques were employed to gather data. Events were recorded relative to the positions of transducers placed at either end of the samples during loading.

Initially, efforts focused on achieving clear acoustic signals with high signal-to-noise ratios, yielding positive results before transitioning to monitoring various parameters. Initial data monitoring included "events versus x-position." Additionally, data was monitored in various configurations. The following details the modes in which data was obtained, compiled, and analyzed.

## 9. OBSERVATIONS MADE FROM DATA ANALYSIS

- A. **Energy Versus X-Position.** It was observed that all samples except one exhibited a significant number of events originating from the center position of the sample [Fig. 9]. This anomaly is likely an experimental aberration rather than a characteristic feature of the defect.
- B. **Cumulative Counts Versus Time.** Both porosity and pinhole defects showed a high rate of count accumulation. The pinhole defect displayed a moderate rate of count accumulation. It was noted that both defects emitted plastic deformation under load [Fig. 10].
- C. **Cumulative Energy Versus Time.** There was considerable variation in cumulative energy over time. Pinhole defects exhibited continuous cumulative emission, whereas porosity defects showed a brief duration for deformation [Fig. 11]. This indicates high energy emission due to the formation of new surfaces.
- D. **Hits Versus Time.** Pinhole defects recorded higher hits compared to porosity defects. After complete deformation in pinhole defects, high emissions were observed. Porosity defects exhibited the highest hits during deformation when new surfaces were formed [Fig. 12].

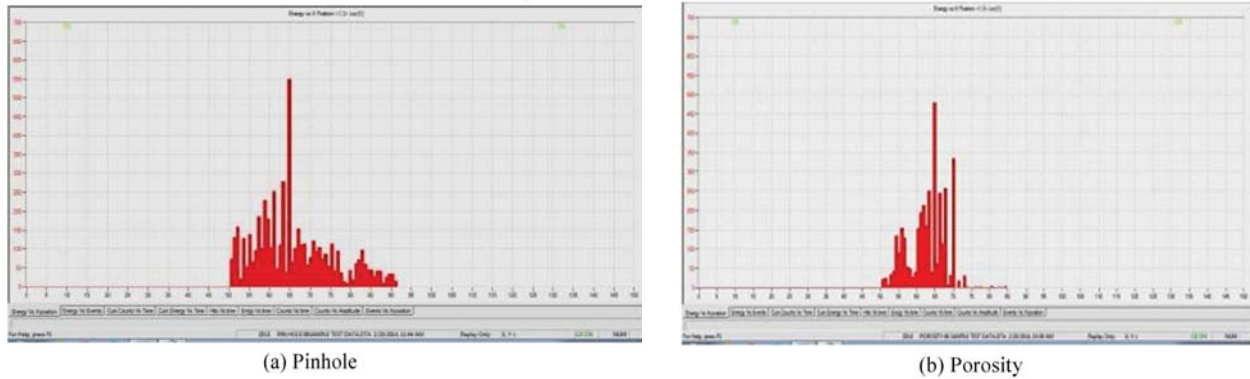


**Fig. 9.** SS 316L Materials showing Energy Vs X-position corresponds to (a) and (b).

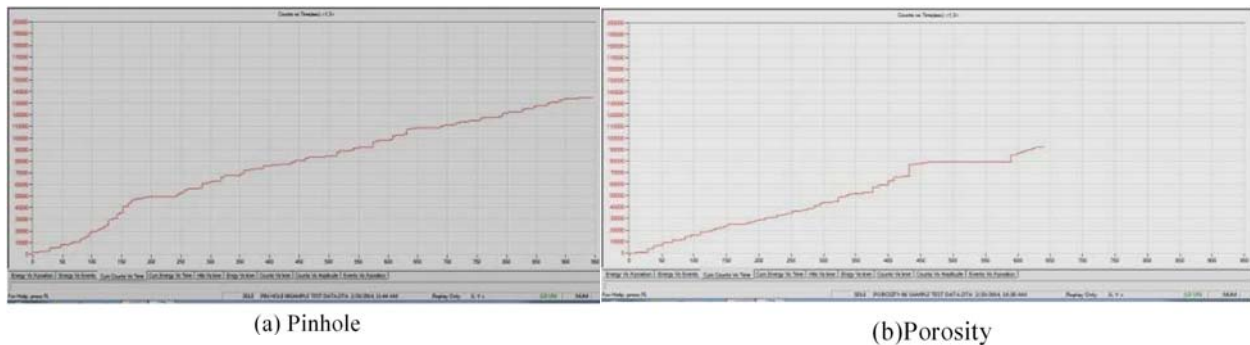


**Fig. 10.** SS 316L Materials showing Cumulative counts Vs Time corresponds to (a) and (b).

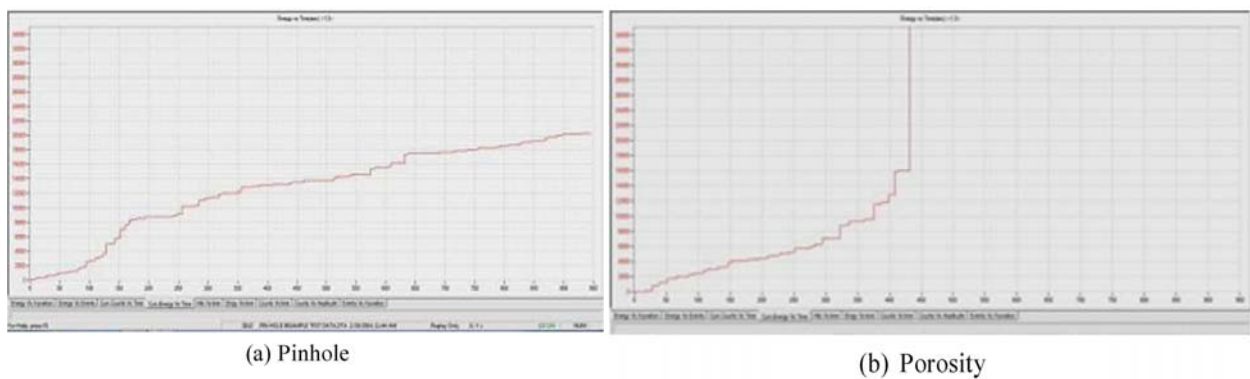


**Fig. 11.** SS 316L Materials showing Cumulative Energy Vs Time corresponds to (a) and (b).

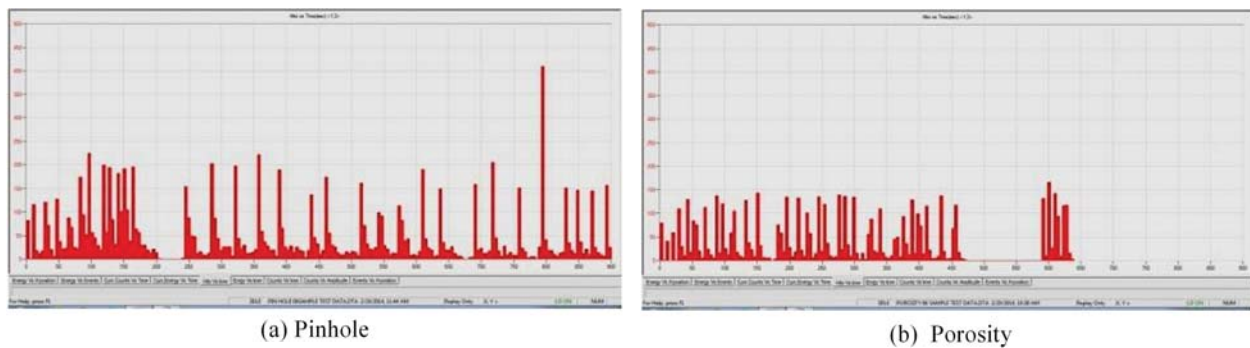
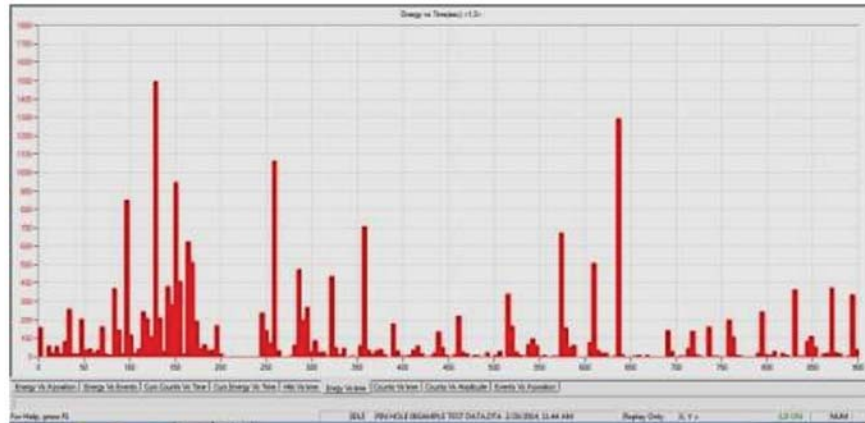


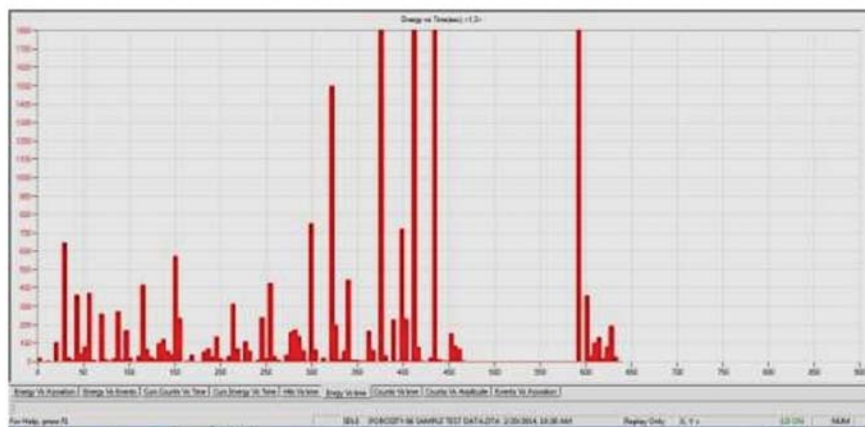
**Fig. 12.** SS 316L Materials showing Hits Vs Time corresponds to (a) and (b).

- E. **Energy Versus Time.** Pinhole and porosity defects recorded the highest energy in that order over time [Fig. 13].
- F. **Counts Versus Time** Samples with porosity defects showed the highest counts over time. Pinhole defects exhibited more counts than porosity defects [Fig. 14].
- G. **Counts Versus Amplitude.** This parameter showed distinct differences for different defects, making it reliable for segregating and characterizing defects alongside other parameters. It was evident that good samples recorded the least amplitudes, while defects like pinhole and porosity recorded the highest count amplitudes [Fig. 15].
- H. **Waveforms Versus Amplitude.** Waveforms were analyzed for selected events with high energy from two tested samples [Fig. 16]. These waveforms plotted amplitude versus time, revealing characteristic features unique to different defects.
- I. **Frequencies Versus Amplitude.** Similarly, amplitude versus frequency graphs showed differences among defects. Some defects exhibited higher frequencies with greater amplitude content than others [Fig. 17].

These observations provide detailed insights into the behavior of defects under testing conditions, highlighting their distinct characteristics in acoustic emission analysis.

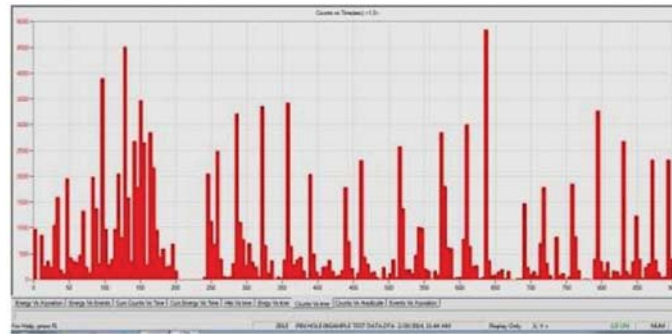


(a) Pinhole

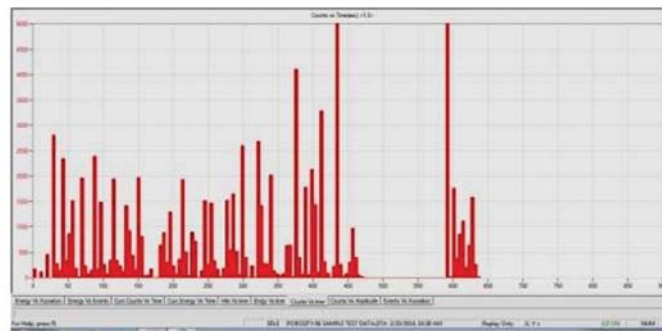


(b) Porosity

**Fig. 13.** SS 316L Materials showing Energy Vs Time corresponds to (a) and (b).

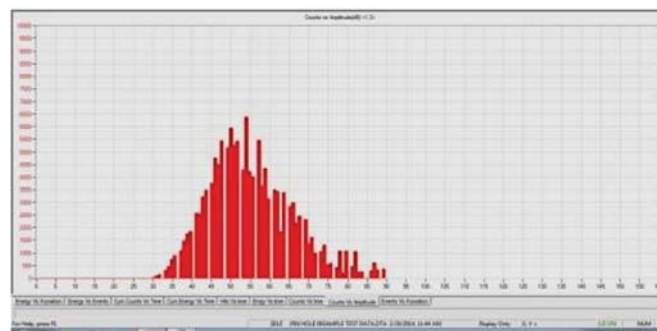


(a) Pinhole

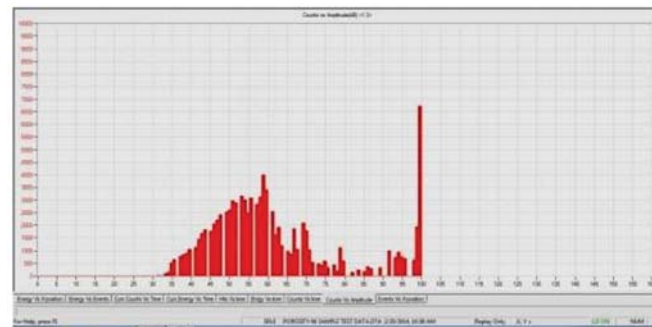


(b) Porosity

Fig. 14. SS 316L Materials showing counts Vs Time corresponds to (a) and (b).

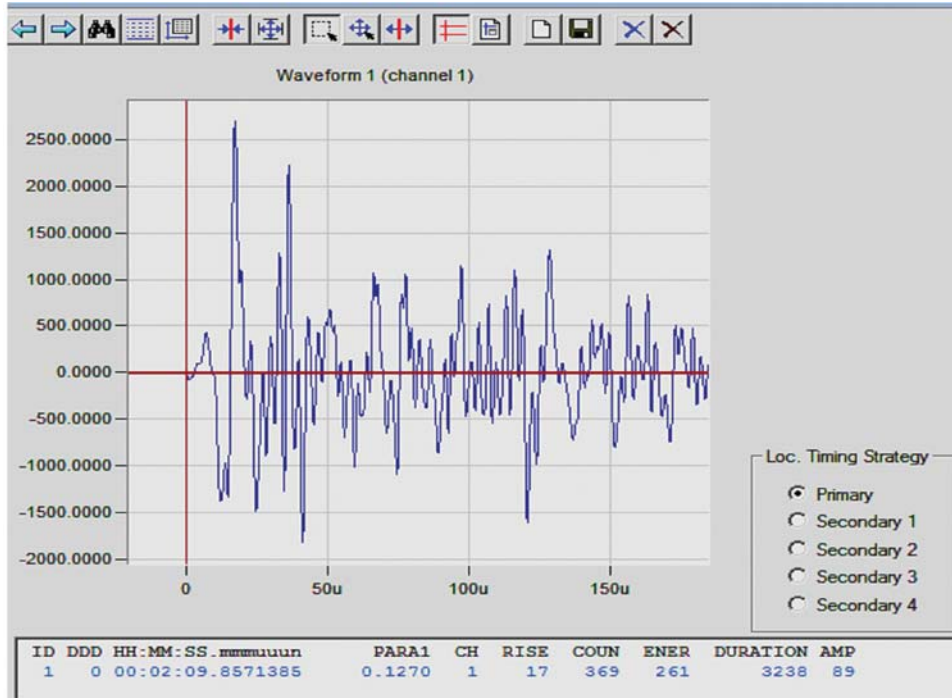


(a) Pinhole

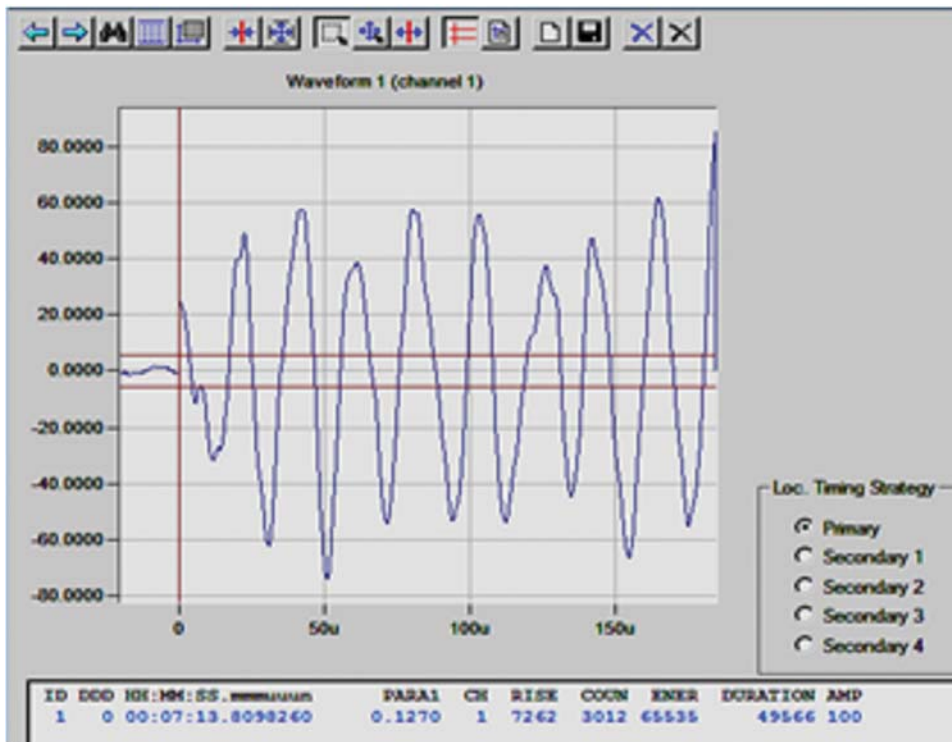


(b) Porosity

Fig. 15. SS 316L Materials showing Counts Vs amplitude corresponds to (a) and (b).

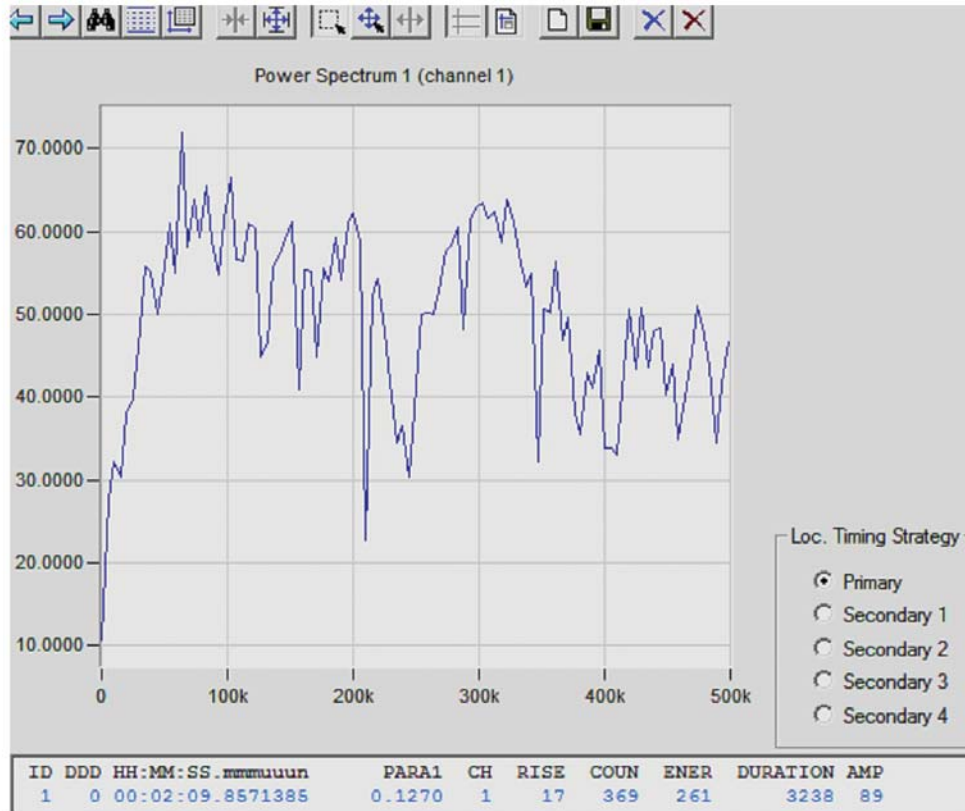


(a) Pinhole

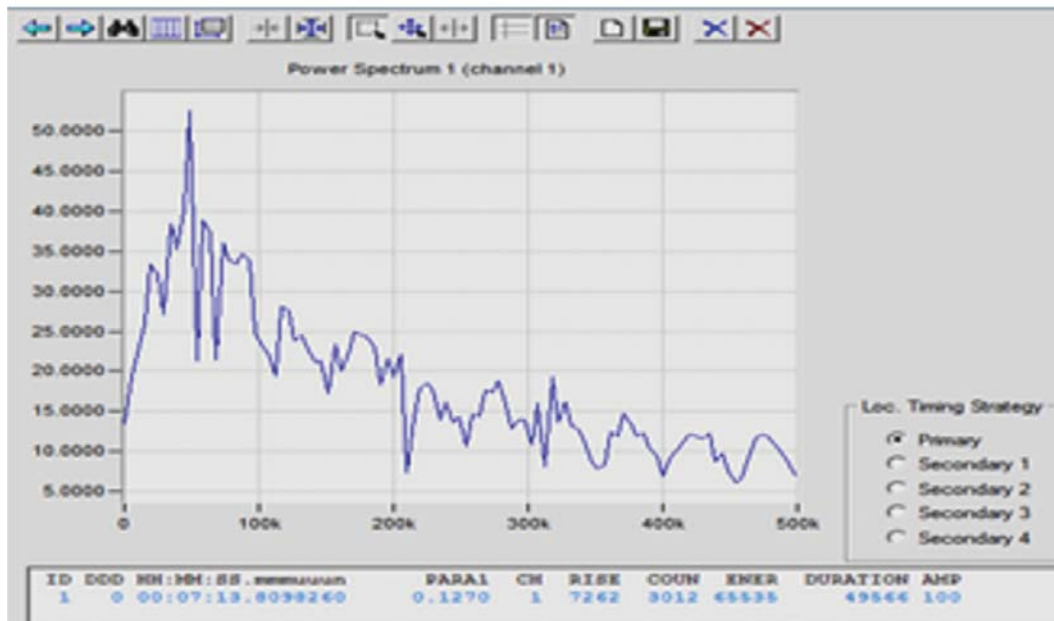


(b) Porosity

Fig. 16. SS 316L Materials showing amplitude Vs time corresponds to (a) and (b).



(a) Pinhole



(b) Porosity

Fig. 17. SS 316L Materials showing frequency Spectrum corresponds to (a) and (b).

## 10. CONCLUSION

Data analysis was conducted on various parameters obtained from testing two samples. Comparison of different AE parameters revealed distinct patterns based on the type of weld defects. It was observed that the "counts versus amplitude" parameter provided the most significant differentiation among defect types. Pinhole and porosity defects exhibited the highest expressions in this regard, showing the highest amplitudes in relation to both counts and event frequencies. These conclusions are drawn from analysis of only two samples.

## 11. ACKNOWLEDGMENT

The authors express gratitude to the members of the Board of Research in Fusion Science & Technology at the Institute for Plasma Research under the Department of Atomic Energy for their financial support (Project no: NFP-MATF12-01) for this project as part of the Nuclear Research Programme. Special thanks are also due to Dr. H S Saini, Managing Director, and Sardar G S Kohli, Vice Chairman, Guru Nanak Institutions, Ibrahimpatnam, for their cooperation and encouragement.

## 12. REFERENCES

- [1] Acoustic Emission Testing. Nondestructive testing handbook. 3<sup>rd</sup> ed., vol. 6. *American Society for Nondestructive Testing*; 2005.
- [2] Gregory C. McLaskey Steven D. Glaser, 2012. "Acoustic Emission Sensor calibration for Absolute Source measurements" *Journal of Nondestructive Evaluation*.
- [3] Baldev Raj and T. Jayakumar, 1990. Acoustic emission during tensile deformation and fracture of austenitic alloys. In: *Acoustic emission: current practices and future directions-ASTM STP 1077*. pp. 218e41.
- [4] C.S. Camerini, J.M.A. Rebello and S.D. Soares, 1992. Relationship between acoustic emission and CTOD testing for a structural steel. *NDT & E Int.* **25**, 127e33.
- [5] Seydou Dia, Thomas Monnier, Nathalie Godin and Fan Zhang, 2012. "Primary Calibration of Acoustic Emission Sensors by the Method of Reciprocity, Theoretical and Experimental Considerations" *30<sup>th</sup> European Conference on Acoustic Emission Testing & 7<sup>th</sup> International Conference on Acoustic Emission University of Granada*.
- [6] Andreas J. Brunner, Thomas Tannert and Till Vallee, 2010. "Waveform Analysis of Acoustic Emission Monitoring Of Tensile Tests on Welded Wood-Joints" *Journal of Acoustic Emission*, **28**, 59-67.
- [7] Jiri Kepert and Petr Benes, 2007. "Determination of Uncertainty in Calibration of Acoustic Emission Sensors" *4<sup>th</sup> international conference on NDT, chania-Greece*.
- [8] D.L. Armentrut and S.H. Carpenter. "An Investigation of Luders band deformation and the Associated Acoustic Emission in Al-4.5% Mg Alloys" *Journal of Acoustic Emission*, **15**(1-4), 43-51.
- [9] S.H. Carpenter, Kani on and D. Aentrut, 2006. "Acoustic Emission of Sensitized 304 Stainless Steel with Simultaneous Hydrogen charging" *Journal of Acoustic Emission*, **24**, 119-126.
- [10] Sotirios J. Vahaviolos. "Acoustic Emission standards and technology update" *ASTM STP 1353* pp-76-77.
- [11] Iri Keepert and petr Benes, 2008. "A comparison of AE sensor calibration methods" *Journal of Acoustic Emission*. **26**, 60-70.
- [12] D.M. Romrell. "Acoustic Emission weld monitoring of nuclear components" *Journal of Welding Research Supplement*, pp 81-92.
- [13] Standard Guide for Radiographic Examination ASTM E94 - 04(2010).
- [14] Standard Reference Radiographs for Steel Fusion Welds ASTM E390 - 11.

- [15] Standard Test Method for Classification of Film Systems for Industrial Radiography ASTM E1815 - 08(2013).
- [16] Standard Test Method for Radiographic Examination of Weldments ASTM E 1032.
- [17] Standard Guide to Obtainable ASTM Equivalent Penetrant Sensitivity for Radiography of Steel Plates 1/4 to 2 in. [6 to 51 mm] Thick with X Rays and 1 to 6 in. [25 to 152 mm] Thick with Cobalt-60, ASTM E 592.
- [18] P. Raasekhar, M.R. Bhat and C.R.L. Murthy C.phanira, T.Jayakumar and Baldev Raj, 2006. "Discrimination of Nuclear grade Steel Samples Subjected to Different heat Treatment Procedures based on Acoustic Emission (AE) data profiling a crack initiation" National Seminar n Non-Destructive Evaluation Dec.
- [19] Dirk Aljets, Alex Chong, Steve Wilcox and Karen Holford, 2010. "Acoustic Emission Source Location in Plate-Like Structures using a Closely Arranged Triangular Sensor Array" *Journal of Acoustic Emission*, **28**, 85-98.
- [20] George Varkey Strategic Electronics group "on-line processing of acoustic Emission Signals" awareness seminar on Digital Signal Processing (ASDSP-2003), Paper 7 pp. 1-12.
- [21] Gerd Manthei, 2010. "Characterization f Acoustic Emission Sensors" European conference on acoustic Emission testing, Venna.
- [22] C. Ennaceur, A. Lakshimi, C. Hervve, M. Ediouni and M. Cherfaui, 2004. "Acoustic Emission technique and potential difference ethd for Detecting the Different Stages of crack propagation in carbon and Stainless Steels" *Journal of Acoustic Emission*. **22**, 71-76.
- [23] C.K. Mukhopadhyay, K.K. Ray, T. Jayakumar and B. Raj, 2000. Acoustic emission stress intensity factor relations for tensile deformation of notched specimens of AISI type 304 stainless steel. *Mater Sci Eng A*; **293**, 137.
- [24] E976-10 "standard guide for determining the reproducibility of Acoustic Emission Sensor Response" ASTM international Standards.

# Ultrasonic investigation on the physicochemical behaviour of acidum lacticum homoeopathic dilutions at different temperatures by using acoustic, volumetric and viscometric methods

Anil Kumar Nain<sup>1\*</sup>, Neha Chaudhary<sup>2</sup>, Preeti Droliya<sup>3</sup>, Raj Kumar Manchanda<sup>4</sup>,  
Anil Khurana<sup>4</sup> and Debadatta Nayak<sup>4</sup>

<sup>1</sup>Department of Chemistry, Dyal Singh College, University of Delhi, New Delhi-110 003, India

<sup>2</sup>Department of Chemistry, Ramjas College, University of Delhi, Delhi-110 007, India

<sup>3</sup>Department of Chemistry, Miranda House, University of Delhi, Delhi-110 007, India

<sup>4</sup>Central Council for Research in Homeopathy, Ministry of AYUSH, New Delhi-110 058, India  
e-mail: ak\_nain@yahoo.co.in

[Received: 27-10-2024; Accepted: 25-01-2025]

## ABSTRACT

Ultrasonic investigations of homoeopathic medicines can deliver better evidence about the presence of medicine and understanding the interactions/mechanism of their action in high dilutions. The physicochemical behaviour of dilutions of acidum lacticum have been studied from the measurements of ultrasonic speeds,  $u$ , densities,  $\rho$  and viscosities,  $\eta$  of pure ethanol control (91% ethanol in water) and 33 dilutions of acidum lacticum with potencies ranging from 1C to 200C at temperatures ranging from 293.15 K to 318.15 K and at atmospheric pressure. Using the experimental data, a number of acoustic parameters, viz., the isentropic compressibilities,  $s$ , intermolecular free length,  $L_f$ , acoustic impedance,  $Z$ , relative association,  $R_A$ , relaxation time,  $\tau$ , ultrasonic absorption,  $\alpha/f^2$ , pseudo-Grüneisen parameter,  $\Gamma$ , deviations in isentropic compressibility,  $\Delta\kappa_s$ , deviations in intermolecular free length,  $L_f$ , deviations in acoustic impedance,  $\Delta Z$ , deviations in viscosity,  $\Delta\eta$  and deviations in pseudo-Grüneisen parameter,  $\Delta\Gamma$  have been evaluated. These parameters show strange behaviour at certain potencies of these homoeopathic dilutions. The results have been qualitatively conversed in terms of interactions of these acidum lacticum homoeopathic formulations. The results indicated that that even in extreme dilutions ( $\approx$  70C and 140C) the molecules of acidum lacticum may be present in these homoeopathic formulations.

## 1. INTRODUCTION

The ultrasonic speed and derived acoustic parameters have been found helpful in understanding the intermolecular interactions in liquids and solutions containing solutes (electrolytes, amino acids, carbohydrates, drugs, etc.) in aqueous and mixed-aqueous solvents<sup>[1-7]</sup>. These studies are useful in

understanding of solute-solvation/hydration behaviour of solute and preferential solvation of solute by the solvent<sup>[1-7]</sup>. As the homeopathic medicines are dilute solutions, their physical properties, viz., ultrasonic speed, density and viscosity can be measured at different concentration and temperature. Various acoustic parameters (evaluated from ultrasonic speed, density and viscosity) can provide valuable information regarding interactions/physicochemical behaviour and action of these homeopathic medicines.

Homeopathy is an alternative system of medicine recognized for its comprehensive healing approach, but it remains controversial due to two main reasons. Firstly, the preparation of homeopathic medicines involves ultra-high dilutions, raising questions about the presence of medicine at extreme dilutions; and secondly, the doubtfulness in biological activity of these homeopathic medicines in which the source drug is diluted beyond Avagadro's limit, *i.e.*, the highly diluted medicine might be similar to the solvent. There have been a few researches to reconnoiter the presence of medicine in ultra-diluted medicines<sup>[8-14]</sup> and its mechanism of action, but the question remains still unanswered. The homeopathic medicines are prepared using the potentization process, which involve a dilution of 1:100 followed by succussion (strokes) and these ultra-diluted solutions show anomalous behaviour in terms of medicinal efficacy when administered in practice. There have been few physicochemical studies on extremely diluted solutions of inorganic salts<sup>[15-18]</sup> and homeopathic medicines<sup>[11,19-22]</sup> by using conductometric and calorimetric methods. These studies provided interesting and convincing info on the behaviour of these extremely diluted solutions. To the best of our knowledge, very few physicochemical studies on homeopathic medicines using volumetric and acoustic methods have been reported in the literature<sup>[23,24]</sup>.

In continuation to our earlier research on the ultrasonic, volumetric and viscometric behaviour of extremely diluted homeopathic formulations<sup>[25-28]</sup>, here we report the results of the ultrasonic study on the physicochemical behaviour of homeopathic dilutions of acidum lacticum. Acidum lacticum is a homeopathic medicine prepared by potentization of lactic acid and it is a remedy used for treating variety of medical problems, viz., helps in treating morning sickness; cures troubles in breasts; treats conditions pertaining to vocal cords; heals pain; swelling; stiffness and tenderness of the joints; useful in nausea and vomiting; manages blood sugar levels; aids anemia and paleness and also treats the problem of excessive urination.

In the present study, the ultrasonic speeds,  $u$ , densities,  $\rho$  and viscosities,  $\eta$  of pure ethanol control (91% ethanol in water) and 33 formulations of acidum lacticum with potencies ranging from 1C to 200C (with intervals of 2C till 30C, and thereafter with intervals of 10C till 200C) at 293.15, 298.15, 303.15, 308.15, 313.15 and 318.15 K and at atmospheric pressure. Using these experimental data, the isentropic compressibilities,  $\kappa_s$ , intermolecular free length,  $L_f$ , acoustic impedance,  $Z$ , relative association,  $R_A$ , relaxation time,  $\tau$ , ultrasonic absorption,  $\alpha/f^2$ , pseudo-Grüneisen parameter,  $\Gamma$ , deviations in isentropic compressibility,  $\Delta\kappa_s$ , deviations in intermolecular free length,  $\Delta L_f$ , deviations in acoustic impedance,  $\Delta Z$ , deviations in viscosity,  $\Delta\eta$  and deviations in pseudo-Grüneisen parameter,  $\Delta\Gamma$  have been evaluated. The results have been discussed qualitatively in terms of interactions/physicochemical behaviour of acidum aceticum in these homeopathic formulations.

## 2. EXPERIMENTAL

The homeopathic formulations of various potencies of acidum lacticum used in the present study were procured from Dr. Wilmer Schwabe India Pvt. Limited, India. The medicines were prepared in accordance with Homoeopathic Pharmacopoeia of India<sup>[29]</sup>. The ethanol control (91% ethanol in water) was prepared by using the ethanol (mass fraction purity, 0.998, E. Merck, India) and triply distilled water. The ultrasonic speeds and densities of the homeopathic dilutions were measured using a highly precise digital vibrating tube Density and Sound Analyzer (DSA 5000M, Anton Paar, Austria). The ultrasonic speed measurements were done using propagation time technique, while the density measurements were based upon oscillating U-tube principle. This instrument is equipped with both ultrasonic and density cells, with reproducibility of  $\pm 1 \times 10^{-2}$  m.s<sup>-1</sup> and  $\pm 1 \times 10^{-3}$  kg.m<sup>-3</sup> for ultrasonic speed and density,

respectively. The temperature for both cells was kept constant by using built in Peltier thermostat within 0.01 K. The equipment was calibrated with triply distilled degassed water and dry air at atmospheric pressure<sup>[5,6]</sup>. The operating working frequency used for ultrasonic speed measurements is 3 MHz. The standard uncertainties related to the measurements of ultrasonic speed, density, and temperature were found within  $\pm 0.5 \text{ m.s}^{-1}$ ,  $\pm 0.05 \text{ kg.m}^{-3}$  and  $\pm 0.01 \text{ K}$ , respectively.

The viscosity of the homoeopathic dilutions was measured by using microviscometer (LOVIS 2000M, Anton Paar, Austria) at temperatures, (293.15 – 318.15) K, and atmospheric pressure  $p = 101 \text{ kPa}$ . The temperature was controlled to  $\pm 0.02 \text{ K}$  by an automatic built in Peltier technique. The rolling ball principle was used in the measurement of viscosity, having a calibrated glass capillary with a steel ball as supplied by manufacturer. The calibration of capillary was accomplished by using viscosity standard fluids. The standard uncertainties for viscosity measurements and temperature were estimated to be within  $\pm 0.5\%$  and  $\pm 0.02 \text{ K}$ .

### 3. RESULTS AND DISCUSSION

The values of densities,  $\rho$ , ultrasonic speeds,  $u$  and viscosities,  $\eta$  of homoeopathic formulations of acidum lacticum as function of potency (in centesimal) at different temperatures are listed in Tables 1-3, and are presented graphically in Figs. 1-3, respectively. A close inspection of Tables 1-3 and Figs. 1-3 specifies that the values of  $u$ ,  $\rho$  and  $\eta$  of acidum lacticum in ethanol control are more than those of pure ethanol control for all the 33 potencies at each investigated temperature and these values decrease with increase in temperature. The values of  $u$ ,  $\rho$  and  $\eta$  are maximum at 1C and then decrease significantly due presence of acidum lacticum on successive dilution to the potency 2C and after that these values increase up to potency 4C and then decrease to exhibit minimum from 6C to 8C and thereafter these values increase to exhibit maximum from 10C to 12C and then decrease up to 14C. After 14C potency these values remain constant till 200C potency, except for potencies 70C and 140C where the values of  $u$ ,  $\rho$  and  $\eta$  exhibit maximum (Figs. 1-3). The observed odd trends (maximum) in  $u$ ,  $\rho$  and  $\eta$  values at some potencies, viz., 1C, 4C, 10C, 12C, 70C and 140C, specify that these potencies show different solution structure as compared to other potencies and pure ethanol control.

The values of the isentropic compressibility,  $\kappa_s$ , intermolecular free length,  $L_f$ , acoustic impedance,  $Z$ , relative association,  $R_A$ , relaxation time,  $\tau$ , ultrasonic absorption,  $(\alpha/f^2)$  and pseudo-Grüneisen parameter, have been calculated by using the following relations<sup>[25,30-35]</sup>.

$$\kappa_s = 1/u^2 \rho \quad (1)$$

$$L_f = K'/u\rho^{1/2} \quad (2)$$

$$Z = u.\rho \quad (3)$$

$$R_A = (\rho / \rho_o)(u_o / u)^{1/3} \quad (4)$$

$$\tau = (4/3) / \kappa_s \eta \quad (5)$$

$$(\alpha/f^2) = 8\pi^2 \eta / 3\rho u^3 \quad (6)$$

$$\Gamma = \alpha_p / \kappa_T \quad (7)$$

where  $K'$  is temperature dependent constant [=  $(93.875 + 0.375T) \times 10^{-8}$ ];  $T$  is the absolute temperature;  $\rho_o$  and  $u_o$  are the density and ultrasonic speed of the ethanol control, respectively;  $\alpha_p$  is the isobaric expansivity and  $\kappa_T$  is the isothermal compressibility. The values of  $\alpha_p$  and  $\kappa_T$  are calculated using the relations<sup>[35,36]</sup>.

**Table 1.** The densities,  $\rho$ /(kg m<sup>-3</sup>) of ethanol control (0 potency, 91% ethanol in water) and 33 dilutions of acidum lacticum in ethanol control as function of potency, C of acidum lacticum (in centesimal) at the temperatures (293.15-318.15) K and atmospheric pressure.

Potency (C)	T/K					
	293.15	298.15	303.15	308.15	313.15	318.15
0	808.248	804.277	800.155	796.005	791.621	787.436
1	918.778	914.821	910.792	906.694	902.530	898.297
2	829.109	824.762	820.361	815.903	811.386	806.803
4	830.355	825.612	821.034	816.387	812.034	807.812
6	827.595	823.243	818.838	814.375	809.855	805.270
8	827.640	823.286	818.885	814.430	809.913	805.334
10	829.811	825.520	821.436	817.122	812.465	807.984
12	829.798	825.591	821.523	817.167	812.552	808.022
14	827.527	823.184	819.078	814.319	809.801	805.218
16	827.628	823.272	818.872	814.417	809.900	805.321
18	827.664	823.311	818.909	814.456	809.941	805.359
20	827.601	823.211	818.824	814.400	809.801	805.200
22	827.544	823.198	818.799	814.341	809.826	805.248
24	827.606	823.259	818.856	814.356	809.879	805.300
26	827.708	823.371	818.957	814.254	809.920	805.408
28	827.583	823.231	818.825	814.368	809.852	805.393
30	827.726	823.373	818.970	814.512	809.994	805.417
40	827.994	823.543	819.324	814.532	810.112	805.622
50	828.055	823.700	819.292	814.539	810.322	805.742
60	828.167	823.811	819.405	814.947	810.430	805.850
70	831.447	827.494	823.093	818.639	814.122	809.543
80	828.071	823.715	819.309	814.854	810.341	805.763
90	828.338	823.985	819.579	815.121	810.603	806.026
100	828.114	823.759	819.353	814.895	810.381	805.803
110	828.445	824.090	819.691	815.235	810.717	806.138
120	828.503	824.152	819.747	815.292	810.777	806.203
130	828.503	824.152	819.747	815.292	810.977	806.203
140	831.404	827.057	822.745	818.088	813.568	809.289
150	828.865	824.509	820.101	815.643	811.128	806.546
160	828.499	824.145	819.739	815.282	810.644	806.365
170	828.532	824.178	819.774	815.317	810.797	806.224
180	828.611	824.245	819.886	815.455	810.888	806.344
190	828.877	824.440	819.998	815.736	810.877	806.555
200	829.008	824.474	819.988	815.731	811.016	806.436

$$\alpha_p = (-1/\rho)(\partial\rho/\partial T)_p \quad (8)$$

$$k_T = (1.71 \times 10^{-3}) / (T^{4/9} u^2 \rho^{4/3}) \quad (9)$$

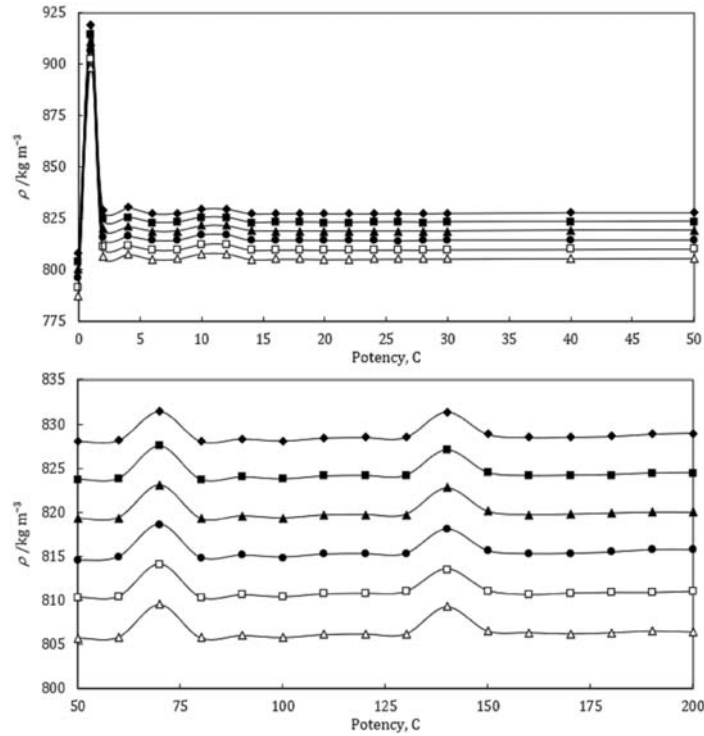


Fig. 1. Plots of densities,  $\rho$  vs. potency,  $C$  of acidum lacticum for homoeopathic dilutions of acidum lacticum at temperatures, 293.15 K,  $\blacklozenge$ ; 298.15 K,  $\blacksquare$ ; and 303.15 K,  $\blacktriangle$ ; 308.15 K,  $\bullet$ ; 313.15 K,  $\circ$ ; and 318.15 K,  $\triangle$ .

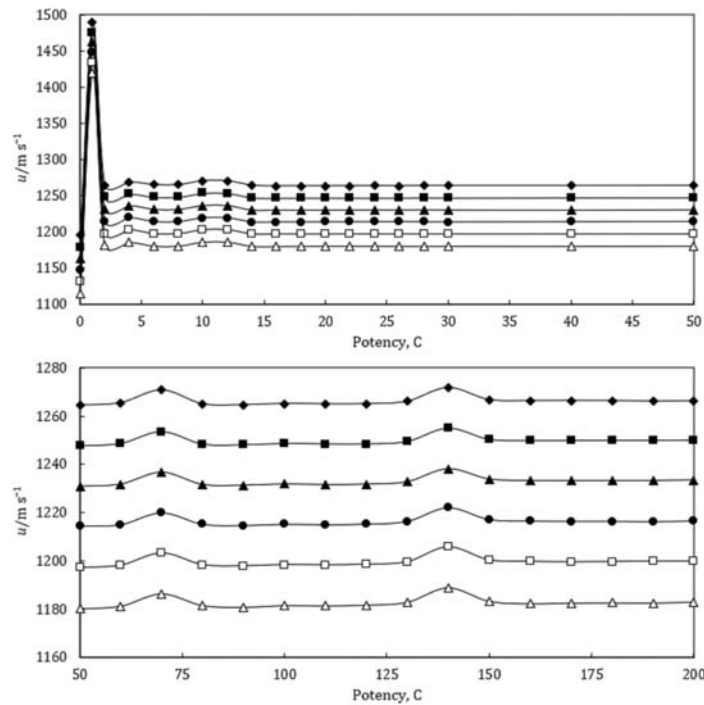


Fig. 2. Plots of ultrasonic speeds,  $u$  vs. potency,  $C$  of acidum lacticum for homoeopathic dilutions of acidum lacticum at temperatures, 293.15 K,  $\blacklozenge$ ; 298.15 K,  $\blacksquare$ ; and 303.15 K,  $\blacktriangle$ ; 308.15 K,  $\bullet$ ; 313.15 K,  $\circ$ ; and 318.15 K,  $\triangle$ .

**Table 2.** The ultrasonic speeds,  $u/(m\ s^{-1})$  of ethanol control (0 potency, 91% ethanol in water) and 33 dilutions of acidum lacticum in ethanol control as function of potency, C of acidum lacticum (in centesimal) at the temperatures (293.15-318.15) K and atmospheric pressure.

Potency (C)	T/K					
	293.15	298.15	303.15	308.15	313.15	318.15
0	1195.93	1179.76	1163.54	1147.33	1131.38	1114.91
1	1489.20	1476.19	1462.66	1448.85	1434.77	1420.43
2	1264.69	1248.38	1231.72	1214.95	1198.13	1181.25
4	1269.27	1253.12	1236.66	1219.94	1203.00	1185.83
6	1265.52	1248.56	1231.44	1214.34	1197.48	1180.36
8	1265.46	1248.49	1231.39	1214.31	1197.43	1180.42
10	1270.85	1254.05	1236.76	1219.59	1203.08	1186.12
12	1270.71	1253.91	1236.71	1219.53	1203.04	1186.11
14	1264.65	1247.86	1230.43	1213.95	1197.13	1180.17
16	1263.72	1247.28	1230.64	1213.95	1197.08	1180.03
18	1263.82	1247.37	1230.61	1213.88	1197.03	1180.13
20	1263.86	1247.44	1230.68	1214.02	1197.21	1180.32
22	1263.87	1247.42	1230.70	1214.02	1197.17	1180.29
24	1263.99	1247.41	1230.79	1214.10	1197.26	1180.25
26	1263.87	1247.42	1230.75	1214.25	1197.14	1180.13
28	1264.10	1247.71	1230.93	1214.03	1197.21	1180.10
30	1264.15	1247.52	1230.74	1213.93	1197.09	1180.20
40	1264.34	1247.76	1230.58	1214.11	1197.25	1180.17
50	1264.53	1247.80	1230.93	1214.44	1197.31	1180.33
60	1265.53	1248.68	1231.83	1215.03	1198.20	1181.31
70	1270.83	1253.60	1236.73	1219.93	1203.27	1186.42
80	1265.01	1248.39	1231.64	1215.17	1198.41	1181.57
90	1264.69	1248.14	1231.37	1214.68	1197.95	1180.87
100	1265.20	1248.67	1231.87	1215.20	1198.47	1181.54
110	1265.04	1248.50	1231.62	1215.00	1198.34	1181.41
120	1265.10	1248.49	1231.80	1215.26	1198.60	1181.75
130	1266.10	1249.49	1232.80	1216.36	1199.60	1182.90
140	1271.80	1255.04	1238.18	1222.04	1205.81	1188.94
150	1266.79	1250.38	1233.93	1217.16	1200.39	1183.34
160	1266.38	1249.86	1233.30	1216.53	1199.76	1182.31
170	1266.43	1249.88	1233.18	1216.43	1199.59	1182.61
180	1266.37	1249.92	1233.25	1216.43	1199.69	1182.67
190	1266.23	1249.90	1233.31	1216.30	1199.88	1182.62
200	1266.30	1250.10	1233.53	1216.56	1199.92	1182.96

The values of  $\kappa_s$ ,  $L_f$ ,  $Z$ ,  $R_A$ ,  $\tau$ ,  $(\alpha/f^2)$  and  $\Gamma$  are given in Tables 4-10. The deviations in  $\kappa_s$ ,  $L_f$ ,  $Z$ ,  $\eta$  and  $\Gamma$  of ethanol control due to addition of acidum lacticum with dilution and succussion are signified by the deviation in the values of these properties. The deviations in isentropic compressibility,  $\Delta\kappa_s$ , deviations in intermolecular free length,  $\Delta L_f$ , deviations in acoustic impedance,  $\Delta Z$ , deviations in pseudo-Grüneisen parameter,  $\Delta\Gamma$  and deviations in viscosity,  $\Delta\eta$  have been calculated by using the following relations<sup>[25,28]</sup>.

**Table 3.** The viscosities,  $\eta/(10^{-3} \text{ N s m}^{-2})$  of ethanol control (0 potency, 91% ethanol in water) and 33 dilutions of acidum lacticum in ethanol control as function of potency, C of acidum lacticum (in centesimal) at the temperatures (293.15-318.15) K and atmospheric pressure.

Potency (C)	T/K					
	293.15	298.15	303.15	308.15	313.15	318.15
0	1.4935	1.3239	1.1844	1.0616	0.9548	0.8677
1	2.5696	2.2605	1.9851	1.7419	1.5131	1.3147
2	1.8022	1.5933	1.4081	1.2521	1.1194	1.0061
4	1.8414	1.6285	1.4549	1.3020	1.1645	1.0452
6	1.7759	1.5693	1.3998	1.2485	1.1155	1.0056
8	1.7530	1.5498	1.3825	1.2355	1.1104	1.0028
10	1.7942	1.5880	1.4165	1.2691	1.1382	1.0308
12	1.7967	1.5885	1.4181	1.2698	1.1395	1.0314
14	1.7598	1.5520	1.3836	1.2352	1.1093	0.9988
16	1.7573	1.5523	1.3832	1.2341	1.1058	0.9972
18	1.7572	1.5524	1.3828	1.2359	1.1066	0.9976
20	1.7578	1.5534	1.3826	1.2365	1.1062	0.9985
22	1.7583	1.5533	1.3829	1.2359	1.1067	0.9982
24	1.7578	1.5536	1.3826	1.2355	1.1064	0.9976
26	1.7568	1.5530	1.3824	1.2358	1.1068	0.9970
28	1.7563	1.5528	1.3828	1.2352	1.1065	0.9971
30	1.7572	1.5535	1.3824	1.2355	1.1055	0.9956
40	1.7566	1.5533	1.3829	1.2352	1.1057	0.9964
50	1.7564	1.5538	1.3824	1.2349	1.1056	0.9967
60	1.7578	1.5556	1.3834	1.2365	1.1066	0.9972
70	1.7867	1.5845	1.4164	1.2669	1.1355	1.0222
80	1.7566	1.5549	1.3866	1.2380	1.1084	0.9983
90	1.7568	1.5539	1.3862	1.2369	1.1078	0.9986
100	1.7561	1.5551	1.3865	1.2367	1.1082	0.9987
110	1.7568	1.5543	1.3867	1.2369	1.1083	0.9984
120	1.7571	1.5551	1.3874	1.2373	1.1081	0.9979
130	1.7576	1.5554	1.3874	1.2379	1.1091	0.9989
140	1.7976	1.5953	1.4248	1.2748	1.1408	1.0297
150	1.7593	1.5550	1.3879	1.2376	1.1085	0.9999
160	1.7598	1.5547	1.3874	1.2370	1.1083	0.9997
170	1.7604	1.5546	1.3869	1.2373	1.1087	0.9994
180	1.7600	1.5541	1.3874	1.2374	1.1086	0.9998
190	1.7597	1.5546	1.3870	1.2375	1.1088	0.9997
200	1.7591	1.5543	1.3875	1.2379	1.1092	0.9996

$$\Delta\kappa_s = \kappa_s - \kappa_s^0 \quad (10)$$

$$\Delta L_f = L_f - L_f^0 \quad (11)$$

$$\Delta Z = Z - Z^0 \quad (12)$$

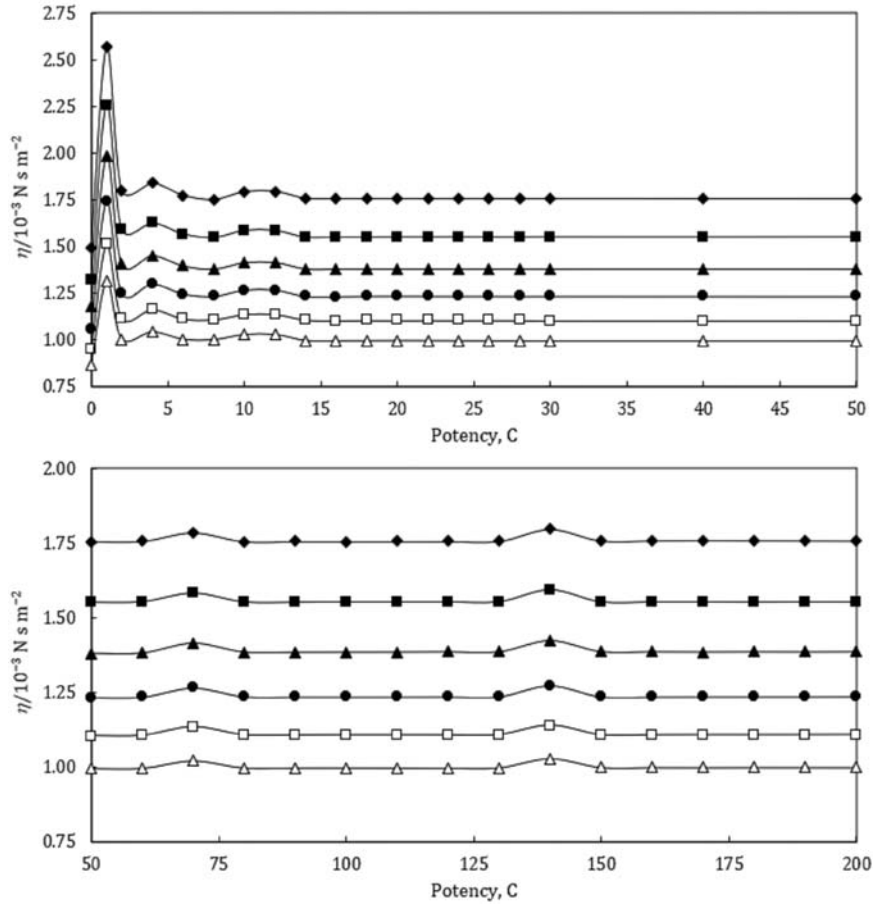


**Fig. 3.** Plots of viscosities,  $\eta$  vs. potency,  $C$  of acidum lacticum for homoeopathic dilutions of acidum lacticum at temperatures, 293.15 K,  $\diamond$ ; 298.15 K,  $\blacksquare$ ; and 303.15 K,  $\blacktriangle$ ; 308.15 K,  $\bullet$ ; 313.15 K,  $\bullet$ ; and 318.15 K,  $\triangle$ .

$$\Delta\eta = \eta - \eta^{\circ} \quad (13)$$

$$\Delta\Gamma = \Gamma - \Gamma^{\circ} \quad (14)$$

where the superscript 'o' represents the values for pure ethanol control (91% ethanol in water). The variations of  $\Delta\kappa_s$ ,  $\Delta L_f$ ,  $\Delta Z$ ,  $\Delta\eta$ ,  $\tau$ ,  $(\alpha/f^2)$  and  $\Delta\Gamma$  with potency,  $C$  of acidum lacticum and temperature are presented graphically in Figs. 4-10, respectively.

A close perusal of Tables 4 and 5 indicate that the values of  $\kappa_s$  and  $L_f$  for acidum lacticum potencies are less than those of ethanol controls for all the potencies at each investigated temperature and these values increase with increase in temperature, which indicates significant interaction between acidum lacticum and ethanol-water molecules. These variations in  $\kappa_s$  and  $L_f$  are expressed in terms of deviations in isentropic compressibility,  $\Delta\kappa_s$  and deviations in intermolecular free length,  $\Delta L_f$  and are shown graphically in Figs. 4 and 5. Figures 4 and 5 indicate that the values of  $\Delta\kappa_s$  and  $\Delta L_f$  are negative and these values are minimum at 1C and then increase significantly due presence of acidum lacticum on successive dilution to the potency 2C and after that these values decrease up to potency 4C and then increase to exhibit maximum from 6C to 8C and thereafter these values decrease to exhibit minimum from 10C to 12C and then increase up to 14C. After 14C potency these values remain constant till 200C potency, except for potencies 70C and 140C where the values of  $\Delta\kappa_s$  and  $\Delta L_f$  exhibit minimum (Figs. 4 and 5). The minimum in  $\Delta\kappa_s$  and  $\Delta L_f$  values at potencies 1C, 4C, 10C, 12C, 70C and 140C indicate that these have more compact

**Table 4.** Isentropic compressibilities,  $\kappa_s/(10^{-10} \text{ m}^2 \text{ N}^{-1})$  of ethanol control (0 potency, 91% ethanol in water) and 33 dilutions of acidum lacticum in ethanol control as function of potency, C of acidum lacticum (in centesimal) at the temperatures (293.15-318.15) K and atmospheric pressure.

Potency (C)	T/K					
	293.15	298.15	303.15	308.15	313.15	318.15
0	8.6506	8.9332	9.2313	9.5435	9.8688	10.2166
1	4.9078	5.0163	5.1321	5.2540	5.3824	5.5175
2	7.5408	7.7800	8.0347	8.3032	8.5855	8.8828
4	7.4753	7.7133	7.9641	8.2305	8.5093	8.8033
6	7.5447	7.7921	8.0533	8.3271	8.6111	8.9131
8	7.5450	7.7925	8.0535	8.3270	8.6112	8.9115
10	7.4616	7.7027	7.9589	8.2278	8.5037	8.7971
12	7.4634	7.7038	7.9587	8.2282	8.5033	8.7968
14	7.5557	7.8014	8.0642	8.3330	8.6167	8.9166
16	7.5659	7.8078	8.0635	8.3320	8.6163	8.9175
18	7.5644	7.8063	8.0635	8.3326	8.6166	8.9156
20	7.5645	7.8064	8.0634	8.3313	8.6155	8.9145
22	7.5649	7.8068	8.0634	8.3319	8.6158	8.9144
24	7.5629	7.8063	8.0617	8.3306	8.6140	8.9144
26	7.5634	7.8051	8.0612	8.3296	8.6153	8.9151
28	7.5618	7.8028	8.0601	8.3314	8.6150	8.9157
30	7.5599	7.8038	8.0612	8.3313	8.6152	8.9139
40	7.5552	7.7992	8.0598	8.3287	8.6116	8.9121
50	7.5524	7.7972	8.0555	8.3241	8.6085	8.9083
60	7.5394	7.7852	8.0427	8.3118	8.5946	8.8924
70	7.4472	7.6898	7.9433	8.2080	8.4837	8.7757
80	7.5465	7.7897	8.0461	8.3109	8.5925	8.8894
90	7.5479	7.7903	8.0470	8.3148	8.5964	8.8971
100	7.5438	7.7858	8.0427	8.3100	8.5913	8.8894
110	7.5427	7.7848	8.0426	8.3093	8.5896	8.8877
120	7.5415	7.7844	8.0397	8.3052	8.5852	8.8819
130	7.5296	7.7719	8.0267	8.2902	8.5688	8.8646
140	7.4362	7.6763	7.9281	8.1852	8.4537	8.7413
150	7.5181	7.7575	8.0085	8.2757	8.5559	8.8542
160	7.5263	7.7674	8.0202	8.2879	8.5700	8.8717
170	7.5254	7.7668	8.0215	8.2889	8.5708	8.8687
180	7.5254	7.7657	8.0194	8.2875	8.5684	8.8665
190	7.5246	7.7641	8.0176	8.2865	8.5658	8.8649
200	7.5226	7.7613	8.0148	8.2830	8.5638	8.8611

solution structure as compared to other potencies, hence, these potencies might show diverse behaviour in terms of properties and efficacy when used in treatment.

A close examination of Table 6 specifies that the acoustic impedances, Z of potencies of acidum lacticum are more than those of ethanol control for all the potencies at each investigated temperature and

**Table 5.** Intermolecular free lengths,  $L_f(10^{-10} \text{ m})$  of ethanol control (0 potency, 91% ethanol in water) and 33 dilutions of acidum lacticum in ethanol control as function of potency, C of acidum lacticum (in centesimal) at the temperatures (293.15-318.15) K.

Potency (C)	T/K					
	293.15	298.15	303.15	308.15	313.15	318.15
0	5.9943	6.1475	6.3062	6.4699	6.6381	6.8140
1	4.5150	4.6066	4.7020	4.8005	4.9023	5.0075
2	5.5966	5.7370	5.8833	6.0348	6.1915	6.3537
4	5.5723	5.7123	5.8574	6.0083	6.1640	6.3252
6	5.5981	5.7414	5.8901	6.0435	6.2007	6.3645
8	5.5982	5.7416	5.8902	6.0435	6.2007	6.3639
10	5.5672	5.7084	5.8555	6.0074	6.1619	6.3229
12	5.5678	5.7088	5.8554	6.0075	6.1618	6.3228
14	5.6022	5.7449	5.8941	6.0457	6.2027	6.3657
16	5.6059	5.7472	5.8938	6.0453	6.2026	6.3661
18	5.6054	5.7467	5.8938	6.0455	6.2027	6.3654
20	5.6054	5.7467	5.8938	6.0450	6.2023	6.3650
22	5.6056	5.7468	5.8938	6.0452	6.2024	6.3650
24	5.6048	5.7467	5.8932	6.0448	6.2017	6.3650
26	5.6050	5.7462	5.8930	6.0444	6.2022	6.3652
28	5.6044	5.7454	5.8926	6.0451	6.2021	6.3654
30	5.6037	5.7458	5.8930	6.0450	6.2022	6.3648
40	5.6020	5.7441	5.8925	6.0441	6.2009	6.3641
50	5.6009	5.7433	5.8909	6.0424	6.1998	6.3628
60	5.5961	5.7389	5.8862	6.0380	6.1948	6.3571
70	5.5618	5.7037	5.8497	6.0001	6.1547	6.3153
80	5.5987	5.7406	5.8875	6.0376	6.1940	6.3560
90	5.5992	5.7408	5.8878	6.0390	6.1954	6.3588
100	5.5977	5.7391	5.8862	6.0373	6.1936	6.3560
110	5.5973	5.7388	5.8862	6.0370	6.1930	6.3554
120	5.5969	5.7386	5.8851	6.0355	6.1914	6.3533
130	5.5925	5.7340	5.8804	6.0301	6.1855	6.3472
140	5.5577	5.6986	5.8441	5.9918	6.1438	6.3029
150	5.5882	5.7287	5.8737	6.0248	6.1808	6.3434
160	5.5912	5.7323	5.8780	6.0293	6.1859	6.3497
170	5.5909	5.7321	5.8784	6.0296	6.1862	6.3486
180	5.5909	5.7317	5.8777	6.0291	6.1853	6.3478
190	5.5906	5.7311	5.8770	6.0287	6.1844	6.3473
200	5.5899	5.7301	5.8760	6.0275	6.1837	6.3459

the values decrease with increase in temperature, which indicates significant interaction between acidum lacticum and ethanol-water molecules. These variations in Z are expressed in terms of deviations in acoustic impedance, Z and are shown in Fig. 6. Figure 6 indicates that  $\Delta Z$  values are positive, *i.e.*, Z values for acidum lacticum potencies are more than those of ethanol control. These  $\Delta Z$  values are maximum at 1C

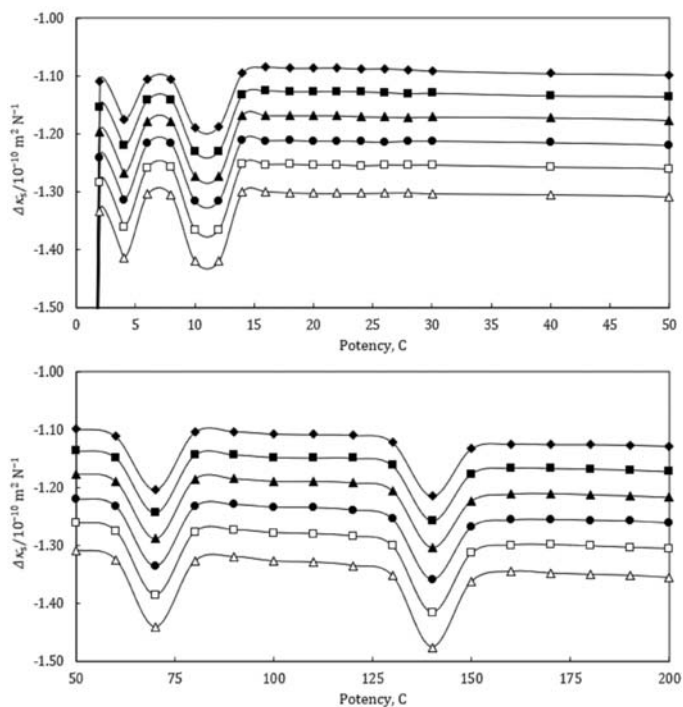


**Fig. 4.** Plots of deviations in isentropic compressibilities,  $\Delta\kappa_s$  vs. potency,  $C$  of acidum lacticum for homeopathic dilutions of acidum lacticum at temperatures, 293.15 K,  $\blacklozenge$ ; 298.15 K,  $\blacksquare$ ; and 303.15 K,  $\blacktriangle$ ; 308.15 K,  $\bullet$ ; 313.15 K,  $\bullet$ ; and 318.15 K,  $\triangle$ .

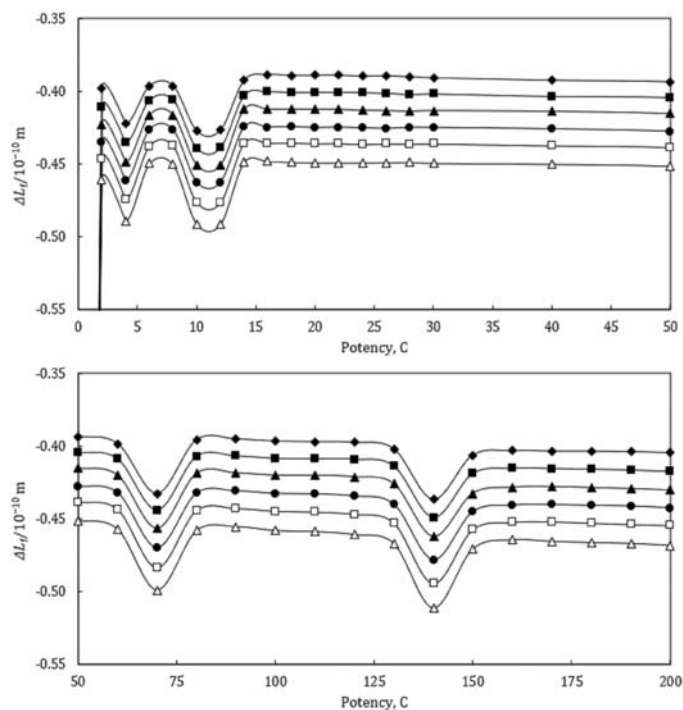


**Fig. 5.** Plots of deviations in intermolecular free length,  $\Delta L_f$  vs. potency,  $C$  of acidum lacticum for homeopathic dilutions of acidum lacticum at temperatures, 293.15 K,  $\blacklozenge$ ; 298.15 K,  $\blacksquare$ ; and 303.15 K,  $\blacktriangle$ ; 308.15 K,  $\bullet$ ; 313.15 K,  $\bullet$ ; and 318.15 K,  $\triangle$ .

**Table 6.** Specific acoustic impedances,  $Z/(10^5 \text{ kg m}^{-2} \text{ s}^{-1})$  of ethanol control (0 potency, 91% ethanol in water) and 33 dilutions of acidum lacticum in ethanol control as function of potency, C of acidum lacticum (in centesimal) at the temperatures (293.15-318.15) K.

Potency (C)	T/K					
	293.15	298.15	303.15	308.15	313.15	318.15
0	9.6661	9.4885	9.3101	9.1328	8.9562	8.7792
1	13.6824	13.5045	13.3218	13.1366	12.9492	12.7597
2	10.4857	10.2962	10.1046	9.9128	9.7215	9.5304
4	10.5394	10.3459	10.1534	9.9594	9.7688	9.5793
6	10.4734	10.2787	10.0835	9.8893	9.6979	9.5051
8	10.4735	10.2786	10.0837	9.8897	9.6981	9.5063
10	10.5457	10.3524	10.1592	9.9655	9.7746	9.5837
12	10.5443	10.3522	10.1599	9.9656	9.7753	9.5840
14	10.4653	10.2722	10.0782	9.8854	9.6944	9.5029
16	10.4589	10.2685	10.0774	9.8866	9.6952	9.5030
18	10.4602	10.2697	10.0776	9.8865	9.6952	9.5043
20	10.4597	10.2691	10.0771	9.8870	9.6950	9.5039
22	10.4591	10.2687	10.0770	9.8863	9.6950	9.5043
24	10.4609	10.2694	10.0784	9.8871	9.6964	9.5046
26	10.4612	10.2709	10.0793	9.8871	9.6959	9.5049
28	10.4615	10.2715	10.0792	9.8867	9.6956	9.5044
30	10.4637	10.2717	10.0794	9.8876	9.6964	9.5055
40	10.4687	10.2758	10.0824	9.8893	9.6991	9.5077
50	10.4710	10.2781	10.0849	9.8921	9.7021	9.5104
60	10.4807	10.2868	10.0937	9.9019	9.7106	9.5196
70	10.5663	10.3735	10.1794	9.9868	9.7961	9.6046
80	10.4752	10.2832	10.0909	9.9019	9.7112	9.5207
90	10.4759	10.2845	10.0920	9.9011	9.7106	9.5181
100	10.4773	10.2860	10.0934	9.9026	9.7122	9.5209
110	10.4802	10.2888	10.0955	9.9051	9.7151	9.5238
120	10.4814	10.2895	10.0976	9.9079	9.7180	9.5273
130	10.4897	10.2977	10.1058	9.9169	9.7285	9.5366
140	10.5738	10.3799	10.1871	9.9974	9.8101	9.6220
150	10.5000	10.3095	10.1195	9.9277	9.7367	9.5442
160	10.4919	10.3007	10.1098	9.9182	9.7258	9.5337
170	10.4928	10.3012	10.1093	9.9178	9.7262	9.5345
180	10.4933	10.3024	10.1112	9.9194	9.7281	9.5364
190	10.4955	10.3047	10.1131	9.9218	9.7296	9.5385
200	10.4977	10.3067	10.1148	9.9239	9.7315	9.5398

and then decrease significantly due presence of acidum lacticum on successive dilution to the potency 2C and after that these values increase up to potency 4C and then decrease to exhibit minimum from 6C to 8C and thereafter these values increase to exhibit maximum from 10C to 12C and then decrease up to 14C. After 14C potency these values remain constant till 200C potency, except for potencies 70C and 140C where the  $\Delta Z$  values exhibit maximums (Fig. 6). This indicates that at potencies 1C, 4C, 10C, 12C, 70C

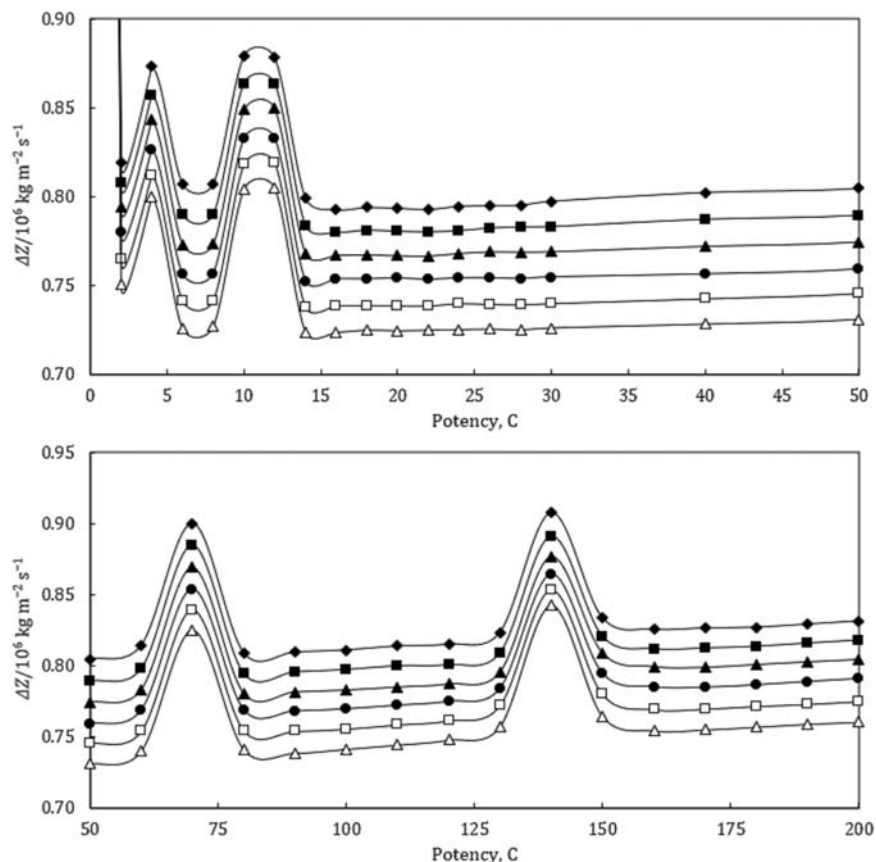


**Fig. 6.** Plots of deviations in acoustic impedance,  $\Delta Z$  vs. potency,  $C$  of acidum lacticum for homeopathic dilutions of acidum lacticum at temperatures, 293.15 K,  $\blacklozenge$ ; 298.15 K,  $\blacksquare$ ; and 303.15 K,  $\blacktriangle$ ; 308.15 K,  $\bullet$ ; 313.15 K,  $\bullet$ ; and 318.15 K,  $\triangle$ .

and 140C offer more resistance to ultrasonic waves due to more compact solution structure than the other potencies. The observed variations in values of  $Z$  and  $\Delta Z$  of these homeopathic dilutions may be due interaction between acidum lacticum and ethanol-water molecules.

A close perusal of Table 7 indicates that the values of  $R_A$  are greater than 1 for all the potencies at each investigated temperature and these  $R_A$  values for 1C, 4C, 10C, 12C, 70C and 140C potencies of acidum lacticum are greater than all other, and the other potencies show nearly constant values with slight variations. The greater values of  $R_A$  of solution in presence of acidum lacticum are due to formation of hydrogen-bonded associates between acidum lacticum and in ethanol-water aggregates.

A close perusal of Fig. 3 indicates that the viscosities,  $\eta$  of potencies of acidum lacticum are more than those of ethanol control for all the potencies at each investigated temperature and the values decrease with increase in temperature, which indicates substantial interaction between acidum lacticum and ethanol-water molecules. These variations in  $\eta$  are expressed in terms of deviations in viscosity,  $\Delta\eta$  and are shown in Fig. 7. Figure 7 indicates that  $\Delta\eta$  values are positive, *i.e.*,  $\eta$  values for acidum lacticum potencies are more than those of ethanol control. These  $\Delta\eta$  values are maximum at 1C and then decrease significantly due presence of acidum lacticum on successive dilution to the potency 2C and after that these values increase up to potency 4C and then decrease to exhibit minimum from 6C to 8C and thereafter these values increase to exhibit maximum from 10C to 12C and then decrease up to 14C. After 14C potency these values remain constant till 200C potency, except for potencies 70C and 140C where the  $\Delta\eta$  values show maximums (Fig. 7). This indicates that at potencies 1C, 4C, 10C, 12C, 70C and 140C offer more resistance to the flow

**Table 7.** The relative associations,  $R_A$  of ethanol control (0 potency, 91% ethanol in water) and 33 dilutions of acidum lacticum in ethanol control as function of potency, C of acidum lacticum (in centesimal) at the temperatures (293.15-318.15) K.

Potency (C)	T/K					
	293.15	298.15	303.15	308.15	313.15	318.15
1	1.0566	1.0556	1.0547	1.0538	1.0533	1.0523
2	1.0069	1.0063	1.0060	1.0056	1.0056	1.0050
4	1.0072	1.0061	1.0055	1.0048	1.0050	1.0050
6	1.0048	1.0044	1.0042	1.0039	1.0039	1.0034
8	1.0049	1.0045	1.0043	1.0040	1.0039	1.0034
10	1.0061	1.0057	1.0059	1.0058	1.0055	1.0051
12	1.0061	1.0059	1.0060	1.0059	1.0056	1.0052
14	1.0050	1.0045	1.0048	1.0039	1.0039	1.0034
16	1.0053	1.0048	1.0044	1.0041	1.0040	1.0035
18	1.0053	1.0048	1.0045	1.0041	1.0041	1.0036
20	1.0053	1.0047	1.0044	1.0040	1.0039	1.0033
22	1.0052	1.0047	1.0043	1.0039	1.0039	1.0034
24	1.0052	1.0048	1.0044	1.0039	1.0039	1.0035
26	1.0054	1.0049	1.0045	1.0038	1.0040	1.0036
28	1.0052	1.0046	1.0043	1.0040	1.0039	1.0036
30	1.0053	1.0049	1.0045	1.0042	1.0041	1.0036
40	1.0056	1.0050	1.0050	1.0042	1.0042	1.0039
50	1.0056	1.0052	1.0049	1.0041	1.0045	1.0040
60	1.0055	1.0051	1.0048	1.0044	1.0044	1.0038
70	1.0081	1.0083	1.0080	1.0076	1.0075	1.0070
80	1.0055	1.0050	1.0047	1.0043	1.0042	1.0037
90	1.0059	1.0054	1.0051	1.0047	1.0046	1.0042
100	1.0055	1.0050	1.0047	1.0043	1.0042	1.0037
110	1.0060	1.0055	1.0052	1.0048	1.0047	1.0042
120	1.0060	1.0056	1.0052	1.0048	1.0047	1.0042
130	1.0058	1.0053	1.0049	1.0045	1.0047	1.0038
140	1.0078	1.0073	1.0071	1.0064	1.0061	1.0060
150	1.0060	1.0055	1.0051	1.0047	1.0046	1.0041
160	1.0057	1.0052	1.0048	1.0044	1.0042	1.0042
170	1.0057	1.0052	1.0049	1.0045	1.0044	1.0039
180	1.0058	1.0053	1.0050	1.0047	1.0045	1.0041
190	1.0062	1.0055	1.0051	1.0050	1.0044	1.0043
200	1.0063	1.0055	1.0050	1.0050	1.0046	1.0041

of liquid due to more compact solution structure and presence of stronger intermolecular interactions between the component molecules (acidum lacticum and ethanol-water) than the other potencies. The variations in values of  $\eta$  and  $\Delta\eta$  are well supported by the trends observed in  $\Delta\kappa_s$ ,  $\Delta L_f$ , and  $\Delta Z$  values for these acidum lacticum dilutions.

A close perusal of Table 8 and Fig. 8 indicates that the relaxation time,  $\tau$  for acidum lacticum potencies is more than those of ethanol controls for all the potencies (except 1C) at each investigated temperature

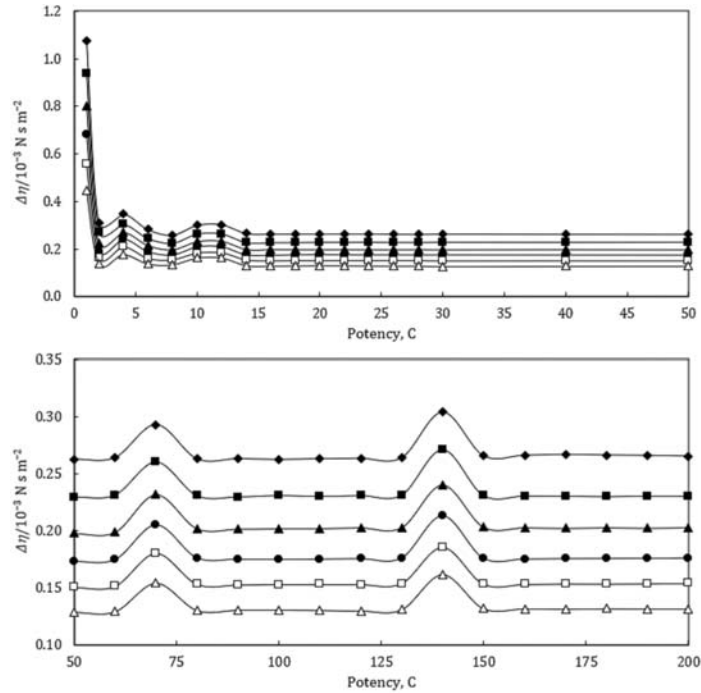


Fig. 7. Plots of deviations in viscosity,  $\Delta\eta$  vs. potency,  $C$  of acidum lacticum for homeopathic dilutions of acidum lacticum at temperatures, 293.15 K,  $\blacklozenge$ ; 298.15 K,  $\blacksquare$ ; and 303.15 K,  $\blacktriangle$ ; 308.15 K,  $\bullet$ ; 313.15 K,  $\bullet$ ; and 318.15 K,  $\Delta$ .

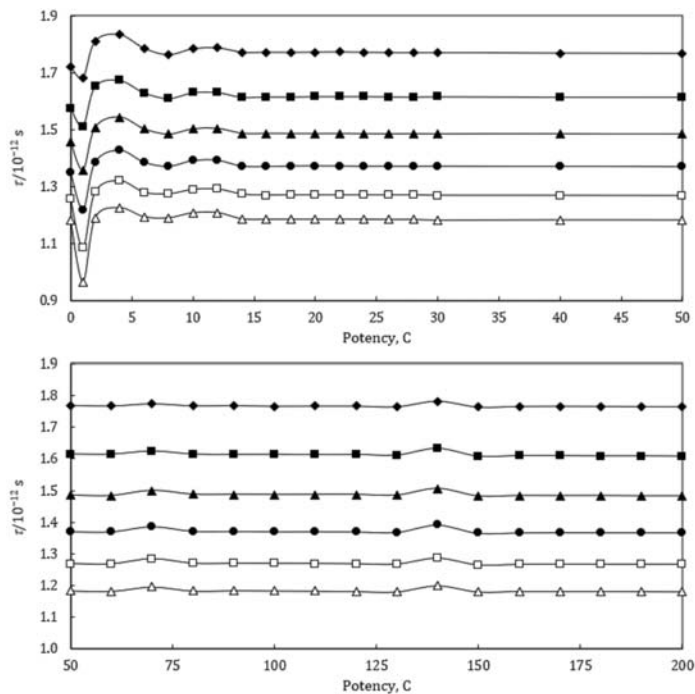


Fig. 8. Plots of relaxation time,  $\tau$ , vs. potency,  $C$  of acidum lacticum for homeopathic dilutions of acidum lacticum at temperatures, 293.15 K,  $\blacklozenge$ ; 298.15 K,  $\blacksquare$ ; and 303.15 K,  $\blacktriangle$ ; 308.15 K,  $\bullet$ ; 313.15 K,  $\bullet$ ; and 318.15 K,  $\Delta$ .

**Table 8.** The relaxation time,  $\tau/(10^{-12} \text{ s})$  of ethanol control (0 potency, 91% ethanol in water) and 33 dilutions of acidum lacticum in ethanol control as function of potency, C of acidum lacticum (in centesimal) at the temperatures (293.15-318.15) K.

Potency (C)	T/K					
	293.15	298.15	303.15	308.15	313.15	318.15
0	1.7226	1.5769	1.4578	1.3509	1.2564	1.1820
1	1.6815	1.5119	1.3584	1.2203	1.0859	0.9672
2	1.8120	1.6528	1.5085	1.3862	1.2814	1.1916
4	1.8353	1.6748	1.5449	1.4288	1.3212	1.2268
6	1.7865	1.6304	1.5031	1.3862	1.2808	1.1951
8	1.7635	1.6103	1.4845	1.3717	1.2749	1.1915
10	1.7850	1.6309	1.5032	1.3923	1.2905	1.2091
12	1.7879	1.6317	1.5048	1.3931	1.2919	1.2097
14	1.7729	1.6144	1.4877	1.3724	1.2745	1.1875
16	1.7728	1.6160	1.4871	1.3710	1.2704	1.1857
18	1.7723	1.6158	1.4867	1.3731	1.2714	1.1859
20	1.7729	1.6169	1.4865	1.3735	1.2707	1.1868
22	1.7735	1.6168	1.4868	1.3730	1.2714	1.1864
24	1.7725	1.6170	1.4861	1.3723	1.2707	1.1857
26	1.7717	1.6162	1.4858	1.3725	1.2714	1.1851
28	1.7708	1.6155	1.4861	1.3721	1.2710	1.1853
30	1.7712	1.6164	1.4858	1.3725	1.2699	1.1833
40	1.7695	1.6153	1.4861	1.3717	1.2696	1.1840
50	1.7687	1.6154	1.4848	1.3706	1.2690	1.1839
60	1.7670	1.6148	1.4835	1.3703	1.2681	1.1823
70	1.7741	1.6246	1.5001	1.3865	1.2844	1.1961
80	1.7675	1.6150	1.4876	1.3718	1.2699	1.1832
90	1.7680	1.6140	1.4873	1.3713	1.2697	1.1846
100	1.7664	1.6144	1.4868	1.3703	1.2694	1.1837
110	1.7668	1.6133	1.4870	1.3704	1.2693	1.1831
120	1.7668	1.6141	1.4872	1.3701	1.2684	1.1818
130	1.7645	1.6118	1.4848	1.3683	1.2671	1.1806
140	1.7823	1.6328	1.5061	1.3913	1.2859	1.2001
150	1.7635	1.6084	1.4820	1.3656	1.2646	1.1804
160	1.7660	1.6101	1.4836	1.3670	1.2664	1.1825
170	1.7664	1.6099	1.4833	1.3675	1.2670	1.1818
180	1.7660	1.6092	1.4835	1.3673	1.2665	1.1820
190	1.7655	1.6093	1.4827	1.3673	1.2664	1.1816
200	1.7644	1.6084	1.4827	1.3671	1.2665	1.1810

and these values decrease with increase in temperature. The  $\tau$  value is the time in which the structural deformation caused by propagation of ultrasonic wave is restored in the medium through translational motion, which indicates significant interaction between acidum lacticum and ethanol-water molecules. These  $\tau$  values are minimum at 1C and then increase significantly due presence of acidum lacticum on successive dilution to the potency 4C and then decrease to exhibit minimum from 6C to 8C and thereafter

these values increase to exhibit maximum from 10C to 12C and then decrease up to 14C. After 14C potency these values remain constant till 200C potency, except for potencies 70C and 140C where the values of exhibit maximum (Fig. 8). This indicates that at potencies 1C, 4C, 10C, 12C, 70C and 140C possess more compact solution structure as compared to other potencies. The maximum in the values of  $\tau$  for 1C, 4C, 10C, 12C, 70C and 140C potencies indicate that the structural deformation by propagation of ultrasonic wave is restored slowly, which may be due substantial interaction between acidum lacticum and water-ethanol molecules.

The loss of energy of ultrasonic waves by the concerned medium is called ultrasonic absorption or attenuation ( $\alpha/f^2$ ). The ( $\alpha/f^2$ ) values for acidum lacticum potencies are more than those of ethanol controls for all the potencies at each investigated temperature and these values decrease with increase in temperature (Table 8 and Fig. 9). As expected, the trends of ultrasonic absorption resemble with the relaxation time (Fig. 8). The viscosity appears to be the main factor accountable for ultrasonic absorption in these homoeopathic dilutions. The ( $\alpha/f^2$ ) values are minimum at 1C and then increase significantly due presence of acidum lacticum on successive dilution to the potency 4C and then decrease to exhibit minimum from 6C to 8C and thereafter these values increase to exhibit maximum from 10C to 12C and then decrease up to 14C. After 14C potency these values remain constant till 200C potency, except for potencies 70C and 140C where the values of ( $\alpha/f^2$ ) exhibit maximum (Fig. 9). The enhancement in ( $\alpha/f^2$ ) values for 1C, 4C, 10C, 12C, 70C and 140C potencies reflect a more ordered structure and significant interactions among the constituents may be due the presence of physical interaction because of hydrogen bonding.

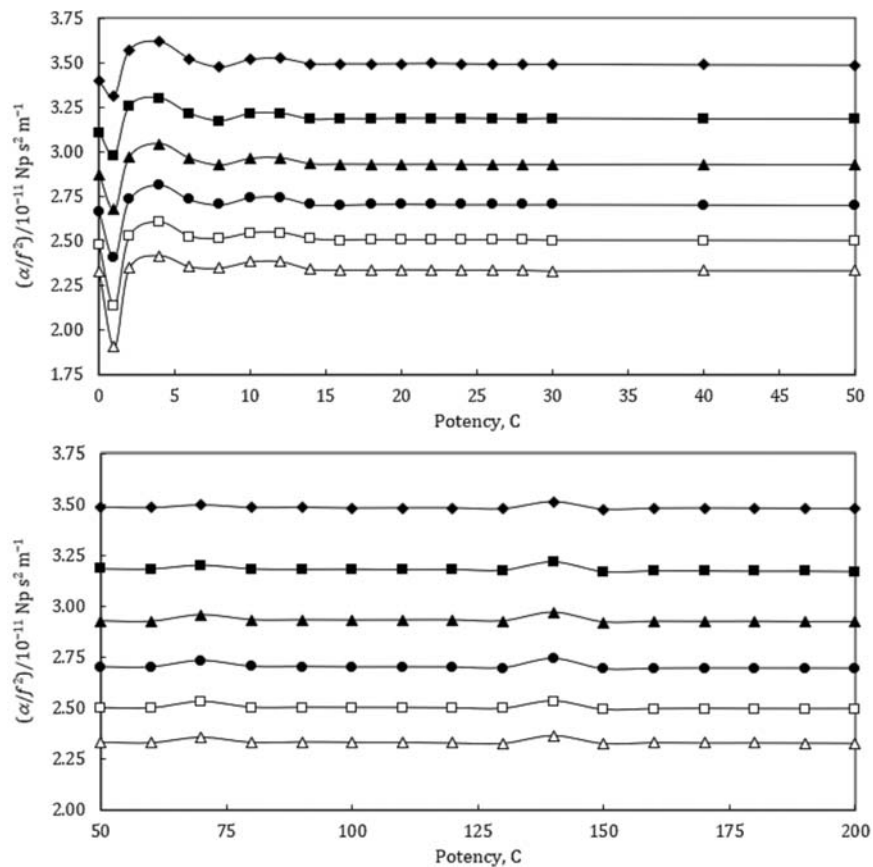


**Fig. 9.** Plots of ultrasonic absorption, ( $\alpha/f^2$ ) vs. potency, C of acidum lacticum for homoeopathic dilutions of acidum lacticum at temperatures, 293.15 K,  $\blacklozenge$ ; 298.15 K,  $\blacksquare$ ; and 303.15 K,  $\blacktriangle$ ; 308.15 K,  $\bullet$ ; 313.15 K,  $\circ$ ; and 318.15 K,  $\triangle$ .

A close perusal of Table 9 and Fig. 10 indicates that the pseudo-Grüneisen parameters,  $\Gamma$  for acidum lacticum potencies is more than those of ethanol controls for all the potencies at each investigated temperature and these values increase with increase in temperature, which indicates substantial interaction between acidum lacticum and ethanol-water molecules. The variations in  $\Gamma$  is expressed in terms of deviations in pseudo-Grüneisen parameter,  $\Delta\Gamma$  and are shown in Fig. 10. Figure 10 indicates that  $\Delta\Gamma$  values

**Table 9.** The ultrasonic absorption,  $(\alpha/f^2)/(10^{-11} \text{ Np s}^{-2} \text{ m}^{-1})$  of ethanol control (0 potency, 91% ethanol in water) and 33 dilutions of acidum lacticum in ethanol control as function of potency, C of acidum lacticum (in centesimal) at the temperatures (293.15-318.15) K.

Potency (C)	T/K					
	293.15	298.15	303.15	308.15	313.15	318.15
0	3.3969	3.1095	2.8747	2.6638	2.4775	2.3308
1	3.3157	2.9813	2.6786	2.4063	2.1413	1.9072
2	3.5731	3.2591	2.9746	2.7335	2.5268	2.3497
4	3.6191	3.3026	3.0465	2.8175	2.6053	2.4192
6	3.5228	3.2150	2.9640	2.7335	2.5255	2.3566
8	3.4775	3.1753	2.9274	2.7049	2.5140	2.3496
10	3.5199	3.2160	2.9641	2.7454	2.5448	2.3842
12	3.5256	3.2175	2.9674	2.7471	2.5476	2.3855
14	3.4960	3.1834	2.9336	2.7063	2.5131	2.3416
16	3.4957	3.1866	2.9325	2.7035	2.5051	2.3381
18	3.4948	3.1862	2.9316	2.7076	2.5070	2.3385
20	3.4961	3.1883	2.9312	2.7085	2.5058	2.3403
22	3.4972	3.1883	2.9318	2.7074	2.5070	2.3396
24	3.4953	3.1887	2.9305	2.7061	2.5058	2.3382
26	3.4936	3.1870	2.9300	2.7065	2.5071	2.3369
28	3.4918	3.1856	2.9304	2.7057	2.5063	2.3373
30	3.4927	3.1875	2.9300	2.7064	2.5041	2.3334
40	3.4894	3.1852	2.9305	2.7048	2.5035	2.3348
50	3.4877	3.1854	2.9279	2.7027	2.5024	2.3345
60	3.4845	3.1842	2.9253	2.7022	2.5006	2.3315
70	3.4984	3.2036	2.9581	2.7341	2.5328	2.3586
80	3.4853	3.1846	2.9334	2.7052	2.5041	2.3333
90	3.4864	3.1828	2.9328	2.7041	2.5038	2.3360
100	3.4831	3.1834	2.9319	2.7021	2.5032	2.3342
110	3.4840	3.1813	2.9323	2.7023	2.5030	2.3330
120	3.4840	3.1828	2.9327	2.7018	2.5012	2.3303
130	3.4795	3.1783	2.9280	2.6982	2.4987	2.3281
140	3.5146	3.2197	2.9699	2.7435	2.5356	2.3665
150	3.4776	3.1716	2.9224	2.6929	2.4936	2.3278
160	3.4823	3.1750	2.9256	2.6955	2.4973	2.3319
170	3.4831	3.1746	2.9250	2.6965	2.4984	2.3304
180	3.4823	3.1731	2.9253	2.6963	2.4975	2.3307
190	3.4814	3.1735	2.9238	2.6961	2.4972	2.3301
200	3.4793	3.1717	2.9238	2.6959	2.4975	2.3289

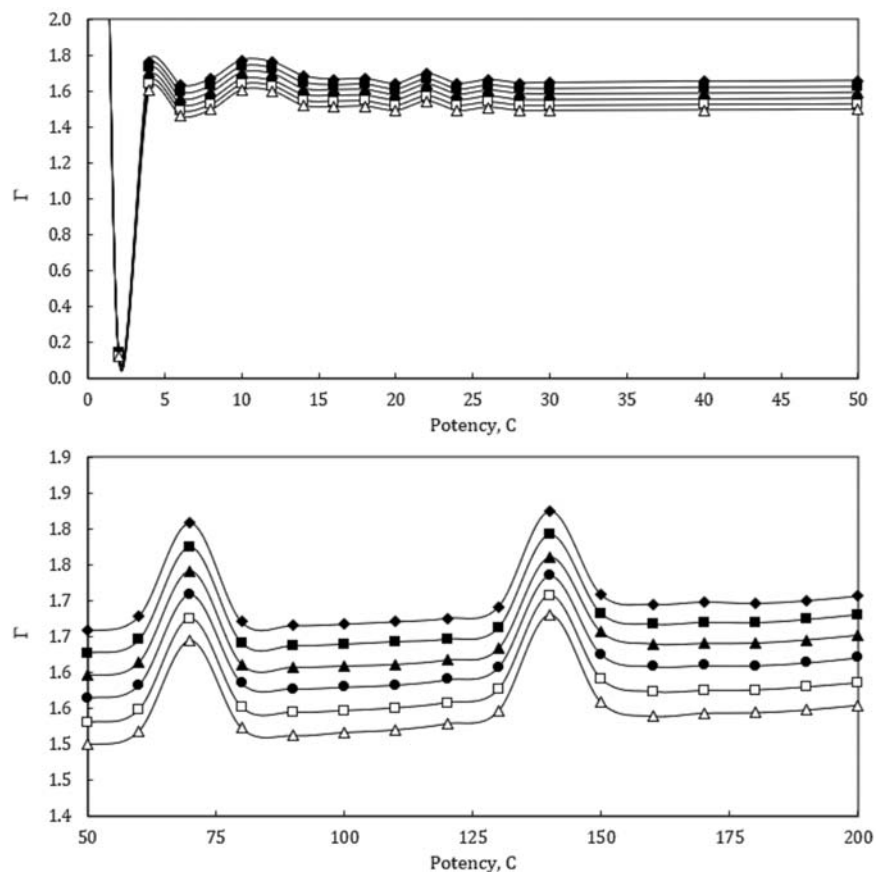


**Fig. 10.** Plots of deviations in pseudo-Grüneisen parameter,  $\Gamma$  vs. potency,  $C$  of acidum lacticum for homoeopathic dilutions of acidum lacticum at temperatures, 293.15 K,  $\diamond$ ; 298.15 K,  $\blacksquare$ ; and 303.15 K,  $\blacktriangle$ ; 308.15 K,  $\bullet$ ; 313.15 K,  $\circ$ ; and 318.15 K,  $\triangle$ .

are positive, *i.e.*,  $\Delta\Gamma$  values for acidum lacticum potencies are more than those of ethanol control. These values are minimum at 1C and then increase significantly due presence of acidum lacticum on successive dilution to the potency 4C and then decrease to exhibit minimum from 6C to 8C and thereafter these values increase to exhibit maximum from 10C to 12C and then decrease up to 14C. After 14C potency these values remain constant till 200C potency, except for potencies 70C and 140C where the values of  $\Delta\Gamma$  exhibit maximum (Fig. 10). The maximum in the values of  $\Delta\Gamma$  for 1C, 4C, 10C, 12C, 70C and 140C potencies may be due substantial interaction between acidum lacticum and water-ethanol molecules.

It has been observed from the scrutiny of the studied acoustic parameters, *viz.*,  $\kappa_s$ ,  $L_f$ ,  $\Gamma$ ,  $\Delta\kappa_s$ ,  $\Delta L_f$ ,  $\Delta Z$ ,  $\Delta\eta$ ,  $\tau$ ,  $(\alpha/f^2)$  and  $\Delta\Gamma$  that all the potencies exhibit more compact solution structure as compared to pure ethanol control; and the potencies 1C, 4C, 10C, 12C, 70C and 140C exhibit more compact solution structure than the other potencies. The difference in the physicochemical properties of these dilutions of acidum lacticum in ethanol control (91% ethanol in water) clearly indicate that the presence of medicine that results in significant structural alterations in solution for all the potencies and is more pronounced in certain potencies. The results can be qualitatively described in terms of interactions prevailing in these acidum lacticum dilutions in ethanol-water controls. The main factors which may be influencing the solution structure are nature of solute, presence of medicine molecules and potentization process.

It has been well-known that hydrogen bonding is one of the most vital weak interactions between molecules in solution leading to the formation of well-defined molecular aggregates, termed as dissipative structures<sup>[11,19]</sup>. It has been reported<sup>[37]</sup> that potentization process permanently changes the

**Table 10.** The pseudo-Grüneisen parameter,  $\Gamma$  of ethanol control (0 potency, 91% ethanol in water) and 33 dilutions of acidum lacticum in ethanol control as function of potency, C of acidum lacticum (in centesimal) at the temperatures (293.15-318.15) K

Potency (C)	T/K					
	293.15	298.15	303.15	308.15	313.15	318.15
0	8.1269	7.9552	7.7821	7.6087	7.4381	7.2613
1	12.5689	12.4241	12.2684	12.1060	11.9374	11.7628
2	8.2736	8.1004	7.9224	7.7428	7.5626	7.3875
4	9.8932	9.6929	9.4904	9.2833	9.0778	8.8714
6	9.7595	9.5528	9.3437	9.1373	8.9321	8.7229
8	9.7953	9.5894	9.3810	9.1724	8.9666	8.7586
10	9.9006	9.6973	9.4894	9.2805	9.0775	8.8703
12	9.8885	9.6867	9.4810	9.2714	9.0689	8.8618
14	9.8120	9.6086	9.3992	9.1947	8.9893	8.7818
16	9.7926	9.5945	9.3929	9.1900	8.9840	8.7751
18	9.7961	9.5976	9.3938	9.1907	8.9850	8.7782
20	9.7692	9.5714	9.3685	9.1669	8.9610	8.7545
22	9.8241	9.6253	9.4227	9.2192	9.0130	8.8058
24	9.7702	9.5706	9.3696	9.1664	8.9618	8.7539
26	9.7901	9.5923	9.3903	9.1862	8.9797	8.7722
28	9.7722	9.5754	9.3719	9.1662	8.9613	8.7537
30	9.7738	9.5731	9.3700	9.1654	8.9602	8.7542
40	9.7816	9.5802	9.3735	9.1691	8.9650	8.7573
50	9.7855	9.5833	9.3782	9.1741	8.9689	8.7614
60	9.8056	9.6014	9.3965	9.1919	8.9866	8.7802
70	9.9358	9.7308	9.5241	9.3182	9.1139	8.9065
80	9.7979	9.5971	9.3938	9.1944	8.9901	8.7844
90	9.7928	9.5932	9.3896	9.1868	8.9830	8.7738
100	9.7948	9.5954	9.3916	9.1890	8.9853	8.7784
110	9.7982	9.5989	9.3936	9.1918	8.9890	8.7820
120	9.8030	9.6024	9.4000	9.1994	8.9965	8.7906
130	9.8187	9.6180	9.4155	9.2162	9.0147	8.8079
140	9.9523	9.7481	9.5430	9.3439	9.1459	8.9424
150	9.8361	9.6383	9.4391	9.2346	9.0297	8.8204
160	9.8224	9.6231	9.4224	9.2177	9.0117	8.8011
170	9.8257	9.6258	9.4230	9.2190	9.0132	8.8052
180	9.8237	9.6252	9.4234	9.2189	9.0139	8.8057
190	9.8274	9.6296	9.4278	9.2227	9.0182	8.8096
200	9.8340	9.6365	9.4343	9.2299	9.0240	8.8161

physicochemical properties of the solution. The succussion process excites the formation of dissipative structures and these dissipative structures are exaggerated by presence of ethanol and medicine molecules<sup>[37]</sup> (lactic acid dissociated into H<sup>+</sup> and lactate ions). The results can be interpreted by considering the interactions that can take place between H<sup>+</sup> and lactate ions and the molecular aggregates of water-ethanol molecules, *i.e.*, dissipative structures<sup>[18]</sup>. The hydrogen bonding in ethanol-water will be

substantially influenced by the presence of H<sup>+</sup> and lactate ions as well as hydroxyl group of lactate ion in solution and it can be assumed that the effect of medicine molecules is likely to alter after successive dilution and succussion on moving from one potency to next potency. A qualitative comparison between various potencies can be considered due to the nature of driving force that leads to formation of complexes (due to solvation of these ions by polar ethanol/water dipoles) between H<sup>+</sup> and lactate ions as well as hydroxyl group of lactate ion and dissipative structures of ethanol-water molecules<sup>[21,38]</sup>. This driving force is supplied by the succussion process in which a vast amount of mechanical energy (~404.3 Newton-meter by 10 strokes)<sup>[39]</sup> is transferred. This transfer of energy due to successive dilution and succussion process is responsible for different/anomalous behaviour of acidum lacticum of different potencies. It has also been observed<sup>[13,14]</sup> that same medicine of different potency displays varied behaviour owing to vehicle-molecule structure (ethanol-water aggregates) generated by potentization process of homeopathy.

#### 4. CONCLUSION

The ultrasonic speeds, densities and viscosities of ethanol control, 33 formulations of acidum lacticum in ethanol control are measured for potencies from 1C to 200C at six different temperatures and atmospheric pressure. Using these experimental data, various acoustic parameters, *viz.*,  $\kappa_s$ ,  $L_f$ ,  $\Gamma$ ,  $\Delta\kappa_s$ ,  $\Delta L_f$ ,  $\Delta Z$ ,  $\Delta\eta$ ,  $\tau$ ,  $(\alpha/f^2)$  and  $\Delta\Gamma$  have been calculated. The results have been qualitatively discussed in terms of interactions/ physicochemical behaviour of these extremely dilute homeopathic formulations of acidum lacticum in ethanol. The potencies 1C, 4C, 10C, 12C, 70C and 140C exhibit more compact solution structure as compared to other potencies and ethanol control. It is found that the interactions can take place between H<sup>+</sup> and lactate ions as well as hydroxyl group of lactate ion and the molecular aggregates of water-ethanol, *i.e.*, dissipative structures. Hence, these potencies might have diverse behaviour in terms of properties and efficacy when utilized in practice. It can be qualitatively concluded that even in high dilutions the molecules of acidum lacticum might be present in these homeopathic formulations, however it needs to be confirmed from other more precise spectroscopic and other techniques.

#### 5. ACKNOWLEDGMENT

The authors are thankful to Central Council for Research in Homeopathy (CCRH), Ministry of AYUSH, Govt. of India for providing financial assistance to carry out this collaborative study.

#### 6. REFERENCES

- [1] A.A. Firdaus, N. Chakraborty and K.C. Juglan, 2024. Thermo-acoustical investigation of monosodium glutamate food preservative in an aqueous solution of poly-ethylene glycols (400 and 600) by using ultrasonic technique, *Chem. Thermodyn. Therm. Anal.*, **13**, 100127.
- [2] A. K. Nain and D. Chand, 2022. Evaluation and analysis of Kirkwood-Buff integrals of 1,4-dioxane + aromatic hydrocarbon binary mixtures using inversion procedure and regular solution theory from ultrasonic speed and density data, *J. Acoust. Soc. India*, **49**, 36-47.
- [3] A. Pal and N. Chauhan, 2012. Interactions of amino acids and peptides with the drug pentifylline in aqueous solution at various temperatures: A volumetric approach, *J. Chem. Thermodyn.*, **54**, 288-292.
- [4] A.K. Nain, 2022. Study of intermolecular interactions in binary mixtures of methyl acrylate with benzene and methyl substituted benzenes at different temperatures: An experimental and theoretical approach, *Chin. J. Chem. Eng.*, **44**, 222-246.
- [5] Ankita and A.K. Nain, 2021. Probing interactions and hydration behaviour of drug sodium salicylate in aqueous solutions of D-xylose/L-arabinose: Volumetric, acoustic and viscometric approach, *J. Mol. Liq.*, **333**, 115985.

- [6] A.K. Nain, 2021. Interactions of some  $\alpha$ -amino acids with antibacterial drug gentamicin sulphate in aqueous medium probed by using physicochemical approaches, *J. Mol. Liq.*, **321**, 114757.
- [7] A. K. Nain, 2020. Volumetric and ultrasonic study of l-arginine/l-histidine and gentamicin sulphate in aqueous medium at different temperatures, *J. Mol. Liq.*, **315**, 113736.
- [8] P.S. Chikramane, A.K. Suresh, J.R. Bellare and S.G. Kane, 2010. Extreme homeopathic dilutions retain starting materials: A nanoparticulate perspective, *Homeopathy*, **99**, 231-242.
- [9] M.K. Temgire, A.K. Suresh, S.G. Kane and J.R. Bellare, 2015. Establishing the interfacial nano-structure and elemental composition of homeopathic medicines based on inorganic salts: a scientific approach, *Homeopathy*, **104**, 1-13.
- [10] V. Elia, E. Napoli and M. Niccoli, 2013. On the stability of extremely diluted solutions to temperatures, *J. Therm. Anal. Cal.*, **113**, 963-970.
- [11] V. Elia, L. Elia, N. Marchettini, E. Napoli, M. Niccoli and E. Tiezzi, 2008. Physico-chemical properties of aqueous extremely diluted solutions in relation to aging, *J. Therm. Anal. Cal.*, **93**, 1003-1011.
- [12] T. Maity, D. Ghosh and C.R. Mahata, 2008. Theory and instrumentation related to potentised homeopathic medicines, *Indian J. Res. Homeopath.*, **2**, 1-5.
- [13] T. Maity, D. Ghosh and C.R. Mahata, 2010. Effect of dielectric dispersion on potentised homeopathic medicines, *Homeopathy*, **99**, 99-103.
- [14] C.R. Mahata, 2013. Dielectric dispersion studies indicate change in structure of water by potentised homeopathic medicines, *J. Inst. Eng. India Ser. B.*, **93**, 231-235.
- [15] V. Elia, M. Marchese, M. Montanino, E. Napoli, M. Niccoli, L. Nonatelli and A. Ramaglia, 2005. Hydrohystretic phenomena of "extremely diluted solutions" induced by mechanical treatments: A calorimetric and conductometric study at 25 °C, *J. Solution Chem.*, **34**, 947-960.
- [16] V. Elia, E. Napoli and M. Niccoli, 2009. A molecular model of interaction between extremely diluted solutions and NaOH solutions used as titrants. Conductometric and pHmetric titrations, *J. Mol. Liq.*, **148**, 45-50.
- [17] V. Elia, E. Napoli and M. Niccoli, 2008. On the stability of extremely diluted aqueous solutions at high ionic strength: A calorimetric study at 298.15 K, *J. Therm. Anal. Cal.*, **92**, 643-648.
- [18] V. Elia, E. Napoli and M. Niccoli, 2010. Thermodynamic parameters for the binding process of the OH<sup>-</sup> ion with the dissipative structures. Calorimetric and conductometric titrations, *J. Therm. Anal. Cal.*, **102**, 1111-1118.
- [19] V. Elia, E. Napoli, M. Niccoli and N. Marchettini, 2008. New physico-chemical properties of extremely dilute solutions. A conductivity study at 25°C in relation to ageing, *J. Solution Chem.*, **37**, 85-96.
- [20] P. Belon, V. Elia, L. Elia, M. Montanino, E. Napoli and M. Niccoli, 2008. Conductometric and calorimetric studies of the serially diluted and agitated solutions. On the combined anomalous effect of time and volume parameters, *J. Therm. Anal. Cal.*, **93**, 459-469.
- [21] V. Elia, L. Elia, P. Cacace, E. Napoli, M. Niccoli and F. Savarese, 2006. Extremely diluted solutions as multi-variable systems: A study of calorimetric and conductometric behaviour as a function of the parameter time, *J. Therm. Anal. Cal.*, **84**, 317-323.
- [22] V. Elia, N. Marchettini, E. Napoli and M. Niccoli, 2014. The role of ethanol in extremely diluted solutions. Calorimetric and conductometric measurements, *J. Therm. Anal. Cal.*, **116**, 477-483.
- [23] J. Wang, F. Zhao, B. Chen, Y. Li, P. Na and J. Zhuo, 2013. Small water clusters stimulate microcystin biosynthesis in cyanobacterial *Microcystis aeruginosa*, *J. Appl. Phycol.*, **25**, 329-336.
- [24] P.P. Singh, H.L. Chhabra, 1993. Topological investigation of the ethanol/water system and its implication for the homeopathic medicines, *Br. Homeopath. J.*, **82**, 164-171.
- [25] A.K. Nain, N. Chaudhary, A. Khurana, R.K. Manchanda and D. Nayak, 2022. Physicochemical

- studies of homoeopathic formulations of ammonium aceticum by using volumetric, acoustic and viscometric measurements at different temperatures. *Organic & Medicinal Chem. I.J.*, **12**, 555830.
- [26] A.K. Nain, P. Droliya, R.K. Manchanda, A. Khurana and D. Nayak, 2016. Physicochemical studies of homoeopathic formulations (extremely diluted solutions) of acidum salicylicum in ethanol by using volumetric, acoustic, viscometric and refractive index measurements at 298.15, 308.15 and 318.15 K, *J. Mol. Liq.*, **215**, 680-690.
- [27] A.K. Nain, P. Droliya, R.K. Manchanda, A. Khurana and D. Nayak, 2015. Physicochemical studies of extremely diluted solutions (homoeopathic formulations) of sulphur in ethanol by using volumetric, acoustic, viscometric and refractive index measurements at different temperatures. *J. Mol. Liq.*, **211**, 1082-1094.
- [28] A.K. Nain, N. Chaudhary, R.K. Manchanda, A. Khurana and D. Nayak, 2024. Physicochemical behaviour of homoeopathic dilutions of ammonium carbonicum at ambient temperatures: Volumetric, ultrasonic and viscometric study, *J. Mol. Chem.*, **4**, 698.
- [29] Homoeopathic Pharmacopoeia of India, 1971. Vol. I. Controller of Publications, Ministry of Health & Family Welfare, Govt. of India, New Delhi.
- [30] N. Chaudhary and A. K. Nain, 2021. Physicochemical studies of intermolecular interactions in 1-butyl-3-methylimidazolium tetrafluoroborate + benzonitrile binary mixtures at temperatures from 293.15 to 318.15 K, *Phys. Chem. Liq.*, **59**, 358-381.
- [31] R.K. Shukla, V.S. Gangwar, S. Shukla, M. Tewari and K. Tenguriya, 2015. Pseudo-Gruneisen parameter and internal pressure of binary mixtures from different approaches, *Int. J. Thermodyn.*, **18**, 150-159.
- [32] R.K. Shukla, K. Tenguriya, S. Shukla, M. Tewari and S. Dwivedi, 2016. Internal pressure, excess internal pressure and pseudo-Gruneisen parameter of binary systems from associated and non-associated models, *Indian J. Chem. Technol.*, **23**, 469-477.
- [33] L. Knopoff and J.N. Shaprio, 1970. Pseudo-Gruneisen parameters for liquids, *Phys. Rev.*, **B1**, 3893-3894.
- [34] S.K. Kor, U.S. Tandon and B.K. Singh, 1972. Pseudo-Gruneisen parameter for liquid argon., *Phys Lett.*, **A38**, 187-188.
- [35] V. Sanguri and R. Sethi, 2017. Interaction studies of binary liquid mixtures through pseudo-Gruneisen parameter, *Int. Acad. Phys. Sci.*, **21**, 83-90.
- [36] J.D. Pandey and R. Verma, 2001. Inversion of the Kirkwood-Buff theory of solutions: Application to binary systems, *Chem. Phys.*, **270**, 429-438.
- [37] L. Ciavatta, V. Elia, E. Napoli and M. Niccoli, 2008. New physico-chemical properties of extremely diluted solutions. Electromotive force measurements of galvanic cells sensible to the activity of NaCl at 25°C, *J. Solution Chem.*, **37**, 1037-1049.
- [38] C. M. Cacace, L. Elia, V. Elia, E. Napoli and M. Niccoli, 2009. Conductometric and pHmetric titrations of extremely diluted solutions using HCl solutions as titrant: a molecular model, *J. Mol. Liq.*, **146**, 122-126.
- [39] R. Shah, 2014. Scientific method of preparing homoeopathic nosodes. *Indian J. Res. Homeopath.*, **8**, 166-174.

# Structure-borne sound source localization using sound level meter measurements in urban residential buildings

**Arun Sulkunte Iyengar**

*Principal Acoustic Consultant, dB Acoustique, No. 95, 1A Main Road,  
Doddanekkundi, Bengaluru-560 037, Karnataka, India  
e-mail: arun@dbacoustique.in*

[Received: 08-09-2024; Accepted: 20-12-2024]

## ABSTRACT

In urban residential settings, particularly in densely populated cities like Bengaluru, India, structure-borne noise poses significant challenges. Traditional noise identification methods often rely on accelerometers, yet their application can be limited due to equipment availability and complexity. This paper introduces a novel method for localizing structure-borne sound sources using a standard sound level meter equipped with octave band or Fast Fourier Transform (FFT) capabilities, specifically focusing on noise from Sewage Treatment Plants (STPs), pumps, and motors in apartment buildings. Additionally, this study explores the use of mobile phones as preliminary tools for residents to identify disturbing frequencies. The methodology, findings, and implications of this approach are discussed, demonstrating its potential as a practical solution for urban noise management.

## 1. INTRODUCTION

### 1.1 Background

In the bustling urban landscapes of cities like Bengaluru, India, the issue of structure-borne noise in residential buildings is increasingly prevalent. The author, an acoustic consultant has frequently addressed noise complaints arising from mechanical sources, such as pumps, motors, and particularly STPs. In these settings, blower motors are often identified as primary contributors to structure-borne noise. A common issue is the lack of appropriate vibration isolation measures, such as customized isolators tailored to the machinery's weight distribution and bellows in piping systems. The enclosed nature of STP rooms, though appropriate for airborne noise control, does not adequately address the transmission of structure-borne sound. This oversight often results in the propagation of vibrations through the building's structure, leading to significant noise disturbances in residential areas.

### 1.2 Problem Statement

The impact of this noise is often localized, affecting a small percentage of residents within an apartment complex. This localized effect presents a unique challenge, as broader community action is often hindered by the limited number of affected individuals. Traditional methods for identifying noise sources,

predominantly based on accelerometers, are limited by their need for specialized equipment and technical expertise. These methods also tend to be costly and complex, making them impractical for widespread use in residential settings.

### **1.3 Research Objective**

This study aims to demonstrate an alternative, more accessible approach for localizing structure-borne sound sources. By utilizing a standard sound level meter with the octave band or Fast Fourier Transform (FFT) capabilities, the research seeks to offer a practical solution for individual apartment owners or small groups within residential complexes to identify and substantiate their noise complaints.

### **1.4 Significance of the Study**

The relevance of this research is highlighted by the growing concerns over urban noise pollution and its impact on quality of life. The capability to effectively identify and mitigate structure-borne noise sources in residential buildings is crucial for urban dwellers, property managers, and urban planners. This study addresses these needs by proposing a method that is both practical and accessible to a broader audience using octave or FFT filter capable sound measuring instruments without the use of accelerometers.

## **2. LITERATURE REVIEW**

### **2.1 Existing Research on Structure-Borne Noise**

Research in the field of acoustics has significantly advanced our understanding of structure-borne noise. Studies have identified various sources of this type of noise in buildings, such as machinery vibrations and architectural elements. Notably, research published in the Journal of the Acoustical Society of America has delved into the complexities of predicting structure-borne sound power input into buildings, highlighting the trade-offs between accuracy and simplicity in measurement and prediction methods.

### **2.2 Methods for Noise Source Identification**

The conventional approach to identifying structure-borne noise sources heavily relies on accelerometer-based techniques. These methods, while precise, often necessitate elaborate setups and specialized knowledge. For instance, the EN 15657:2017 standard proposes detailed characterization methods using low and high-mobility reception plates to measure source characteristics like blocked force and free velocity. However, these methods require extensive data sets and complex calculations, limiting their practicality in residential settings.

### **2.3 Gap in Research**

Despite these advancements, there is a notable gap in research regarding non-accelerometer methods for noise source identification, especially in the context of STP machinery. The existing literature predominantly focuses on technical and equipment-intensive approaches, leaving a void in accessible, cost-effective methods suitable for residential noise issues.

## **3. METHODOLOGY**

### **3.1 Measurement Procedure Details**

**Background :** The research investigates structure-borne noise in a concrete and masonry constructed urban apartment building. The study focuses on the effect of a Sewage Treatment Plant (STP), located inside a masonry enclosure in the basement levels (-1 and -2), on residences two floors above, on Level 1. Despite being over 40 meters horizontally apart and the implementation of airborne noise barriers such as glazing, the unique architectural composition and the distance between the STP and the residences

provided a significant context for exploring the transmission and impact of structure-borne noise in such environments.

**Instrumentation :** In this study, the primary instrument utilized was a standard calibrated NTi XL2 sound level meter, equipped with a class 1 frequency response M2211 microphone, certified as a Class 2 sound measuring Instrument. This equipment is notably capable of conducting 1/3 octave band analysis. To ensure accuracy and consistency, all measurements were made over a period of 10 seconds

### 3.2 Measurement Process

**Initial Measurements :** Initial measurements focused on ascertaining baseline noise levels and excluding intermittent noise. These were conducted with a visual readout of the 1/3 octave band noise spectrum over 2 minutes, specifically when only the blower components of the Sewage Treatment Plant (STP) were operational.

**STP Room Measurements :** Within the STP room, two sets of noise measurements were taken with all STP components operational (Fig. 1) and with only the blower components active (Fig. 2). This dual-measurement approach allowed for a nuanced understanding of the noise contributions from different STP components.

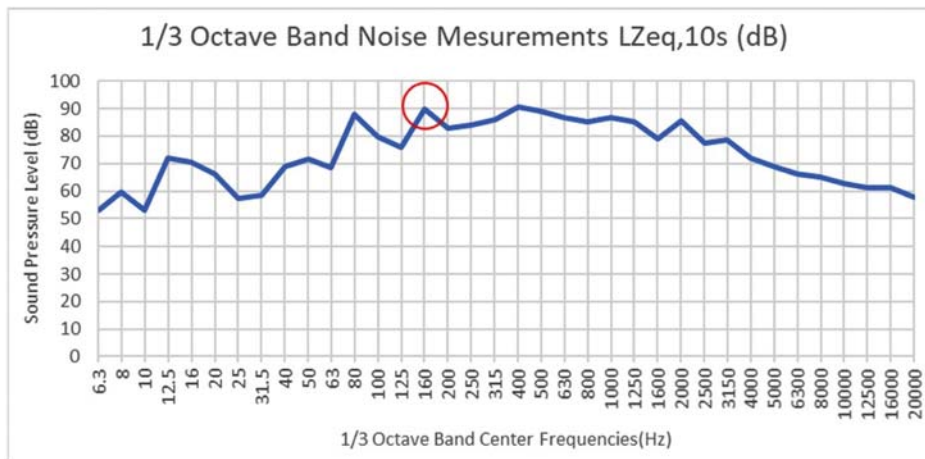


Fig. 1. Noise Levels Measured in the STP room with all STP machinery on.

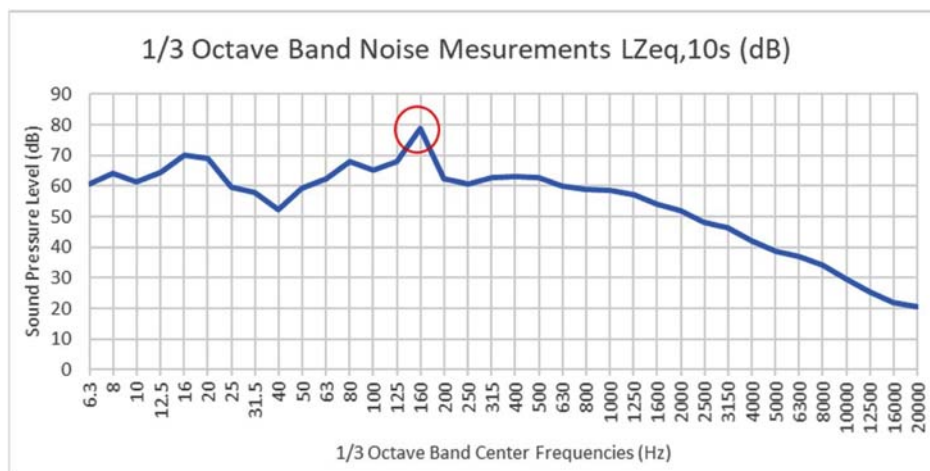
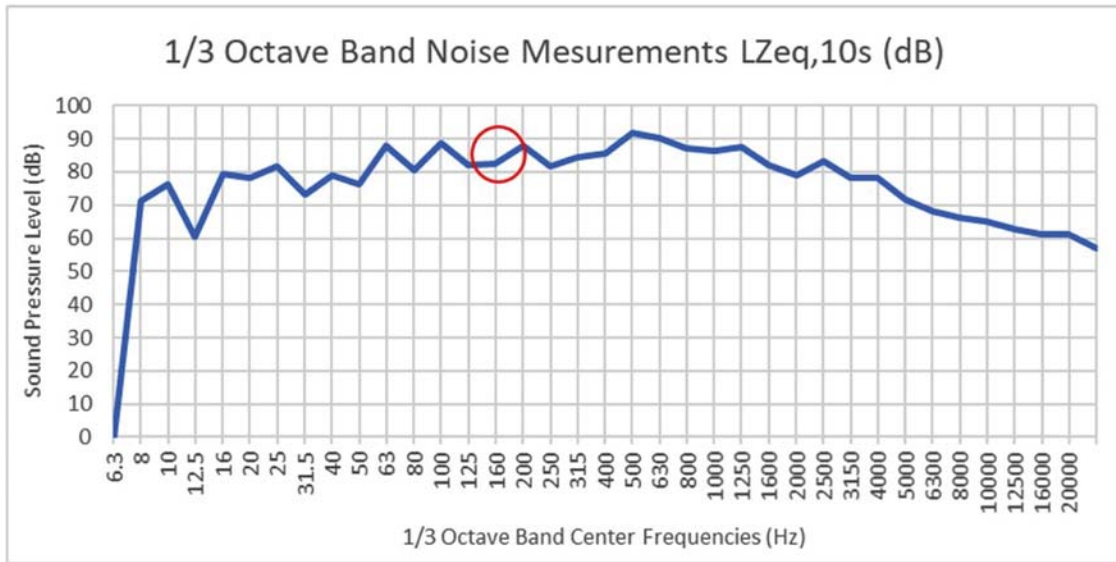
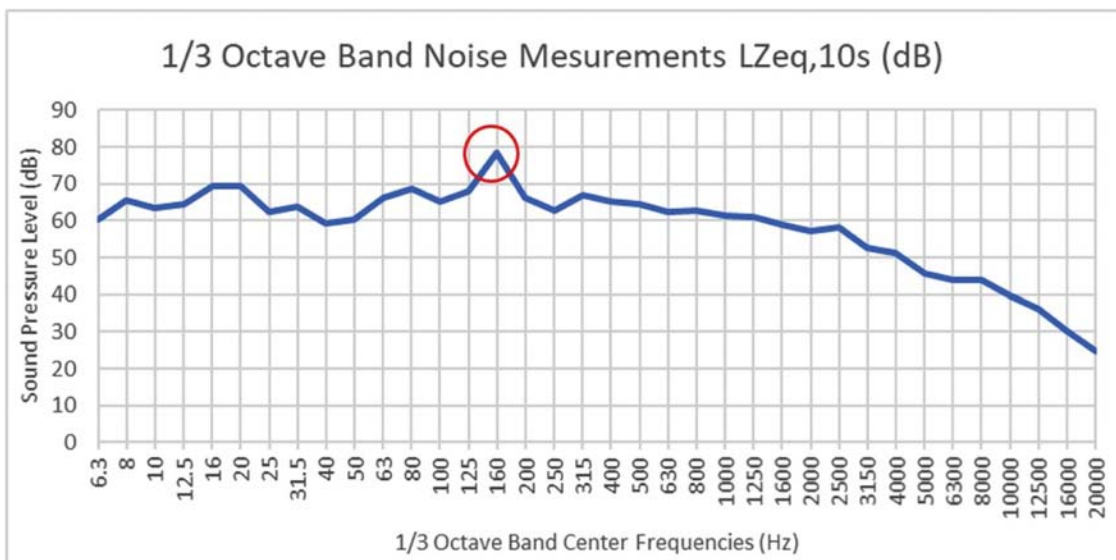


Fig. 2. Noise levels measured in the STP room with only the blower motors on and all other equipment turned off with a noticeable peak in the 160 Hz 1/3 Octave Band.

**External STP Room Measurements :** To assess noise transmission outside the STP room, measurements were taken just outside the STP room access door, which was kept closed, while all equipment was operational (Fig. 3). An additional measurement was conducted 20 meters away from the closed STP room access door to determine if noise characteristics observed near the door were consistent further away (Fig. 4). By measuring 20 meters away from the closed STP enclosure access door, the study aimed to observe an attenuation in airborne noise and a higher peak in the disturbing frequency of the main source of the structure-borne noise, the blower motors. This approach revealed a distinct attenuation pattern as anticipated, with the structure-borne noise becoming more dominant and a peak in the noise levels in the 160 Hz 1/3 octave band observed (Fig. 4).



**Fig. 3.** Noise Levels measured outside the STP enclosure near the STP entrance(access) door when the door was closed.



**Fig. 4.** Noise levels measured 20 meters away from the STP enclosure in the parking lot with the STP enclosure entrance(access) door closed.

**Residential Measurements :** The study extended measurements to the residential areas, beginning with the neighboring apartment of the complainant (Fig. 5) where a less prominent peak is seen in the 1/3 octave band of concern and subsequently within the complainant's apartment (Fig. 6), where the A-weighted measurements particularly highlighted the prominence of the 160Hz 1/3 octave band peak, emphasizing its significance in terms of human hearing perception. During these residential measurements, residents were requested to maintain silence and the doors and windows of the rooms were shut to prevent and minimize interference from human activity or other extraneous noise sources. This comprehensive approach was designed to capture an accurate representation of the noise environment across different locations within the building, with a specific focus on areas impacted by the STP's operation.

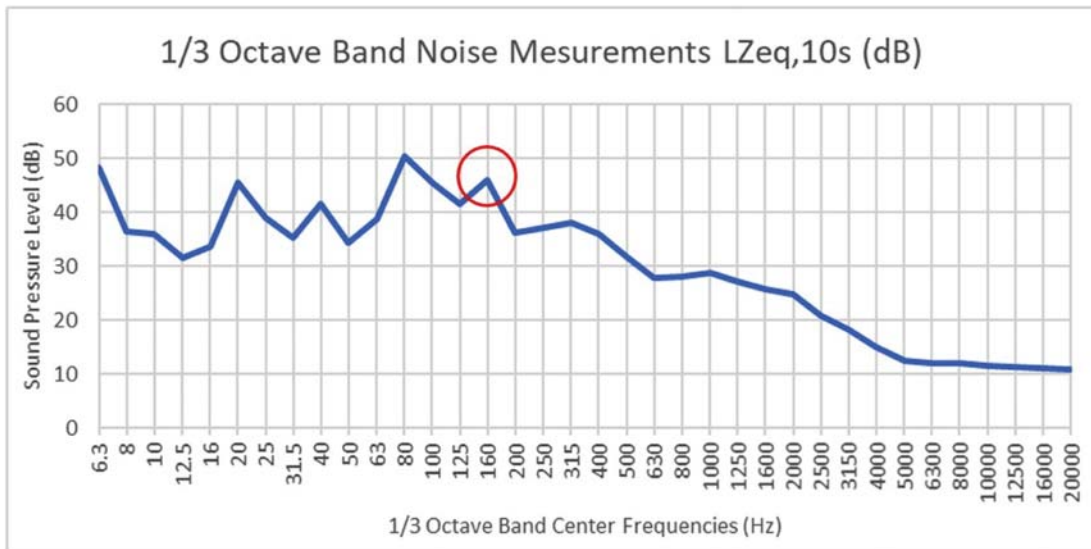


Fig. 5. Noise Levels in one of the bedrooms of the neighbors' apartment.

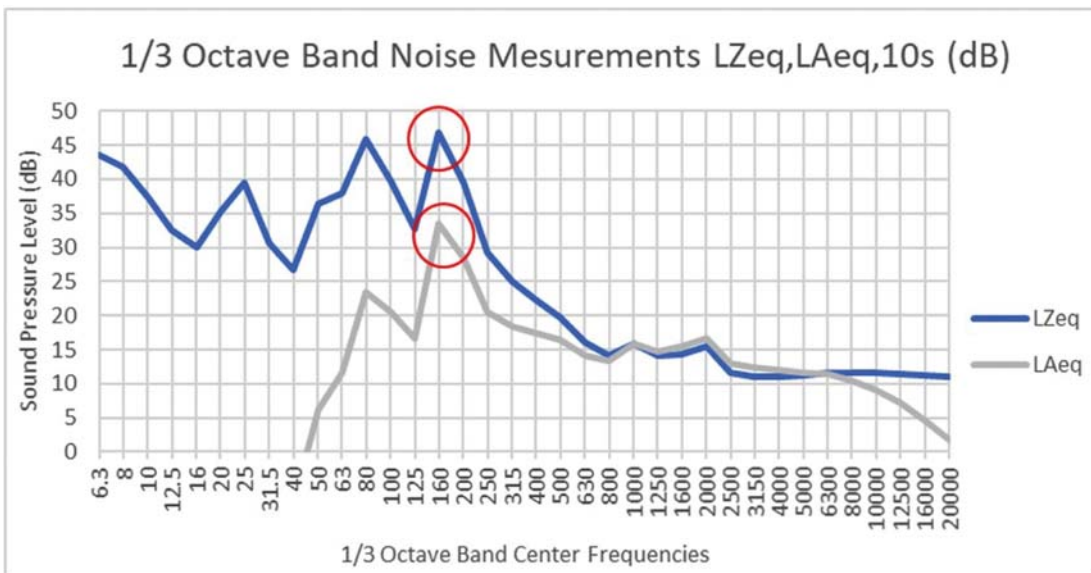


Fig. 6. Figure showing the A-weighted and un-weighted noise levels in one of the bedrooms in the complainant's apartment. The peak in the noise levels in the 160 Hz 1/3 octave band is visible in the A-weighted noise spectrum.

Additionally, the use of mobile phones by residents provided preliminary data on the noise environment within their living spaces (Fig. 7). These recordings, while not as calibrated as the sound level meter, offered valuable insights into the everyday noise experience of the residents.

## 4. RESULTS AND DISCUSSIONS

### 4.1 Noise Characteristics at the Source

The sound level meter readings indicated specific frequencies were prominently emanating from the STP machinery. For instance, certain frequencies were consistently present when specific blower motors were operational.

### 4.2 Noise Transmission to Residences

In the affected residence, similar frequencies were recorded, particularly in areas where structural contact was direct. These findings were corroborated by the mobile phone recordings made by the resident, which, despite their lack of calibration, reflected a similar noise profile to that measured at the source.

### 4.3 Correlation of Data

A clear correlation was observed between the dominant frequencies at the source and those in the residential space. This correlation was crucial in establishing the structure-borne nature of the noise and identifying the specific machinery responsible.

### 4.4 Analysis of Results

The findings from the study significantly contribute to our understanding of structure-borne noise transmission in urban residential buildings. The correlation between the noise signatures measured at the STP source and those within the residence indicates that the dominant noise issues experienced by the residents originate from specific machinery within the STP. This correlation was further substantiated by the preliminary observations made using mobile phones, which, despite their limitations, provided valuable corroborative evidence. The attenuation of airborne sound with distance, also corroborated that the disturbing noise was primarily structure borne.

The effectiveness of using a standard sound level meter for this type of investigation was demonstrated. The detailed frequency analysis provided by the 1/3 octave band capability of the meter was particularly crucial in isolating and identifying the specific machinery responsible for the noise. This method presents a significant advancement over traditional accelerometer-based techniques, which, while accurate, are often impractical for widespread use due to their complexity and cost.

### 4.5 Contextual Comparison

The methodology and findings of this study present a stark contrast to the prevailing practices in structure-borne noise identification as highlighted in existing literature. Traditional methods, as described in sources like EN 15657:2017 and research published in the Journal of the Acoustical Society of America, often involve complex and equipment-intensive procedures. The approach presented in this study offers a simpler, more cost-effective, and accessible alternative, particularly relevant in scenarios where specialized equipment and technical expertise are limited.

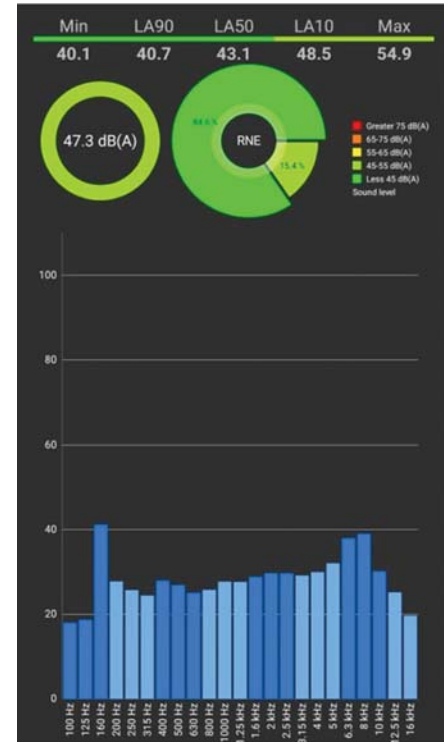


**Fig. 7.** Noise Levels as Measured in the Complainant Bedroom from an Android Phone App by the Resident.

## 5. CONCLUSION AND FUTURE WORK

This research has demonstrated a novel and practical approach to identifying structure-borne noise sources in residential buildings, specifically in the context of urban environments like Bengaluru, India. The use of standard sound level meters, provides a cost-effective and accessible method for localizing structure-borne noise sources, particularly in scenarios where traditional, more technical methods are not feasible.

**Future Work** : Further research is recommended to refine this methodology and explore its applicability in different types of building structures and urban environments. Additional studies could focus on developing guidelines for residents to effectively use mobile phones in preliminary noise investigations and on integrating these findings with professional acoustic analyses. Moreover, exploring ways to enhance the accuracy and reliability of sound measurements using commonly available devices could significantly broaden the scope of community-driven noise management initiatives.

## 6. ACKNOWLEDGMENT

This work was supported by the client and the apartment association of the client's residence where the noise complaint was reported.

**Data Availability** : The data supporting the findings of this study are available in the article as graphs and are also available from the author upon reasonable request.

## 7. REFERENCES

- [1] B.M. Gibbs, 2013. "Uncertainties in predicting structure-borne sound power input into buildings," *J. Acoust. Soc. Am.* **133**(5), 2678-2689, doi: 10.1121/1.4795773.
- [2] European Committee for Standardization, 2017. "Laboratory characterization methods for structure-borne sound sources," EN 15657.
- [3] "Structure-borne sound sources in buildings - Estimating the uncertainty of source properties and installed power from interlaboratory test results," *Acta Acustica*. Accessed from [acta-acustica.edpsciences.org/articles/aa/abs/2017/02/aa16098/aa16098.html](http://acta-acustica.edpsciences.org/articles/aa/abs/2017/02/aa16098/aa16098.html).

# Fundamental frequency perturbation is a consequence of the biomechanics of voicing and not due to phonological status

Indranil Dutta<sup>1\*</sup> and Molly Varghese<sup>2</sup>

<sup>1</sup>*School of Languages and Linguistics, Jadavpur University, Kolkata, India*

<sup>2</sup>*Department of Malayalam, Sree Krishna College, Guruvayur, India*

*e-mail: indranildutta.lnl@jadavpuruniversity.in*

[Received: 11-10-2024; Accepted: 20-01-2025]

## ABSTRACT

Voicing is known to lower  $f_0$  in the following vowel<sup>[18,21,23]</sup>. This lowering has been attributed to biomechanical constraints<sup>[22,28-30]</sup>. On the basis of evidence from typologically, aspiration languages, such as English, where the [voice] feature doesn't manifest itself phonetically, yet is accompanied by  $f_0$  lowering, it has been argued that this lowering serves to enhance the phonological [voice] contrast. We present results from an acoustic study of  $f_0$  perturbation in Malayalam, which exhibits predictable voicing in lexical items from its Dravidian stratum. Voiceless stops appear initially, and are voiced intervocalically. Malayalam also contains a Sanskrit lexical stratum, where phonetic voicing is tied to its stratal affiliation. Results from two experiments on voicing and  $f_0$  perturbation show that even with predictable voicing, in the Dravidian stratum, Malayalam exhibits the crosslinguistic tendency to lower  $f_0$  in the following vowel. We conclude that  $f_0$  lowering is an automatic consequence of the biomechanics of voicing in Malayalam. At the representational level, such lowering could indeed be enlisted for enhancement, however, that is not the only, or the primary purpose of  $f_0$  perturbation.

## 1. INTRODUCTION

Voicing and  $f_0$ , universally, exhibit a covariation, where voiced obstruents are known to lower onset  $f_0$  in the following vowel, while voiceless obstruents tend to raise the  $f_0$ . In typologically aspiration languages, such as English, despite there being a phonological contrast of the feature [voice], phonetically, at least word-initially, this contrast is implemented through aspiration. The accompanying  $f_0$  lowering prompts many to argue that  $f_0$  lowering in aspiration languages serves to enhance the phonological [voice] contrast. In typical, voice languages, that is the ones that indeed have closure voicing, as well, universally onset  $f_0$  perturbation is found. In this paper, we investigate the nature of  $f_0$  perturbation in Malayalam, where in the Dravidian stratum lexical items voicing is predictable, while in the Sanskrit stratum lexical items phonetic voicing does accompany the underlying voiced stops. Our results indicate that voicing and  $f_0$  covariation is a consequence of the biomechanics of voicing and hence automatic. We report on two experiments that help us make this claim. Phonological representations, however, may indeed enlist micro-fluctuations of  $f_0$  to enhance a [voice] contrast.

In section 2 of this paper, we describe in detail the two major accounts that help us understand the nature and role of  $f_0$  perturbation. Following that, in section 3 we detail our experimental methods and the materials used for our study. In section 4, we present the results from two experiments on  $f_0$  perturbation in Malayalam, and following that in section 5, we stress on the need to understand the biomechanical bases of  $f_0$  perturbations.

## 2. VOICING AND $f_0$ PERTURBATION

While voicing is universally known to depress onset  $f_0$  at least in the first 10 ms of the following vowel, voicelessness as a laryngeal setting is known to have the opposite effect<sup>[18,21,23]</sup>. Regardless of the phonetic manifestation of the nature of the voicing contrast, i.e., languages with voiceless stops accompanied by aspiration such as English, and those with stop voicing such as French and Spanish<sup>[19,25]</sup>. Within the literature, the covariation between voicing and  $f_0$  has been shown to function as an enhancement feature for the feature [voice], where even phonetic voicing may be absent or mitigated by contextual influences<sup>[31]</sup>. On the other hand, this covariation has also been understood as governed by automatic biomechanical constraints, regardless of the phonological status of voicing in a given language<sup>[22]</sup>. While the former view ascribes to the notion that voicing related  $f_0$  perturbation in the onset of the vowel cues voicing contrast where even primary voicing cues may be absent or obliterated, the latter view maintains that the acoustic perturbation of  $f_0$  accompanying voicing is a consequence of physiological constraints that have to do with the loosening of the vocal folds<sup>[22]</sup>. A somewhat unified account is provided by<sup>[24 and 20]</sup> who show that phonetic covariation could at once be used for enhancement of contrasts as well as be physiologically governed.

For the intents of this paper, we refer to the covariation as enhancement argument for  $f_0$  perturbation as the phonological account, and the physical-biomechanical explanations for  $f_0$  lowering following voiced obstruents, and raising following voiceless obstruents as the phonetic account. This characterization is operational, rather than representational. Crucial to both these accounts is the phonological status of the feature [voice], since  $f_0$  lowering following [voice] obstruents and concomitant raising following voiceless obstruents implies an underlying [voice] contrast regardless of the phonetic manifestation of such a contrast. While English contrasts the feature [voice], the phonetic manifestation of this contrast is largely cued by variable Voice Onset Times (VOT), in addition to the presence of [voice] related  $f_0$  perturbation. French and Spanish<sup>[19,25]</sup>, on the other hand, represent languages where the phonological feature [voice], phonetically manifests itself in closure voicing, essentially -VOT, where voicing related  $f_0$  perturbation patterns itself with universal tendencies; mainly lowering following voiced, and raising following voiceless obstruents. In as much as these languages could be referred to as 'voice' languages compared to English, which could be characterized as an 'aspiration' language, the voicing related  $f_0$  perturbation could either be understood as [voice] feature enhancement or due to biomechanical constraints. Hence, typological 'voice' languages may indeed pose difficulty in unequivocally attributing  $f_0$  perturbation due to enhancement of a known contrast or biomechanical constraints. Within this context, the phonetic manifestation and phonological status of the feature [voice] in Malayalam provides a potential third typological variant, distinct from aspiration and voice languages, due to the presence of Dravidian and Sanskrit vocabulary lexical items. While speakers may not have explicit knowledge of the etymology of Dravidian and Sanskrit source lexical items, they may indeed group these words according to the variable application of phonological rules to Dravidian and Sanskrit strata lexical items. To that end<sup>[26]</sup> proposes the features [+Dravidian] and [+Sanskrit] that are specified in the lexicon for the application of rules sensitive to these features. For instance, in Malayalam compounding, if the stem-initial stop of the second stem in the compound has the feature [+Dravidian] then that stop is geminated while if it is [+Sanskrit] it is not. This reflects the ubiquitous presence of intervocalic voiceless geminates in Malayalam and absence of voiced geminates in this environment. The Dravidian stratum and vocabulary as expressed in<sup>[26]</sup> consists of predictable, non-contrastive voicing, the Sanskrit stratum consists of several high-usage lexical items that exhibit phonetic voicing and also share the four-way laryngeal contrast seen in typical Indo-Aryan

languages. The status of the feature [voice] in Malayalam, therefore, is tied to the stratal affiliation of the lexical item. In this paper, we would like to offer a two-fold view; first that in order to ascertain the phonetic and phonological basis for  $f_0$  perturbation, it is crucial to look at languages such as Malayalam, where the phonological status of the feature [voice] is ambiguous at best, or stratally determined. Secondly, the presence of  $f_0$  perturbation in Malayalam voiced and voiceless obstruents would lend support to the claim that  $f_0$  lowering has physiological and biomechanical basis as has been shown by<sup>[22]</sup>.

Stiffening and loosening of the vocal folds is governed by three muscles, namely, Cricothyroid (CT), vocalis, and Thyroartynoid (TA)<sup>[29]</sup>. Voicing during stop closure is enabled by lowering the larynx which helps expand the supraglottal cavities in order to allow voicing during oral closure. During this period, the relaxation in the Cricothyroid (CT) muscle resets the vocal fold tension and results in  $f_0$  lowering<sup>[22]</sup>. Cricoid cartilage (CC) moves downward making the posterior plate parallel to the curvature of the cervical spine. This rotation of the Cricoid cartilage CC leads to shortening of the vocal folds.

### 3. MATERIALS AND METHODS

#### 3.1 Experiment 1

Data were collected from 6 native speakers of Malayalam, 3 male and 3 female. The target words consisted of word-initial (I) and word medial (M) consonants: 6 C(vl)V and 6 Nasal+Vowel (NV) words for the I context, 3  $V_1C(vd)V_2$ , 4  $V_1C:(vl)V_2$  words and 6  $V_1N:V_2$  words for the M context. The 25 target words along with distractors were embedded in a carrier sentence, with 4 repetitions of each word. Time normalized  $f_0$  was measured at 10 intervals into the vowel using ProsodyPro<sup>[32]</sup>, 5 ms offset from the vowel onset. Total 600 items made up the corpus for this experiment. Since the Dravidian stratum lexical items do not exhibit initial voicing, nor intervocalic voiceless singletons, singleton nasals were used in place of voiced stops. In an effort to control for any effects of gemination on  $f_0$  nasal geminates were used to contrast with voiceless geminates.

#### 3.2 Experiment 2

The data were collected from 6 native speakers of Malayalam, 3 male and 3 female. Target words consisted of word-initial (I) and word medial consonants (M): 9 C(vl)V and C(vd)V words for the I context, where C(vd)V words were mainly words from the Sanskrit stratum that are in common use among Malayalam speakers (as confirmed from a Malayalam corpus). 9  $V_1C(vl)V_2$  and  $V_1C(vd)V_2$  words for the M context. 2 prosodic conditions, strong and weak, were also used. This led to a total of 27 words\* 2 (I and M) \* 2 prosodic conditions \* 4 repetitions \* 6 subjects = 2592 items in all. Malayalam is reported to exhibit intervocalic lenition of voiced stops<sup>[27]</sup> such that they become frictionless approximants. These lenited stops were excluded from our study, hence the final number of items analysed were 2056. Since intervocalic stops get voiced in Malayalam,  $V_1C(vl)V_2$  items were taken from compounds where the second stem is a borrowed word from Sanskrit. According to compounding rules in Malayalam, second stem Sanskrit compounds, unlike second stem Dravidian compounds, do not undergo gemination. Instead, the vowel at the end of the first stem is lengthened<sup>[26]</sup>, and the initial consonant of the second stem remains singleton voiceless, as observed from the examples from<sup>[26]</sup>. As in Experiment 1, the target words along with distractors were embedded in a frame sentence, with 4 repetitions of each word. Time normalized  $f_0$  was measured at 10 intervals into the vowel with ProsodyPro<sup>[32]</sup>, 5 ms offset from the vowel onset. For both the experiments data was manually segmented and annotated. In order to control the effects of gender and subject, all  $f_0$  values in Hz were converted to their corresponding z-score normalized values grouped by subject for both experiments.

### 4. $f_0$ PERTURBATION IN MALAYALAM

Results from both experiment 1 and experiment 2 show that despite the phonological status of [voice] in Malayalam, voiced stops significantly lower  $f_0$  in the following vowel. There is also a significant effect

of segment context, with word-initial stops, lowering  $f_0$  more than the word-medial stops. Results from Experiment 1 show that the z-score normalized  $f_0$  ( $z f_0$ ) values are lower for voiced stops and nasals compared to their voiceless counterparts (Fig. 1). A noticeable effect is also the segment position, *i.e.*, the word-initial stops and nasals have lower onset  $f_0$  compared to the stops and nasals in word-medial position.

As can be seen in Fig. 2, we do not find an effect of manner of articulation on the onset  $f_0$ , and nasals are not known to effect  $f_0$  perturbation on account of nasal airflow or velic lowering. However, there is a significant interaction between nasal stops and context. Word initial nasals have lower  $f_0$  compared to word medial nasals. We elaborate on this interaction and the implications for our study below.

We performed a linear mixed effects analysis of the relationship between  $z f_0$  and laryngeal setting, voiceless (VL) and voiced (VD), and with context; word initial (I) and word media (M)<sup>[17]</sup>. The fixed effects, laryngeal setting and context were fitted on the model. An interaction term between context and manner of articulation was also included in the model. The model also consisted of items (words), and iteration as random effects. We obtained p-values by using likelihood ratio tests, *i.e.*, comparison of the full model with the null model. At T1, corresponding to  $f_0$  at 5% of the vowel,  $z f_0$  is significantly predicted by laryngeal setting,  $p=0.02643$ , while context and manner interaction is also found to have a significant effect,  $p=0.022$ . At T2, *i.e.*, 20% of the vowel,  $z f_0$  is not significantly predicted by laryngeal setting and neither

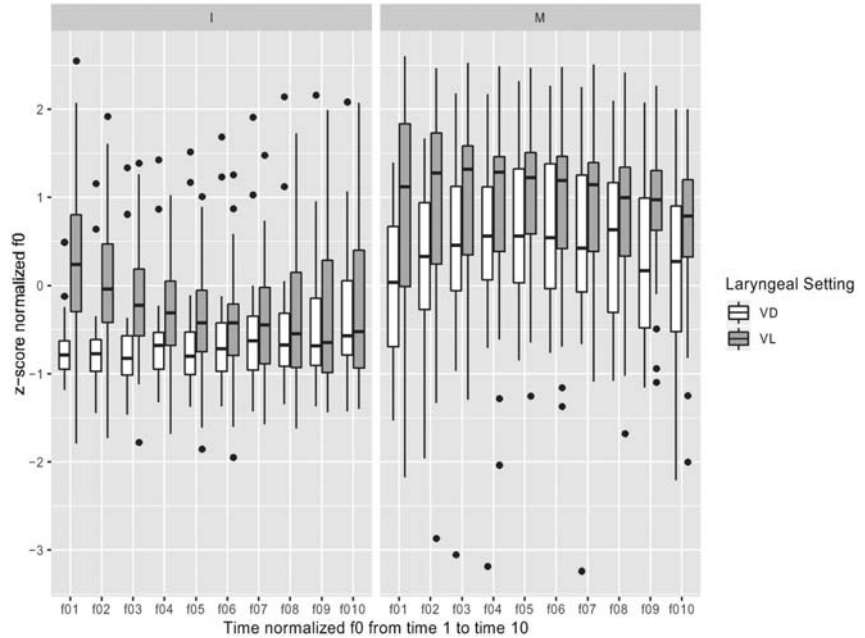


**Fig. 1.** z-score normalized  $f_0$  values for 10 time normalized periods in the following vowel (Experiment 1).

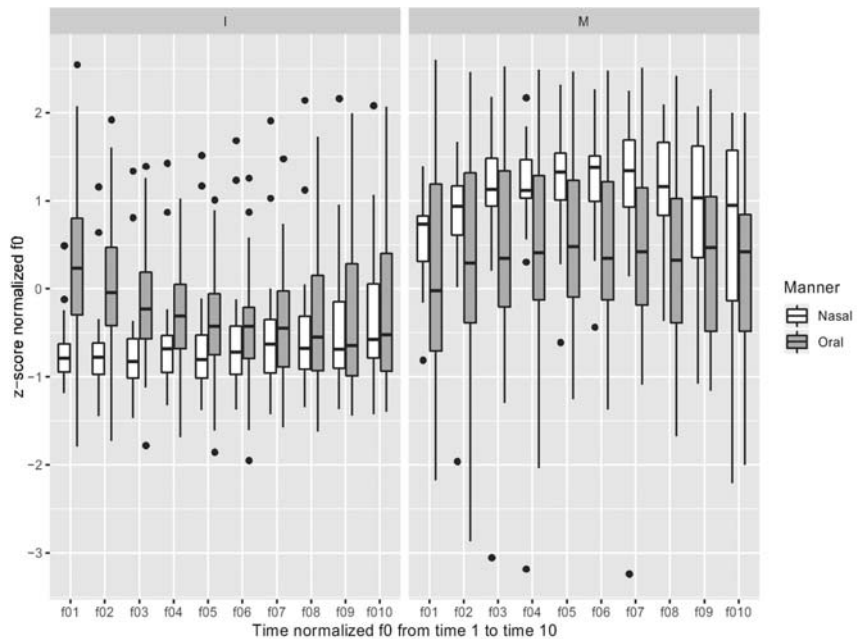


**Fig. 2.** z-score normalized  $f_0$  values for 10 time normalized periods for oral and nasal manner of articulation (Experiment 1).

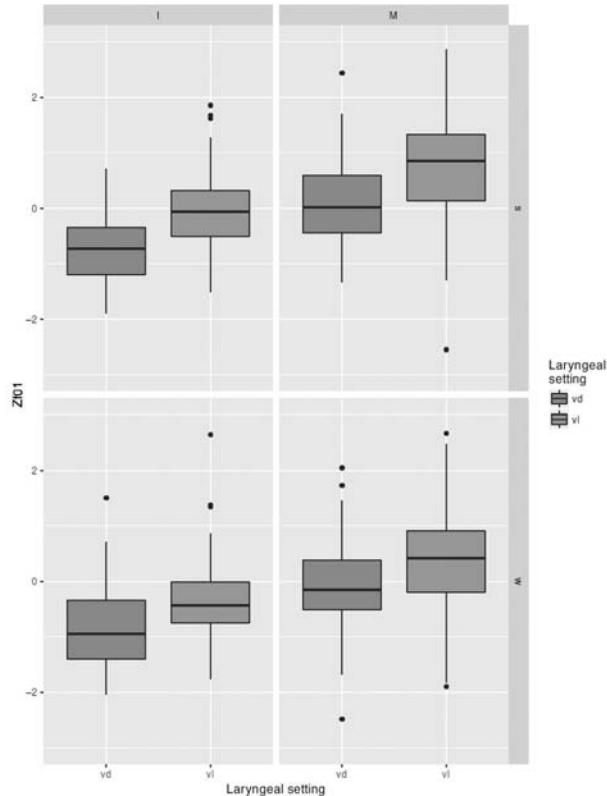


**Fig. 3.** z-score normalized  $f_0$  values for time T1 that corresponds to 10% of the vowel.

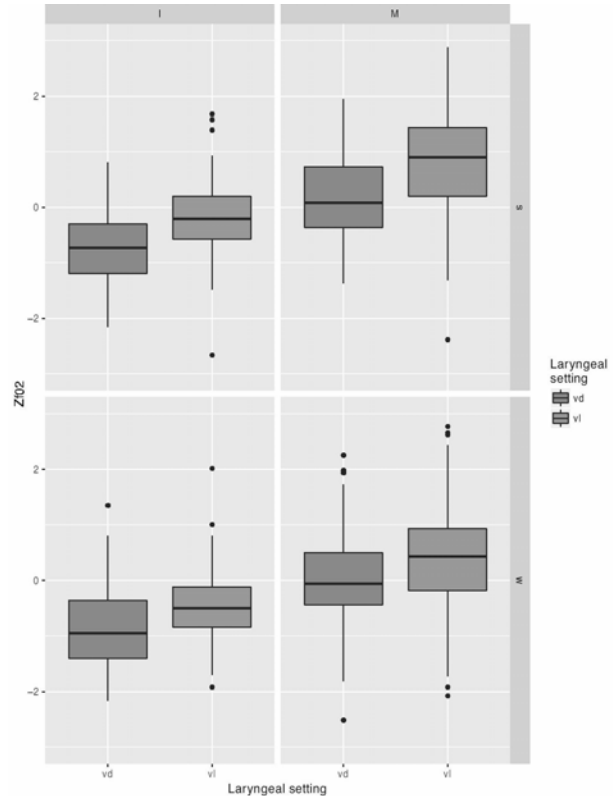


**Fig. 4.** z-score normalized  $f_0$  values for time T2 that corresponds to 20% of the vowel.

context nor manner show significant effects on  $z f_0$ . We did not find any significant effect of laryngeal setting on  $z f_0$  for the remaining time frames.

As can be seen in Fig. 4 the z-score normalized  $f_0$  for voiced stops is lower than that of the voiceless stops at 10% of the vowel. Similar to the results in experiment 1, there is an effect of segmental context, in that word-initial stops lower  $f_0$  in general, compared to word-medial stops. This pattern persists till about 30% of the vowel, with there being an interaction between the effect of the laryngeal setting and segmental context. The effect of the laryngeal setting wanes into the vowel, from it being the greatest at vowel onset, compared to the effect of the segmental context. We also do find a marginal effect of prosodic context; a focal-strong position and non-focal weak position.

For experiment 2, we performed a linear mixed effects analysis of the relationship between  $z f_0$  and laryngeal setting with two levels; voiced (VD) and voiceless (VL). The fixed effects in our model were laryngeal setting and context; word initial (I) and word medial (M), prosodic position (strong and weak) and gender. The random effects had intercepts for subjects, items, and iterations, as well as by-subject, by-item and by-iteration random slopes for the effect of laryngeal setting. We obtained a p-value of  $p=0.011792$  by conducting likelihood ratio tests of the full model with laryngeal setting against a model without laryngeal setting for the effect of laryngeal setting on  $z f_0$  at vowel onset (T1). Introducing an interaction term between laryngeal setting and segmental context we obtained a p-value of  $p=0.0355$  which was significant at the  $p<0.05$ . These results suggest the laryngeal setting, voiced or voiceless is significant in determining the onset  $f_0$  of the vowel, regardless of the phonological status of voicing in a language. In addition we find that the effect of segmental context; word-initial and word-medial, is such that  $f_0$  is significantly lower word initially than word medially. Prosodic context was also found to have a significant

$f_0$  perturbation is automatic not phonologically motivated

effect on  $z_{f_0}$  at vowel onset (T1) with significantly higher  $z_{f_0}$  values for stronger prosodic positions compared to the weaker prosodic context.

## 5. PHYSIOLOGICAL FACTORS BEHIND $f_0$ PERTURBATION

Microprosodic local  $f_0$  fluctuations most definitely play a role in enhancement of segmental contrasts, in this case a laryngeal contrast (where presumably there is none). The processes involved, however, for these local fluctuations are patently biomechanical, and phonological representations recruit these available acoustic cues for discrimination. Cricothyroid (muscle) applies a sudden stretch to the vocal folds to stop vocal fold vibration for voiceless stops and hence raises  $f_0$ , the Cricothyroid due to the rotation shortens the length of the folds which lowers the  $f_0$  in voiced stops. In this paper, we observe that Malayalam due to the variable nature of the status of the feature [voice] in its lexicon provides an excellent testing ground for the automatic versus controlled accounts of  $f_0$  perturbation. Our results indicate that  $f_0$  perturbations are biomechanical in nature, even in a typologically non-contrastive [voice] language, which also exhibits phonetic voicing in the Sanskrit stratum.

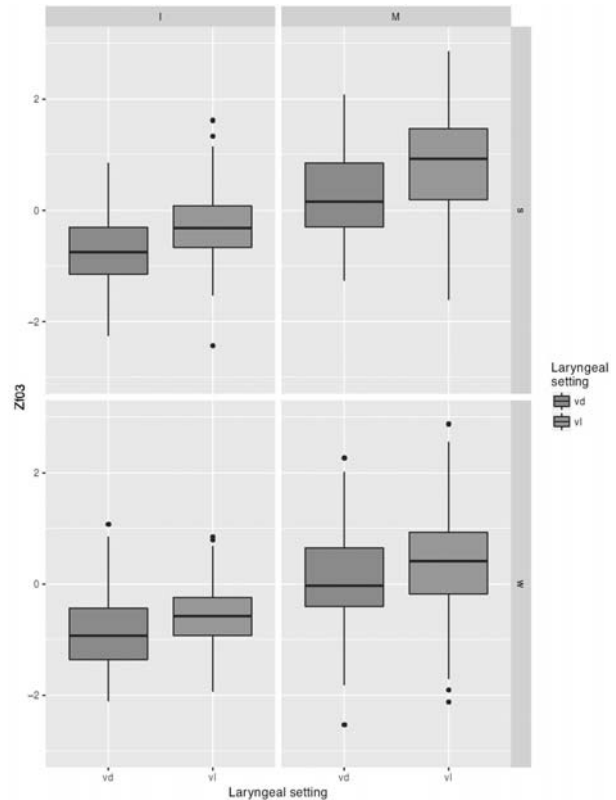


Fig. 5.  $z$ -score normalized  $f_0$  values for time T3 that corresponds to 30% of the vowel.

## 6. ACKNOWLEDGMENT

We acknowledge the help provided by Jasmine Maria George and Minu Sara Paul during collection of acoustic data for experiment 1.

## 7. REFERENCES

- [1] D. Bates, M. Mächler, B. Bolker and S. Walker, 2015. Fitting linear mixed-effects models using lme4 *Journal of Statistical Software*, **67**(1), 1-48, doi: 10.18637/jss.v067.i01.
- [2] L. Chistovich, 1969. Variations of the fundamental voice pitch as a discriminatory cue for consonants *Soviet Phys. Acoust*, **14**, 372-378.
- [3] O. Dmitrieva, F. Llanos, A. A. Shultz and A. L. Francis, 2015. Phonological status, not voice onset time, determines the acoustic realization of onset  $f_0$  as a secondary voicing cue in Spanish and English *Journal of Phonetics* **49**, 77-95, <http://www.sciencedirect.com/science/article/pii/S0095447014001053>, doi: <http://dx.doi.org/10.1016/j.wocn.2014.12.005>.
- [4] L. L. Holt, A. J. Lotto and K. R. Kluender, 2001. Influence of fundamental frequency on stop-consonant voicing perception: A case of learned covariation or auditory enhancement? *The Journal of the Acoustical Society of America*, **109**(764), 131-174.
- [5] J. M. Hombert, 1978. Consonant types, vowel quality, and tone in *Tone: A linguistic survey*, edited by V. A. Fromkin (Academic Press, New York), pp. 77-111.

- [6] K. Honda, 2004. Physiological factors causing tonal characteristics of speech: from global to local prosody *Speech Prosody* .
- [7] A. S. House and G. Fairbanks, 1953. The influence of consonant environment upon the secondary acoustical characteristics of vowels. *The Journal of the Acoustical Society of America*, **25**, 105-113.
- [8] J. Kingston and R. L. Diehl, 1994. *Phonetic knowledge in Language*, edited by S. Everson (Cambridge University Press), pp. 419-454.
- [9] A. Löfqvist, T. Baer, N. S. McGarr and R. S. Story, 1989. The cricothyroid muscle in voicing control. *The Journal of the Acoustical Society of America*, **85**, 1314-1321.
- [10] K. Mohanan, 1986. *Studies in Natural Language and Linguistic Theory. The Theory of Lexical Phonology* (Reidel), <https://books.google.co.in/books?id=bGZiAAAAMAAJ>.
- [11] K. Mohanan and T. Mohanan, 1984. Lexical phonology of the consonant system in malayalam *Linguistic Inquiry*, **15**, 575-602.
- [12] R. N. Ohde, 1984. Fundamental frequency as an acoustic correlate of stop consonant voicing. *Journal of the Acoustical Society of America*, **75**, 224-230.
- [13] K. Stevens, 2001. *Acoustic Phonetics* (MIT Press).
- [14] J. O. Svantesson and D. House 2006. Tone production, tone perception and kammu tonogenesis. *Phonology*, **23**, 309-333, [http://journals.cambridge.org/article\\_S0952675706000923](http://journals.cambridge.org/article_S0952675706000923), doi: 10.1017/S0952675706000923.
- [15] D. H. Whalen, A. S. Abramson, L. Lisker and M. Mody, 1993.  $F_0$  gives voicing information even with unambiguous voice onset times. *The Journal of the Acoustical Society of America*, **93**, 2152-2159.
- [16] Y. Xu, 2013. Prosodypro - a tool for large-scale systematic prosody analysis. *In Proceedings of Tools and Resources for the Analysis of Speech Prosody*, pp. 7-10.
- [17] Bates, D., Mächler, M., Bolker, B. and Walker, S. (2015). Fitting linear mixed-effects models using lme4. *Journal of Statistical Software*, **67**(1), 1-48, doi: 10.18637/jss.v067.i01.
- [18] L. Chistovich, 1969. Variations of the fundamental voice pitch as a discriminatory cue for consonants. *Soviet Phys. Acoust*, **14**, 372-378.
- [19] O. Dmitrieva, F. Llanos, A. A. Shultz and A. L. Francis, 2015. Phonological status, not voice onset time, determines the acoustic realization of onset  $f_0$  as a secondary voicing cue in Spanish and English. *Journal of Phonetics*, **49**, 77-95, <http://www.sciencedirect.com/science/article/pii/S0095447014001053>, doi: <http://dx.doi.org/10.1016/j.wocn.2014.12.005>.
- [20] L. L. Holt, A. J. Lotto and K. R. Kluender, 2001. Influence of fundamental frequency on stop-consonant voicing perception: A case of learned covariation or auditory enhancement? *The Journal of the Acoustical Society of America*, **109**(764), 131-174.
- [21] J. M. Hombert, 1978. Consonant types, vowel quality, and tone in *Tone: A linguistic survey*, edited by V. A. Fromkin (Academic Press, New York), pp. 77-111.
- [22] K. Honda, 2004. Physiological factors causing tonal characteristics of speech: from global to local prosody *Speech Prosody* .
- [23] A. S. House and G. Fairbanks, 1953. The influence of consonant environment upon the secondary acoustical characteristics of vowels. *The Journal of the Acoustical Society of America*, **25**, 105-113.
- [24] J. Kingston and R. L. Diehl, 1994. *Phonetic knowledge in Language*, edited by S. Everson (Cambridge University Press), pp. 419-454.
- [25] A. Löfqvist, T. Baer, N. S. McGarr and R. S. Story, 1989. The cricothyroid muscle in voicing control. *The Journal of the Acoustical Society of America*, **85**, 1314-1321.
- [26] K. Mohanan, 1986. *Studies in Natural Language and Linguistic Theory. The Theory of Lexical Phonology* (Reidel), <https://books.google.co.in/books?id=bGZiAAAAMAAJ>.

$f_0$  perturbation is automatic not phonologically motivated

- [27] K. Mohanan and T. Mohanan, 1984. Lexical phonology of the consonant system in Malayalam. *Linguistic Inquiry*, **15**, 575-602.
- [28] R. N. Ohde, 1984. Fundamental frequency as an acoustic correlate of stop consonant voicing. *Journal of the Acoustical Society of America*, **75**, 224-230.
- [29] K. Stevens, 2001. *Acoustic Phonetics* (MIT Press).
- [30] J.O. Svantesson and D. House, 2006. Tone production, tone perception and kammu tonogenesis. *Phonology*, **23**, 309-333, [http://journals.cambridge.org/article\\_S0952675706000923](http://journals.cambridge.org/article_S0952675706000923), doi: 10.1017/S0952675706000923.
- [31] D. H. Whalen, A. S. Abramson, L. Lisker and M. Mody, 1993.  $F_0$  gives voicing information even with unambiguous voice onset times. *The Journal of the Acoustical Society of America*, **93**, 2152-2159.
- [32] Y. Xu, 2013. Prosodypro - a tool for large-scale systematic prosody analysis. In *Proceedings of Tools and Resources for the Analysis of Speech Prosody*, pp. 7-10.

# INFORMATION FOR AUTHORS

## ARTICLES

The Journal of Acoustical Society of India (JASI) is a refereed publication published quarterly by the Acoustical Society of India (ASI). JASI includes refereed articles, technical notes, letters-to-the-editor, book review and announcements of general interest to readers.

Articles may be theoretical or experimental in nature. But those which combine theoretical and experimental approaches to solve acoustics problems are particularly welcome. Technical notes, letters-to-the-editor and announcements may also be submitted. Articles must not have been published previously in other engineering or scientific journals. Articles in the following are particularly encouraged: applied acoustics, acoustical materials, active noise & vibration control, bioacoustics, communication acoustics including speech, computational acoustics, electro-acoustics and audio engineering, environmental acoustics, musical acoustics, non-linear acoustics, noise, physical acoustics, physiological and psychological acoustics, quieter technologies, room and building acoustics, structural acoustics and vibration, ultrasonics, underwater acoustics.

Authors whose articles are accepted for publication must transfer copyright of their articles to the ASI. This transfer involves publication only and does not in any way alter the author's traditional right regarding his/her articles.

## PREPARATION OF MANUSCRIPTS

All manuscripts are refereed by at least two referees and are reviewed by the Publication Committee (all editors) before acceptance. Manuscripts of articles and technical notes should be submitted for review electronically to the Chief Editor by e-mail or by express mail on a disc. JASI maintains a high standard in the reviewing process and only accept papers of high quality. On acceptance, revised articles of all authors should be submitted to the Chief Editor by e-mail or by express mail.

Text of the manuscript should be double-spaced on A4 size paper, subdivided by main headings-typed in upper and lower case flush centre, with one line of space above and below and sub-headings within a section-typed in upper and lower case understood, flush left, followed by a period. Sub-sub headings should be italic. Articles should be written so that readers in different fields of acoustics can understand them easily. Manuscripts are only published if not normally exceeding twenty double-spaced text pages. If figures and illustrations are included then normally they should be restricted to no more than twelve-fifteen.

The first page of manuscripts should include on separate lines, the title of article, the names, of authors, affiliations and mailing addresses of authors in upper and lower case. Do not include the author's title, position or degrees. Give an adequate post office address including pin or other postal code and the name of the city. An abstract of not more than 200 words should be included with each article. References should be numbered consecutively throughout the article with the number appearing as a superscript at the end of the sentence unless such placement causes ambiguity. The references should be grouped together, double spaced at the end of the article on a separate page. Footnotes are discouraged. Abbreviations and special terms must be defined if used.

## EQUATIONS

Mathematical expressions should be typewritten as completely as possible. Equation should be numbered consecutively throughout the body of the article at the right hand margin in parentheses. Use letters and numbers for any equations in an appendix: Appendix A: (A1, (A2), etc. Equation numbers in the running text should be enclosed in parentheses, i.e., Eq. (1), Eqs. (1a) and (2a). Figures should be referred to as Fig. 1, Fig. 2, etc. Reference to table is in full: Table 1, Table 2, etc. Metric units should be used: the preferred form of metric unit is the System International (SI).

## REFERENCES

The order and style of information differs slightly between periodical and book references and between published and unpublished references, depending on the available publication entries. A few examples are shown below.

### Periodicals:

- [1] S.R. Pride and M.W. Haartsen, 1996. Electro seismic wave properties, *J. Acoust. Soc. Am.*, **100** (3), 1301-1315.
- [2] S.-H. Kim and I. Lee, 1996. Aeroelastic analysis of a flexible airfoil with free play non-linearity, *J. Sound Vib.*, **193** (4), 823-846.

### Books:

- [1] E.S. Skudrzyk, 1968. *Simple and Complex Vibratory Systems*, the Pennsylvania State University Press, London.
- [2] E.H. Dowell, 1975. *Aeroelasticity of plates and shells*, Nordhoff, Leyden.

### Others:

- [1] J.N. Yang and A. Akbarpour, 1987. Technical Report NCEER-87-0007, Instantaneous Optimal Control Law For Tall Buildings Under Seismic Excitations.

## SUBMISSIONS

All materials from authors should be submitted in electronic form to the JASI Chief Editor: B. Chakraborty, CSIR - National Institute of Oceanography, Dona Paula, Goa-403 004, Tel: +91.832.2450.318, Fax: +91.832.2450.602, (e-mail: bishwajit@nio.org) For the item to be published in a given issue of a journal, the manuscript must reach the Chief Editor at least twelve week before the publication date.

## SUBMISSION OF ACCEPTED MANUSCRIPT

On acceptance, revised articles should be submitted in electronic form to the JASI Chief Editor (bishwajit@nio.org)